SCREENING OF MICROFILTRATION AND ULTRAFILTRATION CERAMIC MEMBRANES FOR PRODUCED WATER TREATMENT AND TESTING OF DIFFERENT CLEANING METHODS

A Thesis

Submitted to the Faculty of Graduate Studies and Research

In Partial Fulfillment of the Requirements

For the Degree of

Master of Applied Science

in

Process Systems Engineering

University of Regina

By

Ali Heydari Beni

Regina, Saskatchewan

April, 2014

UNIVERSITY OF REGINA

FACULTY OF GRADUATE STUDIES AND RESEARCH

SUPERVISORY AND EXAMINING COMMITTEE

Ali Heydari Beni, candidate for the degree of Master of Applied Science in Process Systems Engineering**,** has presented a thesis titled, ***Screening of Microfiltration and Ultrafiltration Ceramic Membranes for Produced Water Treatment and Testing of Different Cleaning Methods,*** in an oral examination held on April 16, 2014. The following committee members have found the thesis acceptable in form and content, and that the candidate demonstrated satisfactory knowledge of the subject material.

External Examiner:	Dr. Mohamed ElDarieby, Software Systems Engineering
Supervisor:	Dr. Amr Henni, Process Systems Engineering
Committee Member:	Dr. Hussameldin Ibrahim, Process Systems Engineering
Committee Member:	Dr. Mohamed Ismail, Industrial Systems Engineering
Chair of Defense:	Dr. Allan East, Department of Chemistry & Biochemistry

Abstract

Membrane filtration, as a physical treatment method, was used to treat produced water (PW). Two ceramic microfiltration (MF) membranes and two ceramic ultrafiltration (UF) membranes were tested. The treatment target was to reach a contamination level suitable for further treatment by nanofiltration (NF)/reverse osmosis (RO) polymeric membranes, discharge into sea or injection into oil wells for enhanced oil recovery (EOR).

MF 0.3 μm TiO2/ZrO2 and MF 0.1 μm SiC membranes were initially tested. The MF 0.1 μm SiC membrane was selected based on the permeate flux and rejection performances. The selected MF membrane was used as the first filtration step. The two UF membranes, UF 0.04 μm SiC and UF 150 KDa TiO2/ZrO2, were used for further treatment of the permeate. Finally, the UF membranes were directly tested for the treatment of PW, as a result, the UF 0.04 μm SiC membrane was selected as the most suitable UF membrane for the PW used. When the selected MF and UF membrane, the UF 0.04 μm silicon carbide (SiC) membrane appeared to be the most suitable membrane since it could totally remove the oil, but, it also had the disadvantage of lower permeate flux than the selected MF membrane.

The effects of transmembrane pressure (TMP) and cross flow velocity (CFV) on the permeate quality and flux of the selected MF and UF membranes were investigated. Different membrane cleaning methods including cleaning-in-place

(CIP), backwashing and backpulsing were used to clean the fouled UF membrane.

Hermia's models were used to investigate the fouling mechanisms involved in all the filtration operations conducted. It was found that the cake layer formation and at a lesser degree the intermediate blocking were the predominant fouling mechanisms which controlled the permeate flux of filtrations at all operating conditions tested.

Acknowledgements

I would like to express my sincere appreciation and deep gratitude to my supervisor, Dr. Amr Henni for his advice and encouragement during my study. I am deeply indebted to him for providing me the opportunity to pursue my M.A.Sc. under his supervision. I greatly thank him for his endless support and guidance even during his busiest times. This research would not be conducted without his kind help which was far beyond the regular requirements for an academic supervisor.

I would also like to appreciate Dr. Hussameldin Ibrahim and Mr. Robert Jones for their outstanding and kind support.

The STEPS program, Western Economic Diversification, Enterprise Saskatchewan, and the Petroleum Technology Research Centre are acknowledged for funding and financial support. I would like to thank the Faculty of Engineering and Applied Science and Faculty of Graduate Studies and Research at the University of Regina for their financial support in terms of Teaching Assistantships and Scholarships.

Also, I would like to thank Rangarajan Tharakshi Duraisamy for his kind assistance.

I express my deepest gratitude to my parents and my brother for their support and encouragement throughout this research. Finally, I give my heartfelt thanks to my wife, Niloofar, for her patience, understanding, and continuous encouragement throughout my studies.

Dedication

To my true love, Niloofar

Table of Contents

List of Tables

List of Figures

Nomenclature

A	Membrane surface area (m^2)
A_0	Membrane porous surface area (m^2)
API	American Petroleum Institute
CBM	Coal bed methane
CFV	Cross flow velocity (m/s)
CIP	Cleaning-in-place
COD	Chemical oxygen demand
Da	Dalton
DAF	Dissolved air flotation
EOR	Enhanced oil recovery
FR	Flux recovery
J_0	Initial permeate flux (m/s)
J_P	Permeate flux (m/s)
J_{wi}	Permeate flux of reverse osmosis water through the clean membrane
K	Constant in Equation (2.1) (unit depends on the parameter n in Equation (2.1))
K_A	The blocked area of the membrane per unit of the total permeate volume (m^{-1})
K_B	The decrease in cross-sectional area of the membrane pores per unit of the total permeate volume (m^{-1})
K_C	Complete blocking model parameter (s^{-1})
K_D	Cake layer area per unit of the total permeate volume (m^{-1})

K_g	Cake layer formation model parameter (s/m^2)
K_i	Intermediate blocking model parameter (m^{-1})
K_S	Standard blocking model parameter ($m^{-1/2}s^{-1/2}$)
MF	Microfiltration
MWCO	Molecular weight cut-off
n	Constant in Equation (2.1) that depends on the fouling mechanism
NF	Nanofiltration
NTU	Nephelometric Turbidity Units
O&G	Oil and grease
PW	Produced water
R_g	Cake layer resistance (m^{-1})
RIS	Resistance-in-series
R_m	Membrane resistance (m^{-1})
RO	Reverse osmosis
SAGD	Steam assisted gravity drainage
SD	Standard deviation
SiC	Silicon carbide
t	Time (s)
TDS	Total dissolved solids
TMP	Transmembrane pressure
TOC	Total organic carbon
TSS	Total suspended solids
U_E	Electrophoretic mobility

UF	Ultrafiltration
z	Zeta potential
ε	Dielectric constant
η	Viscosity

CHAPTER 1: Introduction

1.1 Overview

Membrane technology is an alternative treatment method of produced water which can convert produced water into a potable water resource. Produced water is the water produced in conjunction with produced oil/gas from oil/gas reservoirs.

The goals of this study were to determine, among the available membranes, what are the best ceramic membranes for the treatment of produced water, investigate the effect of the filtration operating conditions for the selected membranes, and study the effectiveness of different membrane cleaning methods.

1.2 Produced water

Oil and gas exploration and production processes produce their largest volume of waste as produced water. This wastewater is also called oilfield brine. The generated volume of produced water depends on the amount of formation water, and if oil is produced by water injection into the reservoir (as an enhanced oil recovery method), the production of PW will increase. Oil field produced water is formation water which exists in oil reservoirs and in the case of gas reservoirs; produced water is the condensed water. If sea water was injected into a reservoir, produced water will mainly be sea water (Ray and Engelhardt, 1992). Oily wastewater produced from other sources such as refineries and

petrochemical plants are considered as major pollutants of the aquatic environment (Mueller et al., 1997). PW contains oil and grease, organics, dissolved and suspended solids, salts and different trace metals. The typical composition ranges for total oil and grease, total suspended solids (TSS), and total dissolved solids (TDS) in produced water are 50-1000 mg/L, 50-350 mg/L, and 200-170000 mg/L, respectively. The TDS content for potable water should be less than 500 mg/L, and for other uses such as irrigation and stock ponds it should be between 1000 and 2000 mg/L. The average TDS content of sea water is about 35000 mg/L (Chakrabarty et al., 2008).

Production of produced water increased from 2.1 million bbl per day in 1990 to more than 6 million bbl per day in 2002 as reported by Shell co. (Scurtu, 2009; Khatib and Verbeek, 2003). When the production life of a crude oil well reaches its end time, around 98% of the produced fluid can be PW. In contrast, coal bed methane (CBM) wells produce large volumes of produced water at the early stages of production and the volume of water produced decreases with time (International Advanced Resources, 2002).

Produced water composition is different from one field to another, and also changes with the age of the reservoir. PW of gas wells usually contains condensed water in the early stages of their production and the amount of salts, and inorganic compounds is very low but this type of water contains high concentration of dissolved light hydrocarbons.

In oil field reservoirs, the ratio of PW to produced oil is low at the early stages of operation, but this amount increases and may reach high values (50:1). The composition of oil field PW changes with time, but this change is lower than that of gas field PW (Lee et al., 2011). Water is often injected into oil wells for enhanced oil recovery in order to maintain the reservoir pressure. The injected water dilutes the formation water and makes the composition of produced water approach the composition of injected water (OGP, 2005).

In Canada, the production of bitumen using the Steam Assisted Gravity Drainage (SAGD) process demands high volume of water (about 3 barrels of water for every barrel of oil produced) (Syncrude, 2004). River water is usually used in SAGD process and as the winter flows of the rivers are low, it is not clear whether this amount of water is enough for higher water demands of the future (Peachey, 2005). Providing this enormous amount of water will be limited by governments since this water is also needed for domestic and agricultural purposes (Environment Canada, 2004). Therefore, it is important to find new water treatment methods to treat the generated PW and make it reusable for production of steam in SAGD process. Table 1.1 presents the characteristics of oilfield produced water at 18 heavy oil recovery operations in Western Canada (Vachon et al., 1991). The total concentration of oil and grease varies widely (between 3.3 and 1571 mg/L). The variations of oilfield produced water from different offshore regions are presented in Table 1.2.

Table 1.1: Heavy oilfield produced water characteristics in Western Canada (Vachon et al., 1991)

Parameter	Range of Dada (mg/L)	
	Min	Max
Alkalinity (CaCO3)	68.0	1196.0
Hardness	3.3	11170.0
Total Suspended Solids	8.0	1955.0
Total Dissolved Solids	2110.0	76185.0
Total O&G	3.3	1571.0
Dissolved O&G	0.0	103.3
Filterable Organic Carbon	0.8	548.0
CO3	40.8	745.2
Cl	85.0	43500.0
SO4	0.10	820.0
Ca	0.40	2576.0
Mg	0.03	1200.0
K	11.0	884.0
Na	520.0	36000.0

Table 1.2: Oilfield produced water characteristics comparison between different offshore regions

Parameter	**Eastern Canada** (Canada Oil and Gas Lands Administration, 1990)	**Gulf of Mexico** (Thomas et al., 1983)	**North Sea** (Thomas et al., 1983)
Temperature	-	20-48.2	-
pH	5.6-7.1	5.8-7.6	-
TDS (mg/L)	81000-196000	6000-300000	35000-130000
TSS (mg/L)	-	20-90	-
Cl (mg/L)	49000-119000	16000-170000	-
SO_4^{-2} (mg/L)	71-853	0-70	0-400
TOC (mg/L)	300	70-650	-
Oil (mg/L)	35	2-400	6-250

Produced water has been a major concern for oil and gas industry due to the high cost of produced water management. In onshore wells in United States, more than 98% of the produced water was injected into reservoirs in 2007. Around 59% of this amount was injected into oil producing reservoirs to enhance oil production and the remainder was injected to nonproducing reservoirs for storage (Clark and Veil, 2009). The injection cost for storage and the capital cost is $0.50 to $1.75 per bbl and $400,000 to $3,000,000, respectively. Around 4% of the produced water was disposed into the environment after some pre-treatment methods which may cause some environmental problems (Wandera, 2012). Therefore, finding a promising way to manage the produced water will help oil and gas companies to save money in produced water management.

1.3 Treatment targets

The level of produced water treatment is based on the final required quality of produced water. In offshore oil production platforms, produced water is usually disposed of and the average discharge limit for oil in produced water in Canada is 40 mg/L (maximum of 80 mg/L for 48 h), but regulatory levels are anticipated to be more stringent in the future (Glimmerman, 2006). Oil companies are encouraged to reduce bulk disposal and consider injection as an alternative method for produced water management. There is no required oil concentration in produced water, but it is preferable to reduce the oil level in produced water to prevent the risks of formation plugging. Treatment of produced water to such a level (removal of all detectable oil) suitable for the generation of steam for SAGD

is an alternative method for produced water management in onshore heavy oilfields (Zaidi et al., 1992).

1.4 Produced water treatment technologies

Different types of physical and chemical separation technologies have been developed for treatment and purification of PW. As there are many types of PWs with different characteristics, it has been difficult to develop a single proven PW treatment method. A variety of treatment methods are applied based on the type and characteristics of PW.

1.4.1 Conventional methods

Conventional treatment methods of produced water include coalescence, plate interceptors, granular media filtration, skimming, dissolved air floatation, coagulation, flocculation (Thoma et al., 1999; El-Kayar and Hussein, 1993), filtration, adsorption, gravity separation (Zeevalkink and Brunsmann, 1983), and chemical demulsification (Zhang and Fang, 2008; Kukizaki and Masahiro, 2008; Thompson et al., 1985). As one of the primary technologies for oily wastewater treatment, it was shown that gravity separation has been effective especially when it was used together with skimming. The separation of smaller oil droplets can be enhanced by using air to increase the buoyancy of the oil droplets in dissolved air flotation (DAF). De-emulsification or thermal treatment can be used to remove the emulsified oil before gravity separation and skimming or DAF. Chemicals are also used to destabilize the oil-water emulsion (de-emulsification) and then gravity separation can be used after de-emulsification. Thermal treatment includes evaporation and incineration and can be used to treat many

types of oily wastewaters but the amount of energy consumption is high and the condensate needs to be treated as it contains some amount of oil. The effluents from gravity separation may not meet the discharge limits. Production of large volumes of sludge and high operating costs are some other disadvantages of conventional methods (Wandera, 2012).

Removal of oil/grease and suspended solids has been the ultimate target of different treatment methods. Removal of oil and grease has been a challenge in the past. Usage of hydrocyclones and centrifuges has been restricted due to limitations in the removal of oil. Absorption methods are another PW treatment methods but they are limited by the presence of suspended solids and other contaminants in different PWs that react with absorbent and create new contaminants which requires further removal. Membrane separation technology is an alternative PW treatment method that can be used to remove both the oil/ grease and suspended solids in PW.

1.4.2 Membrane technology

Membrane technology is considered to be a new technology for the treatment of produced water. Membranes are classified into different types based on their nominal size or molecular weight cut-off (MWCO) including microfiltration (MF), ultrafiltration (UF), nanofiltration (NF), and reverse osmosis (RO). Microfiltration membrane rejects suspended solids in the size range of 0.10 to 100 μm. Ultrafiltration membrane rejects macromolecules and suspended solids in the size of 0.001 to 0.02 μm (or 1000 to 100000 MWCO). Nanofiltration membrane rejects divalent salts and dissociated acids with size lower than 1000 MWCO.

Reverse osmosis membrane can be used to reject all the remaining ions except water (Cheryan, 1998).

Membranes also come into four different configurations including tubular, hollow fiber, plate and frame, and spiral. Tubular membranes are suitable for handling large size particles and high flow rates, and they have easier cleaning-in-place methods but the surface area to volume ratios of these membranes are low. Hollow fiber membranes have the highest surface area to volume ratios but the particle sizes passing through should be small to prevent plugging. Plate and frame membranes can be easily replaced onsite. Spiral membranes have feed spacers to provide turbulent flow, high surface area to volume ratio, low energy consumption as operate at low feed flow rates. They also have a low pressure drop, and tend to witness high turbulence (Cheryan, 1998).

Membranes are manufactured from polymeric, ceramic or hybrid materials. There are different polymeric membranes including cellulose acetate, polysulfone, polypropylene, polyamide, Polytetrafluoroethylene and PVDF (Duraisamy et al., 2013). The majority of the ceramic membranes are made of metal oxides including aluminium oxide or alumina (Al_2O_3), titanium oxide or titania (TiO_2), zirconium oxide or zirconia (ZrO_2), and silicium oxide or silica (SiO_2) (Mallada and Menéndez, 2008). There are some other materials used for ceramic membranes including zeolites, microporous carbon and silicon carbide (SiC).

Ceramic membranes have higher temperature and chemical stabilities than the cheaper polymeric membranes. The typical maximum operating temperature

for polymeric membranes is 100 ℃. Polymeric membranes may dissolve in acids and bases. But ceramic membranes can be cleaned at high temperatures with strong acids and bases to recover the permeate flux of the fouled ceramic membranes (Mallada and Menéndez, 2008).

However, ceramic membranes have different stabilities. For example, TiO_2 has better chemical and thermal stability than α-Al_2O_3 (the common phase of Al_2O_3 used as a support layer). TiO_2 ceramic membranes can also be produced at lower costs than α-Al_2O_3 (Mallada and Menéndez, 2008). Because of the high stabilities of the TiO_2 membrane, Tami Industries manufactured TiO_2 membranes in different pore sizes (Lescoche and Bergel, 2004). TiO_2 ceramic membranes were reported to have the highest chemical stability. ZrO_2 has lower chemical stability than TiO_2. But the α-Al_2O_3 and SiO_2 have the lowest chemical stabilities for ceramic membranes (Mallada and Menéndez, 2008).

An α-Al_2O_3 ceramic MF membrane with 50 nm pore size was tested for the treatment of oily wastewater (Hua et al., 2007). The Total Organic Carbon (TOC) removal efficiencies were higher than 92.4% for all the experiments. The highest permeate flux was found at the highest CFV (1.68 m/s) and TMP (0.3 MPa). The cleaning efficiencies of the fouled α-Al_2O_3 ceramic membranes purchased from ECO-CERAMICS were assessed (Silalahi and Leiknes, 2009). Different commercial products including Ultrasil 115, Ultrasil 73, Surfactron CD 50, Derquim+, etc, were tested. Ebrahimi et al. (2009) tested different MF, UF and NF ceramic membranes (in different materials including Al_2O_3, TiO_2/Al_2O_3 and TiO_2), in series, for the treatment of a synthetic produced water. Oil removal

percentage of up to 99 % was observed. Abbasi et al. (2010) manufactured mullite and mullite-alumina MF membranes from kaolin clay and α-Al_2O_3 powder and used it for treating the real and synthetic oily wastewaters. The highest rejection was observed for the mullite ceramic membrane.

A highly concentrated oil-water emulsion was treated with a 300 kDa TiO_2 UF membrane and the critical fluxes were determined (Falahati and Tremblay, 2011). A 99.5 % oil removal was reached in this study. A tubular MF α-Al_2O_3 was used for the treatment of oily wastewater (Rezaei Hosein Abadi, 2011). The permeate had an oil content of 4 mg/L. The mechanical, thermal and chemical stability of the porous SiC materials are high (Facciotti et al., 2014). The thin Al_2O_3 was deposited over the commercial MF 0.04 μm SiC membranes. The retention percentage for polyethylene glycol molecules was about 75 %. It was found that the permeate flux and selectivity of α-Al2O3 can be enhanced by improvement of the commercial MF SiC surface smoothness (Facciotti et al., 2014).

CoMem asymmetric silicon carbide (SiC) MF and UF membranes were manufactured by LiqTech for separation of oil and suspended solids from solutions. It was reported (LiqTech, 2014) that the SiC membranes have high thermal (up to 800℃) and chemical (pH 0 - 14), stabilities and they also have very high permeate flux due to high porosity (about 45 %).

Membrane technology has been used since 1973 for treatment of oily wastewater and membrane technology was suggested to be one of the best solutions for treatment of produced water on near-shore platforms (United States

Environmental Protection Agency, 1991). Membrane technology has some advantages over conventional treatment methods (Duraisamy et al., 2013):

- Lower variation of permeate quality by variation of feed water quality
- Recycling of selected streams within a plant
- Not required to add chemicals prior to separation
- Small space requirement, suitable for places having space limitation
- Lower energy cost than thermal treatments
- Probable automation of separation process
- Lower capital cost
- Reduced sludge
- High quality permeate
- Ease of operation

These advantages have made membrane technology a competitive method for treatment of wastewaters (Kong and Li, 1999; Wandera, 2012; Lin, 2006).

Despite the several advantages of membrane technology in treatment of oily wastewater, this technology suffers from permeate flux decline with time as a result of fouling or concentration polarization effect.

Feed water quality, flow rate, turbulence, and temperature affect the membrane filtration. The permeate flux of the membrane is affected by these factors due to the change in concentration polarization (Cheryan, 1998). Concentration polarization effect is the formation of a layer on the membrane surface that provides a barrier to permeate flow. The increase in cross flow

velocity (CFV) and consequently increase in turbulence or lowering the transmembrane pressure (TMP) minimizes the concentration polarization effect.

Fouling is also another reason for permeate flux reduction during membrane filtration of PW. Fouling is due to adsorption and accumulation of suspended solids, rejected oil, and other rejected components on the membrane surface which causes external fouling. If the rejected components enter the membrane pores and block the membrane pores, it will cause internal fouling (Wandera, 2012).

Several membrane cleaning strategies including air sparging, vibration, relaxation ultrasonication, backwashing, backpulsing, and chemical cleaning have been used to reduce the fouling. These methods are effective in mitigation of reversible fouling, but they are not effective for irreversible fouling, and therefore the original flux cannot be recovered in the case of irreversible fouling (Wandera, 2012).

In a study by Cheryan and Rajagopalan (1998), it was reported that membranes are suitable for treatment of stable oil-water emulsions of the three categories of oily wastewaters (free-floating oil, unstable oil-water emulsions, and highly stable oil-water emulsions).

The application of membranes in produced water treatment depends on the feed and desired water quality after treatment. Polymeric membranes are cheaper than ceramic membranes, but they are less stable than ceramic membranes at high temperatures and at harsh cleaning conditions, and they are not suitable for highly concentrated oily wastewaters (Wandera, 2012; Lin, 2006).

MF membranes (pore size: 0.1-10 μm) have been used for the treatment of oily wastewater (Abbasi et al., 2010). There are several complicated issues in usage of membranes for treatment of produced water including droplet deformation, coalescence, phase inversion, and change in droplet size distribution. The oil droplets will pass through the membrane below a critical droplet size for a given membrane pore size and operating conditions. If the pore size of the membrane is larger than oil droplet size, oil droplets will adsorb on the membrane pore surface (internal fouling) (Wandera, 2012).

UF membranes (pore size 1-100 nm) have been used for treatment of oily wastewater (Badrnezhad and Heydari Beni, 2013). The permeate flux of UF membranes are lower than MF membranes due to the lower pore size of UF membranes. If the particle sizes of oil droplets are smaller than the pore size of the MF membrane, the oil droplets will pass through the MF membrane pores. Therefore, UF membranes can be used for further treatment. Selection of membrane pores should also be based on the concentration and size distribution of suspended solids and size of oil droplets. The membrane pore size should be smaller than particle size of suspended solids and the oil droplets to reject the particles and to prevent them from entering the pores of the membrane (Wandera, 2012).

NF and RO membranes (pore size less than 2 nm) can also be utilized to remove salts from produced water. Some pretreatment methods like MF, UF, addition of anti-scalants, and pH adjustment should be used before NF or RO treatment of produced water (Wandera, 2012).

1.5 Scope of the study

The main objectives of this research can be summarized as:

1) Studying the feasibility of using certain types of ceramic membranes for treatment of produced water,
2) Assessing the MF and UF processes for produced water treatment and the most suitable membrane with specific pore size will be recommended,
3) Studying the effects of different operating conditions including transmembrane pressure (TMP) and crossflow velocity (CFV) on the permeate flux and quality,
4) Assessing the efficiency of different membrane cleaning methods including backwashing, backpulsing, and Cleaning-In-Place in terms of flux recovery,
5) Modeling the fouling of the membranes.

CHAPTER 2: Literature review

2.1 Types of oily wastewaters used as feed for membranes

2.1.1 Synthetic oily wastewater

Lobo et al. (2006) used tubular ceramic ultrafiltration membranes (50 and 300 kDa) for the treatment of a model metal working o/w emulsion (1 wt %). The membrane and feed characteristics are presented in Table 2.1. The concentration polarization was found to be the fouling mechanism at low crossflow velocities. The properties of the o/w emulsion were independent from pH value, but COD retention and permeate flux decreased at low pH values since the membrane surface gained a positive charge at low pH values; therefore, anionic surfactants were adsorbed onto the membrane surface and made it more hydrophobic. The resistance-in-series (RIS) model was used to check the fouling mechanism. Surfactant adsorption and concentration polarization were found to be the major fouling mechanisms. COD retention was higher than 92% for all the operating conditions for both membranes. It was recommended to use the 300 kDa membrane for ultrafiltration of this oil/water emulsion. A summary of the used synthetic oily wastewaters for membrane filtration is presented in Table 2.1.

Table 2.1: Review of synthetic oily wastewaters used as feed for membrane filtration

Reference	Year	Model	Description
Nandi et al. (2009) and Vasanth et al. (2011)	2009	Oily wastewater	Crude oil containing a high degree of aromatic and wax content and distilled water were used to prepare 40, 50, 125, and 250 mg/L o/w emulsion using a sonicator tank (Make: Elmasonic; Model: S30H) for 15 hours at temperature of 25℃. When the oily layer on the water surface disappeared, it was supposed that emulsification process was successful. No surfactant was used and the natural surfactants in crude oil were used for emulsion stabilization. After two weeks, a thin oil film was formed on the water surface. Therefore, prepared emulsions were used within 10 days of preparation date.
Zhang et al. (2013)	2013	Oilfield produced water	NaCl was dissolved in distilled water (0.1%, 3%, and 25% w/w) and different concentrations of polyacrylamide (PAM, 5, 15, 30, and 50 mg/L) which is widely used for polymer flooding in oil production, was added to NaCl solutions. The solution was mixed for 30 min at a speed of 150 rpm.
Mueller et al. (1997)	1997	Oily wastewater	A heavy crude oil (API 12 weight, density 0.972 g/cm-3) was mixed with tap water at various concentrations at high shear rates for 2 min using a blender (Osterizer Model 890-28M). Natural surfactants in heavy oil were used to stabilize the emulsion. The emulsion was centrifuged for 60 min at 1850 rpm in 100 ml pear-shaped, glass centrifuge tubes (International Portable Centrifuge Model IPC-2) to remove all droplets larger than 0.5 μm in diameter.
Cui et al. (2008)	2008	Oily wastewater	0.1 g of lubricant oil was emulsified in 1000 mL of distilled water with 5 mL surfactant (0.01 g/L), polyoxyethylene (80) sorbitan monooleate (Tween 80, Wako) using an ultrasonic mixing (B2200S, Branson) for 60 min.

Reference	Year	Model	Description
Abbasi et al. (2010) and Abbasi et al. (2011)	2010, 2011	Oily wastewater	Condensate gas, distilled water, and Triton X-100 (0.01 wt %) as emulsifier were mixed using a blender at shear rate of 6000 rpm for 30 min to prepare 1000 ppm o/w emulsion. The emulsion was highly stable as no separation was seen after 12 h.
Ebrahimi et al. (2009), Ebrahimi et al. (2010) and Czermak et al. (2008)	2009, 2010, and 2008	Oilfield produced water	Waste oil (5%, 10%, 20% w/w) and distilled water were mixed in a heated stirred tank for 30 min at 60℃. The mixture was left for 30 min to clarify and the free oil was removed. The oil content of model solutions was not constant (32-180 mg/L). The mixture had a uniform yellowish color.
Lue et al. (2009)	2009	Oily water	Kerosene was used to make a 0.2-2% surfactant-free oil-water emulsion.
Yang et al. (2011)	2011	Oil-water emulsion	P-xylene, deionized water, and firefighting foam were used to prepare the oil-water emulsion using the membrane filtration loop at a crossflow velocity of 4 m/s and a pressure of 0.05 MPa for 20 min while the permeate valve was closed.
Salahi et al. (2010b)	2010	Oily wastewater	Commercial grade gas-oil (Tehran refinery, Iran), deionized water, and surfactant (Triton X-100, Merck) were used to prepare a synthesized emulsion (0.1% oil concentration). Surfactant was dissolved in water, then after 10 min, gas-oil was added to the solution. The mixture was blended at 6000 rpm for 30 min.
Chakrabarty et al. (2008)	2008	Oil-water emulsion	Crude oil (Guwahati Refinery, India) and Millipore water were kept in a sonicator tank (S30H Elmasonic) for 5-15 h at a temperature of 30℃ to prepare the emulsion (75, 100, and 200 mg/L oil concentration). No surfactant was added and the emulsion was stable for at least 2 weeks.
Gorouhi et al. (2006)	2006	Oily wastewater	Gas-oil and distilled water were stirred without using any surfactant because the emulsion was stable at low oil concentrations (5 wt. % of oil in water).

Reference	Year	Model	Description
Sutrisna et al. (2012)	2012	Oil-water emulsion	Kerosene or crude oil, distilled water, and SPAN 80 as surfactant (1 wt. %) were mixed to prepare the feed (6.25 v%, 10 v%, and 13.75 v%).
(Madaeni et al. (2013)	2013	Oily wastewater	Commercial grade oil (Tehran refinery, Iran), deionized water, and Tween 85 (Merck) as surfactant were used for emulsion preparation (0.3% oil in water). The surfactant was dissolved in water and after 10 min gas-oil was gradually (during 1.5 h) added to the solution.

2.1.2 Field oily wastewater

It was found that most of the studies were conducted using synthetic oily wastewaters as feeds for membranes. However, a few researchers used field oily wastewater for membrane filtration. A summary of these studies are presented in Table 2.2.

Table 2.2: Review of field oily wastewaters used as feed for membrane filtration

Reference	Year	Wastewater	Description
Kyllönen et al. (2006)	2006	Industrial wastewater	Two types of industrial wastewater including Bark and fabric press filtrate was used.
Rezaei Hosein Abadi et al. (2011)	2011	Oily wastewater	Outlet of the API unit of Tehran refinery was used. As the droplet size distribution was below 20 μm, the oil was emulsified in water.
Pedenaud et al. (2011)	2011	Produced water	The produced water from skim tanks was passed through 500 μm pre-filters to remove large particles to avoid membrane damage.
Madaeni et al. (2012)	2012	Oily wastewater	The wastewater from olefin plant of the Marun petrochemical Co. (Iran, Mahshahr) produced in quenching process of the cracked gas was passed through the stainless steel guard filters for elimination of the coke particles to some extent.

Reference	Year	Wastewater	Description
Fakhru'l-Razi et al. (2010)	2010	Produced water	Produced water from a Malaysian oilfield (Petronas BCOT, Sarawak) was collected and stored at 4℃ before use. The concentration of TDS, O&G, TOC, and SS were 16400 mg/L, 15 mg/L, 540 mg/L, and 168 mg/L, respectively.
Salahi et al. (2010d)	2010	Oily wastewater	The effluent of sand filter of Tehran Refinery wastewater treatment unit was used. The concentration of TDS, O&G, TOC, and TSS were 1953 mg/L, 7.2 mg/L, 48.0 mg/L, and 4.0 mg/L, respectively.
Salahi et al. (2010a)	2010	Oily wastewater	Outlet of the API unit of Tehran refinery was used for polymeric UF process. The concentration of TDS, O&G, TOC, and TSS were 2028 mg/L, 78 mg/L, 81 mg/L, and 60 mg/L, respectively.
Çakmakce et al. (2008)	2008	Produced water	Two types of produced water were used (Vakiflar and Devecatagi). The concentration of conductivity, O&G, and SS for Vakiflar/Devecatagi fields were -/47600 mg/L, 1565/- mg/L, and 35830/- mg/L, respectively. Sodium and chlorine ions were responsible for the measured conductivities.

In this study, two samples of field produced waters were analyzed by analytical instruments. Table 3.2 shows the characteristics of these two water samples. These two samples pertain to two different oil producing areas.

2.2 Membrane cleaning methods

2.2.1 Overview

Two types of membrane fouling exist for treatment of oily wastewater:

i) Reversible fouling

ii) Irreversible fouling

Reversible fouling occurs when solutes or colloidal particles deposit on the surface and in the pores of the membrane. Pure water backwash can be used to recover the flux decline caused by reversible fouling. Irreversible fouling is caused by strong physical or chemical sorption of particles and solutes on the membrane surface or pores. Acid or alkali solutions can only be used to recover the flux decline caused by irreversible fouling. However, the initial permeate flux cannot be reached even after using aggressive cleaning solutions. The selection of chemical solution for the cleaning the membrane is based on the feed type, concentration and type of materials precipitated on the membrane surface. Most of the time, the selection of chemical solution for cleaning of the fouled membranes is performed by trial and error (Munoz-Aguado et al., 1996). The selected materials should efficiently remove the precipitated materials on the membrane surface and be washable with water. These materials should be cheap, safe, and chemically stable and do not degrade the membrane surface.

Different chemicals including disinfectants, surfactants, enzymes, bases, and acids or a mixture of these chemicals can be used for membrane cleaning. The operating parameters like washing time, concentration, pH, crossflow velocity, pressure, and temperature have effects on the extent of membrane cleaning.

2.2.2 Chemical cleaning

Ceramic membranes have high chemical stabilities and make it possible to be cleaned by chemicals at any pH and high temperature levels. Cleaning-In-Place (CIP) which is membrane cleaning without dismantling the setup is performed when backpulsing and backwashing is not sufficient to maintain the permeate

flux. CIP uses a combination of chemical cleanings with intermediate water flushings. The typical duration of CIP is 30 min to 120 min.

A general cleaning procedure is outlined below:

1. Pure water flushing
2. Cleaning at 60℃ with an alkaline detergent for 30 min
3. Pure water flushing
4. Cleaning at 60℃ with an acidic detergent for 30 min
5. Pure water flushing

Intermediate water flushing will hinder the generation of poisonous gases when changing the chemicals, and it helps make a stronger acidic solution for acidic cleaning. The volume of pure water used for intermediate water flushing should be sufficient to make sure that the previous water in the setup is displaced. Intermediate water flushing can be more efficient by back pulses to remove the foulants mechanically and reduce the required amount of chemicals for CIP.

Chemicals used for CIP are categorized into two groups including alkaline and acidic chemicals. Alkaline chemicals are used for removal of organic foulants (crude oil in this study) and acidic chemicals are suitable for precipitated salts. In this study, Nitric acid (HNO_3) was used for the removal of precipitated salts. Nitric acid is cheap and does not corrode stainless steel. Sodium hydroxide (NaOH) was used as an alkaline chemical to remove organic fouled materials. NaOH is relatively cheap, does not lead to stainless steel corrosion problems, and can be disposed of, after neutralization, without any issues. Table 2.3 presents a review

of the methods used for chemical cleaning of membranes. In this table, when the membrane was cleaned without dismantling the setup, which was noted as a CIP method. Otherwise, the method was mentioned as “chemical cleaning”.

In a study (Salahi et al., 2010c), different chemicals including NaOH (as alkali); H_2SO_4, HCl, HNO_3 and H_3PO_4 (as acids); EDTA (as metal chelating agent) and SDS (as surfactant) were used to clean the fouled polyacrylonitrile (PAN) membrane in treatment of oily wastewater from effluent of API (American Petroleum Institute) separator of Tehran refinery. The concentration of all chemical cleaning solutions was 5 mM. The efficiency of cleaning methods was assessed by a permeate flux measurement after the cleaning. It was found that acids had the worst results in the regeneration of the permeate flux, and the effect of alkali solution was moderate while EDTA as a chelating agent was successful to combine with metals. SDS solution as a surfactant was effective in the cleaning of membranes. The cleaning efficiency of membranes increased with the SDS and EDTA solution concentrations. SDS and EDTA solution concentrations of 4 mM and 30 mM are recommended. A combination of 30 mM EDTA and 4 mM SDS was more effective in cleaning the membranes. Oil and grease were cleaned by SDS and minerals were removed by EDTA. At a pH of 10, a cleaning time of 30 min, at a temperature of 45℃, and the CFV of 1.25 m/s were suggested as the best operating conditions.

In another study (Yan et al., 2009), tubular UF PVDF membranes were used for oily wastewater treatment and the fouled membranes were backwashed for 10 minutes with a cleaning solution. Different cleaning solutions were used

including 1% OP-10, 1% OP-10 solution at pH 10, 2% sodium dodecylbenzenesulfate, and 2% sodium hydroxide and permeate flux recovery ratios of membrane were 95%, 97.67%, 93.67%, and 89.67%, respectively. Flux recovery ratio was calculated based on permeate flux after washing divided by initial flux. Membrane flux was recovered to about 90% which means that most of the membrane fouling was reversible fouling.

Various cleaning agents such as H_2SO_4, NaOH, HNO_3, EDTA and SDS were used to clean the RO and NF membranes fouled by licorice aqueous solutions (Sohrabi et al., 2011). The permeate fluxes of water before fouling, after fouling, and after cleaning were measured for 10 minutes at 25℃, a crossflow velocity of 1.5 m/s, and a pressure of 12 bars. The fouled membrane was washed with water for 5 minutes and the permeate flux of water was measured. A cleaning agent was used to clean the membrane at 25℃ without pressure for 5 minutes. Membrane was washed with water for 5 minutes and then the permeate flux of water was measured. Precipitated salts can be removed by acidic solutions. Organic foulants are removed by alkaline solutions. The organic gel network can be broken down using SDS by rearranging the complex between the organic foulant and the divalent action Ca^{2+}. Natural organic matter in the presence of calcium ion can be removed by using EDTA solution. Chemical cleaning solutions were used at concentrations of 0.1 wt. % at 25℃, with 5 m/s velocity at 0 bar for 5 min. A mixture of SDS, EDTA, and NaOH had the best efficiency in cleaning the fouled membrane.

Table 2.3: Review of the membrane chemical cleaning methods

Reference	Cleaning method	Description
Lobo et al. (2006)	CIP	1. 1vol.% Derquim+(commercial detergent supplied by Panreac) was used for 45 min at 40℃, 1 bar and of 5 m/s 2. Water flushing 3. 0.3 vol% HNO_3 aqueous solution at 40℃, 1 bar and 5 m/s for 45 min 4. Water flushing 5. Measurement of permeate flux at 20℃ and various TMPs to check the efficiency of membrane cleaning
Nandi et al. (2009)	Chemical cleaning	"Surfexcel", a laboratory detergent solution, was used to clean the membranes.
Vasanth et al. (2011)	Chemical cleaning	1. Membrane was soaked in hot water at 90℃ for 20 min 2. Membrane was soaked in detergent water solution for 30 min 3. Membrane was rinsed with Millipore water to remove the detergent on the membrane surface 4. When a 20% reduction in pure water flux was observed, membrane was soaked in alkali solution (1N) 5. Pure water flux was measured to check the membrane cleaning
Zhang et al. (2013)	CIP	1. Water flushing to remove the residual process water 2. NaOH solution (pH>12) was used for cleaning at 40℃ for 2 h 3. Water flushing to neutralization 4. Measurement of pure water flux
Mueller et al. (1997)	CIP	1. Cleaning the filtration setup and ceramic membrane with tap water 2. Then cleaning with 0.2 wt% NaOH 3. Finally, 1.0% HNO3 at 40℃ was used for cleaning
Ramirez and Davis (1998)	Chemical cleaning	1. Membrane was backwashed by 5 L of a caustic detergent (1 w/v% of Alconoz) 2. Membrane was removed from setup and cleaned with detergent solution 3. Cleaned with pure ethyl alcohol and rinsed with water

Reference	Cleaning method	Description
Rezaei Hosein Abadi et al. (2011)	CIP	1. Membrane was rinsed with water at room temperature 2. Cleaned it with a 2% NaOH solution at 70-80℃ 3. Re-rinsed the membrane with water at room temperature 4. Cleaned it with a 2% citric acid at 70-80℃ 5. Rinsed the membrane with water at room temperature
Lue et al. (2009)	Chemical cleaning	1. Membrane was soaked in a 30% NaOH solution for 12 h 2. Rinsed with tap water and then with 2 L of deionized water 3. Membrane was soaked in a 30% nitric acid for more than 12 h 4. Re-rinsed with tap water and deionized water 5. Membrane was installed in the filtration setup and 4 L deionized water used to clean the filtration setup and membrane
Yang et al. (2011)	CIP	1. Filtration setup was emptied and tap water was used for rinsing 2. A 1 wt% nitric acid solution at 50℃ was used for cleaning for 40 min 3. A 1 wt% NaOH solution at 50℃ was used for cleaning for 60 min 4. Membrane and setup was rinsed with deionized water

2.2.3 Backwashing and backpulsing

In backpulsing, very short pulses are generated from the permeate side and the foulants are loosened and removed by the cross flow. Backpulsing can be used at a certain frequency or when the TMP reaches a certain level to maintain the permeate flux. Typical frequency for backpulsing is 10 s^{-1} to 1 h^{-1} and the typical duration for backpulsing is 0.8 s. A negative pressure of -3 bars is applied in backpulsing (LiqTech, 2013a).

A TMP of -3 bars is recommended in backpulsing to reach the inner channels of the membrane. The maximum time length of backpulsing should be less than 1 second. It is very important to generate a “block pulse” on the permeate side (Figure 2.1). Block pulse can loosen the fouling material over the entire surface of membrane while the “sine pulse” (Figure 2.2) can only loosen the easiest removable fouling material.

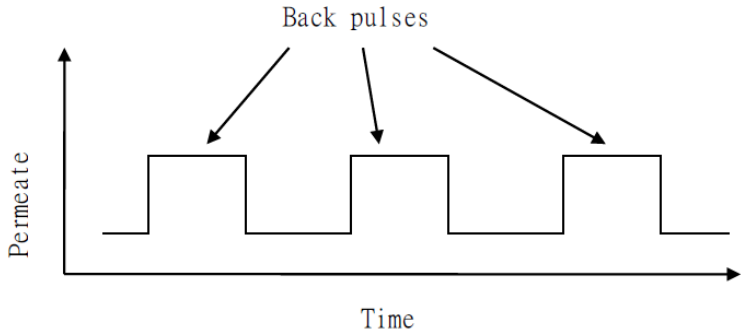

Figure 2.1: Block pulses (adapted from (LiqTech, 2013a))

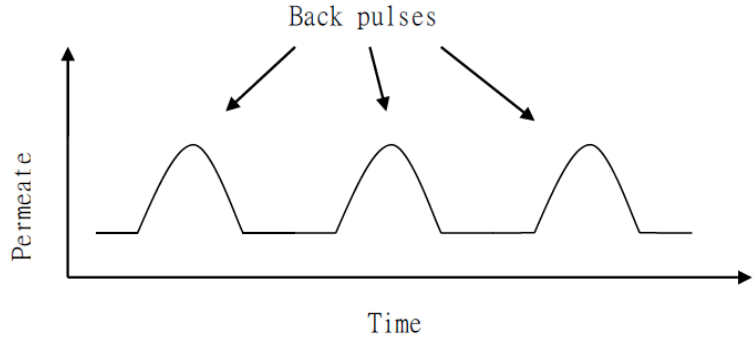

Figure 2.2: Sine pulses (adapted from (LiqTech, 2013a))

Backpulsing uses a low amount of permeate and has a short duration. Pressure oscillation to the setup due to the backpulsing is a disadvantage which should be considered in the design of membrane plant.

backwashing uses a similar concept as backpulsing which is to reverse the permeate flow by means of a pump, and the foulants on membrane surface are washed and removed by a cross flow. Backwashing is often used when the permeate flux decline is 50% or more or when the TMP reaches to a certain level (LiqTech, 2013a). A reversed flow of 1 $m^3/m^2 \cdot h$ is applied in backwashing (LiqTech, 2013a).

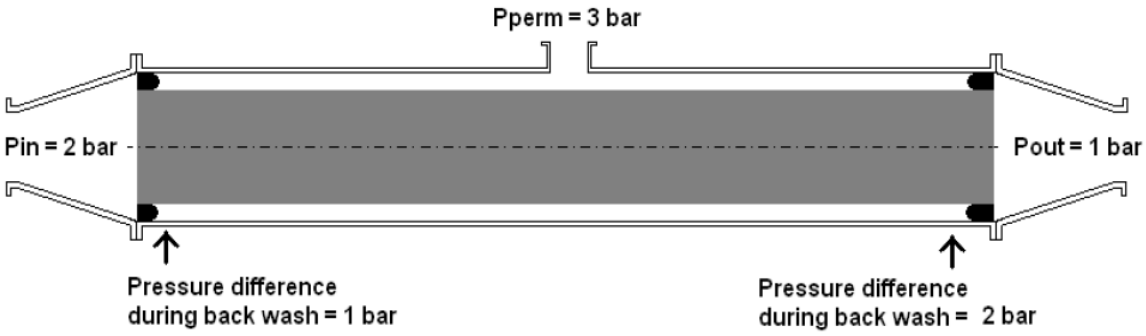

Figure 2.3: Backwashing pressures in the membrane housing (adapted from (LiqTech, 2013a))

Figure 2.3 demonstrates the pressure differences between permeate and inlet and between permeate and outlet of membrane housing. There is a difference between the two pressure difference values which is due to cross flow of feed. The majority of permeate flows through the outlet section of the membrane due to higher the pressure difference at the outlet than the pressure difference at the inlet. Therefore, the inlet section of the membrane will not be cleaned as much as the outlet. This can be solved by using low cross flow velocities (LiqTech, 2013a).

Backwashing can easily be used by adding a pump to the permeate side in order to reverse the flow, and chemicals can be used to enhance the cleaning efficiency of backwashing (Chemically Enhanced Back Wash). If the membrane

has a high internal pressure drop, backwashing efficiency will be limited. One of the major disadvantages of backwashing is the usage of permeate for cleaning of membrane as the permeate production is costly. Backwashing may not be an ideal cleaning method since filtration has to be paused for backwashing (Lee et al., 2001).

In a study, hot distilled de-ionized water at 90℃, a flow velocity of 0.02 m/s, and 100 kPa were used for backwashing every 50 minutes of operation for a duration of 60 s (Cui et al., 2008). When the permeate flux dropped below 20% of the initial flux, hot alkali solution (1wt% NaOH) at the same operating condition and duration as hot water backwashing was used for backwashing, and then hot DDI water at 0.02 m/s and 100 kPa was backwashed to reach a neutral pH (Cui et al., 2008). In another study, backwashing was performed at a maximum pressure of 2 bars for 15 s (Rezaei Hosein Abadi et al., 2011).

2.2.4 Other membrane cleaning methods

Some other methods have been employed to minimize fouling and enhance flux rate in produced water treatment. Table 2.4 presents some of these methods.

Table 2.4: Fouling mitigation methods

Direct methods	**Indirect methods**
Use of turbulence promoters	Pre-treatment
Use of abrasive particles	Surface modification of membranes
Rotatory/vibrating membranes (Vigo et al., 1990)	Preparation of hydrophilic membranes
Rotating blade on the membrane surface	Identification of optimum operating conditions
Crossflow electrofiltration	Identification of suitable operating mode
Ultrasonic enhancement	

In a study, ultrasonic irradiation method as an on-line cleaning method was used (Kyllönen et al., 2006). Ultrasonic cleaning method could reduce chemical cleaning frequencies with no need to pause the filtration. Ultrasound helps to break the cake layer and reduces the solute concentration on the membrane surface which helps to increase the permeate flux (Chai et al., 1999).

2.3 Fouling mechanisms in microfiltration and ultrafiltration

Although many studies have been conducted on the effect of different parameters on the fouling mechanism of microfiltration and ultrafiltration, further research is still necessary to quantify the relationship between the basic parameters (CFV, TMP, temperature, and size of the particles in feed) and the MF and UF fouling mechanisms. The currently developed theoretical models are not very accurate in describing the fouling mechanism of MF and UF for design purposes. Many studies are based on empirical models (Bhattacharjee and Datta, 2003) and in a lower extent on semi-empirical (Badrnezhad and Heydari Beni, 2013; Zydney and Ho, 2002) models can be found in the literature. The accuracy of the empirical models is very good but they cannot describe the fouling mechanism very well. On the other hand, the theoretical models give a better understanding of fouling mechanism, but they are not very precise in predicting the permeate flux with time, and they also need some experimental data to find some of the model parameters (Vincent Vela et al., 2008). Consequently, semi-empirical models which have parameters with a physical meaning, better accuracy than theoretical models, and more accurate description

about the fouling mechanism are more suitable. Hermia's (Hermia, 1982) models are one type of the semi-empirical models.

Hermia's models were initially developed for dead-end filtration but they were also utilized for modeling the cross-flow filtration (Badrnezhad and Heydari Beni, 2013; Sarfaraz et al., 2012; Vincent Vela et al., 2008). Therefore, it was assumed that the type of fouling in Hermia's models for dead-end filtration may also happen for cross-flow filtration.

There are four types of Hermia's models including complete blocking, intermediate blocking, standard blocking, and cake layer formation. These models have some parameters which have a physical meaning which help to understand the fouling mechanisms involved in MF and UF processes. Developed models by Hermia are based on the constant pressure filtration law presented in the following equation:

$$\frac{d^2t}{dV^2} = K\left(\frac{dt}{dV}\right)^n \tag{2.1}$$

For different fouling mechanisms, n has different values. The different fouling mechanisms are presented in Figure 2.4.

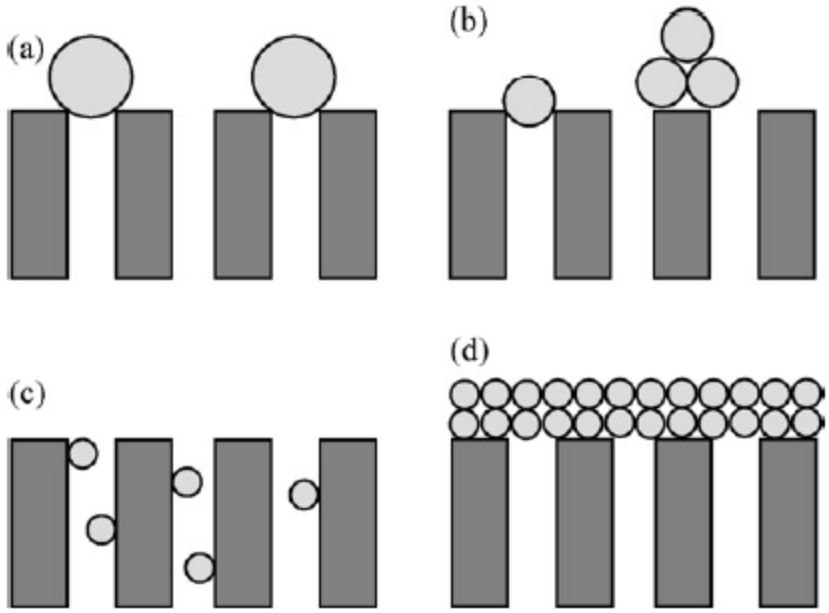

Figure 2.4: Different fouling mechanisms: (a) complete blocking; (b) intermediate blocking; (c) standard blocking and (d) cake layer formation (adapted from (Vincent Vela et al., 2008))

2.3.1 Complete blocking

Based on this fouling mechanism, the entrance of the membrane pores are completely blocked by all the molecules that reach the membrane surface, and molecules do not settle on molecules which have previously deposited on the surface of the membrane. Based on these assumptions, the parameter n was assumed to be 2 and Eq. (2.1) was linearized to the following equation (Lim and Bai, 2003):

$$\text{Ln } J_P = \text{Ln } J_0 - K_C t \qquad (2.2)$$

The parameter K_C was represented as a function of the initial permeate flux, J_0, and the membrane surface which was blocked per unit of the total permeate volume, K_A (Bowen et al., 1995):

$$K_C = K_A J_0 \quad (2.3)$$

This implies that the blockage of the pores results in decreasing the active membrane surface (de Barros et al., 2003). When the size of solute molecules is greater than the size of the membrane pores, the complete blocking mechanism is more likely to occur (Badrnezhad and Heydari Beni, 2013).

2.3.2 Intermediate blocking

The intermediate blocking mechanism is similar to complete blocking mechanism. The membrane pores are blocked by molecules which approach the membrane surface, but the molecules can deposit on the molecules which have previously settled. Therefore, all the molecules do not attribute in blocking the membrane pores. Hermia (Hermia, 1982) considered that n was 1 in this model.

The Eq. (2.1) was linearized (Mohammadi et al., 2003) when n was 1 and expressed in the following form:

$$\frac{1}{J_P} = \frac{1}{J_0} + K_i t \quad (2.4)$$

The parameter K_i was presented (Bowen et al., 1995) as a function of surface of membrane which is blocked per unit of the total permeate volume, K_A. When the size of particles is similar to the pore size of membrane, the intermediate blocking will occur.

2.3.3 Standard blocking

In this model, the particles enter the membrane pores and deposit on the pore walls. As more permeate passes through the membrane, the cross sectional area

of the membrane pores decreases. It was assumed that the length and diameters of the membrane pores are constant.

The n was equal to 3/2 and the Eq. (2.1) was linearized (Bowen et al., 1995) into:

$$\frac{1}{J_P^{1/2}} = \frac{1}{J_0^{1/2}} + K_S t \quad (2.5)$$

The parameter K_S was expressed in the following form:

$$K_S = 2\frac{K_B}{A_0} A J_0^{1/2} \quad (2.6)$$

where K_B is the cross-sectional area of the membrane pores per unit pf the total permeate volume (m^{-1}), A_0 is the membrane porous surface area (m^2), and A is the membrane surface area (m^2).

When the size of particles is smaller than the pore size of membrane, the standard blocking will occur (Mohammadi et al., 2003).

2.3.4 Cake layer formation

In cake layer formation mechanism, a cake layer forms on the membrane surface. The size of particles is greater than the membrane pore sizes (like complete blocking mechanism) and therefore, particles cannot enter the membrane pores (Hwang and Lin, 2002). The molecules deposit on the membrane surface and they can also deposit on the previously settled molecules. The n was considered as 0 and after linearization, the following equation was obtained (Lim and Bai, 2003):

$$\frac{1}{J_P^2} = \frac{1}{J_0^2} + K_g t \quad (2.7)$$

The parameter K_g was presented in the following form (Bowen et al., 1995):

$$K_g = \frac{2R_g K_D}{J_0 R_m} \quad (2.8)$$

where R_g is the cake layer resistance (m^{-1}), K_D is the cake layer area per unit of the total permeate volume (m^{-1}), and R_m is the membrane resistance (m^{-1}).

CHAPTER 3: Experimental part

3.1 Introduction

The first part of the experiments was to screen the MF ceramic membranes to find the most suitable one for the tested synthetic PW. The MF membranes were compared based on their permeate flux and the percentage rejection values for different water parameters analyzed. The MF membrane which had the highest permeate flux and the highest rejection percentage for different contaminants was selected.

The permeate of the selected MF membrane was then used as feed for the UF membranes (MF and UF membranes in series). The percentage rejections of the UF membranes were compared.

As an alternative method, the synthetic PW was directly used as a feed for the UF membranes. The permeate flux and percentage rejection of the two membranes were compared and the most suitable UF membrane tested with synthetic PW was selected. Finally, the selected MF and UF membranes were compared, and the best membrane for the prepared PW was chosen.

After completion of the screening part of the experiments, the operating conditions (TMP and CFV) of the selected membrane were changed to investigate the effect of operating conditions on MF and UF of PW.

In this study, one type of synthetic PW was used as feed to find the best membrane for PW treatment. Determination of a suitable treatment method for field PWs is difficult due to variability of PWs. The treatment system needs to handle high potential contaminants in PW. The usage of different treatment

methods in series may be more suitable to pre-treat the highly contaminated PWs into a certain level, and then different filtration technologies can be utilized to treat the PW to the desired quality. Fouling of the membranes will be the concern if the PW has high level of contaminants like suspended solids. Cross-flow filtration helps to reduce the accumulation of oil and suspended solids on the membrane surface and therefore, the frequency of membrane cleaning will be reduced.

3.2 Selection of membranes

No specific membrane material or pore size has been proven to be the most appropriate for produced water treatment, but the desirable membrane should have the following specifications: long operating lifetime, low cost, high resistivity against chemical cleaning agents, pressure and temperature tolerance, surface hydrophilicity, and high porosity.

Hydrophilic membranes have been used more often than hydrophobic membranes in the treatment of oil-in-water emulsions (Ohya et al., 1998; Daiminger et al., 1995; Zhao et al., 2005). Since hydrophobic membranes are more sensitive to adsorb oil than hydrophilic membranes; Therefore, fouling resistance can be reduced, and permeate flux can be increased by the selection of hydrophilic membranes (Koltuniewiz and Field, 1996; Field et al., 1994).

Two MF tubular membranes and two UF tubular membranes with the same length and external diameter were selected. Therefore, it was possible to test all the membranes using a single membrane cell. The specifications of these membranes are presented in Table 3.1. All of the membranes have a length of

305 mm, external diameter of 25 mm, and can be used in all pH values (0-14). The largest MF membrane (0.3 μm) and the finest UF membrane (150 kg/mol) were purchased from TAMI Industries (INSIDE CéRAM, Montréal, Canada). The MF membrane with 0.3 μm pore size had a support made of TiO2 and an active layer manufactured from TiO2+ZrO2. The UF membrane with the size of 150 kg/mol had also a support and an active layer made from TiO2 and ZrO2, respectively. These two membranes were originally manufactured in longer sizes (1178 mm), but were cut into 305 mm lengths to have the same size as the membranes received from LiqTech. Purchased membranes from TAMI Industries had 23 channels with a hydraulic diameter of 3.5 mm each, and they could resist up to a maximum temperature of 350 ℃. The other MF and UF membranes with pore sizes of 0.1 μm and 0.04 μm, respectively, were purchased from LiqTech International (Ballerup, Denmark). These membranes had more channels (31) than the TAMI membranes, each channel had a hydraulic diameter of 3 mm, and the maximum operational temperature of these membranes was higher (800℃). The filtration area (about 0.09 m2) and cross-sectional area (about 2.2E-4 m2) of both the TAMI and LiqTech membranes were about the same values.

Table 3.1: Membranes used in this study

Membrane	**MF**	**MF**	**UF**	**UF**
Material	Support: TiO_2, Active layer: TiO_2 + ZrO_2	Silicon Carbide (SiC)	Silicon Carbide (SiC)	Support: TiO_2, Active layer: ZrO_2
Pore size/MWCO	0.3 μm	0.1 μm	0.04 μm	150 kg/mol
External diameter, mm	25	25	25	25
Number of channels	23	31	31	23
Hydraulic diameter of channels, mm	3.5	3	3	3.5
Length, mm	305	305	305	305
pH	0-14	0-14	0-14	0-14
Max temperature,℃	350	800	800	350
Filtration area, m^2	0.0906	0.0891	0.0891	0.0906
Cross-sectional area , m^2	2.213E-4	2.191E-4	2.191E-4	2.213E-4
Company	TAMI Industries (INSIDE CéRAM)	LiqTech International	LiqTech International	TAMI Industries (INSIDE CéRAM)
Product code	MTB252311M030	COM0250305010-03	COM0250305004-03	MTB252311U150

3.3 Materials

Calcium chloride and magnesium chloride with purities of 95% and 99% were purchased from Fluka and Alfa Aesar, respectively. Sodium bicarbonate, potassium chloride and sodium sulfate having a purity of 99.5%, 99.5% and 99%, respectively, were purchased from Sigma-Aldrich. Sodium chloride and sodium hydroxide with ACS grade qualities were purchased from EMD. Nitric acid with concentration of 69-70% was purchased from BDH Chemicals. The oil with a density of 0.81 g/cc was received from the Bakken area.

3.4 Feed preparation

In this study, two field produced waters were received from Lloydminster (Alberta, Canada) and Weyburn (Saskatchewan, Canada) and analyzed immediately. Table 3.2 presents the characteristics of two field produced waters. Synthetic PW was used as feed because the feed would have constant properties for all the experiments and it was easier to make the feed for all the experiments (24 liters per experiment) than testing real field produced water as it was impossible to test the fresh field produced water for all the experiments. Preserving a large volume of field PW for the duration of all the experiments was not suitable as it is also known that produced water characteristics changes with time.

Another membrane filtration flow setup (purchased from Sterlitech Corporation, U.S.A.) equipped with CF042 316 stainless steel membrane cells for testing flat sheet polymeric membranes has been used to prepare the synthetic PW for screening of the polymeric membranes in the same research

group. Therefore, to have a consistent feed preparation method, the same setup was used to prepare the synthetic PW. For each experiment, about 24-36 liters (4 to 6 batches) of synthetic PW were prepared. The feed tank volume of the Sterlitech setup was about 5 gallons (18.9 liters), but only about 6 liters (one batch) of PW was prepared at each time to make a more turbulent condition in the feed vessel and have better oil and water mixing. Each batch of PW was made by dissolving a combination of salts in 6 liters of reverse-osmosis (RO) water and then adding 4 mL of crude oil which was received from Bakken area, and mixing for 30 minutes using the Sterlitech setup pump. The speed of the pump was adjusted to 70 Hz and brine valve of setup was closed while the bypass valve was completely opened. Totally, 24 to 36 liters of PW were prepared for each experiment of ceramic membrane filtrations.

The concentration ranges of different ions in the Heavy Oilfield Brines from Western Canada (Vachon et al., 1991) were presented in Table 1.1. The average concentration and percentage of these ions were calculated and presented in Table 3.3. Therefore, different salts containing these ions were purchased and the desired combination of these salts was used to make the synthetic PW. Table 3.4 shows the amounts of different salts dissolved in 6 liters of water to make one batch of PW.

Table 3.2: Analyzes of two field produced water samples

Parameter	PW 1	PW 2	Unit
Turbidity	293	106	NTU
TSS	162.75	-	mg/L
pH	6.86	6.70	
Conductivity	201.9	81.6	mS
TDS	101650	40600	ppm
TOC	660.2	28.78	ppm
IC	28.04	38.78	ppm
Zeta Potential	29.2	-11	mV
Oil content	106	17	ppm
Chloride	24820	16901	ppm

Table 3.3: Average concentration of ions in heavy oilfield brines from Western Canada

Ion	Average Concentration	Percentage
CO_3	393	0.9
Cl	21793	50.5
SO_4	410	0.9
Ca	1288	3.0
Mg	600	1.4
K	448	1.0
Na	18260	42.3

Table 3.4: Quantity of different salts per 6 liters of RO water for synthetic PW preparation

Salt	gram/ 6 liters of RO water
Calcium chloride	8.05
Magnesium chloride	5.29
Sodium chloride	63.56
Sodium bicarbonate	1.08
Potassium chloride	1.85
Sodium sulphate	1.35

Table 3.5: Quantity and percentage of ions used to make 6 liters of PW

Ion	gram/6 liter	Percentage
CO3	0.77	0.95
Cl	48.52	59.78
SO4	0.91	1.12
Ca	2.91	3.58
Mg	1.35	1.66
K	0.97	1.20
Na	25.74	31.71

After dissolving the presented quantities (Table 3.4) of salts in 6 liters of RO water, the quantity and percentage of each ion was calculated and presented in Table 3.5. By comparison of the ions percentages between Table 3.3 and Table 3.5, it was found that the used ion percentages (Table 3.5) are very close to the average values in the literature. The small deviations are due to presence of some ions like sodium and chloride in different salts and therefore, it was impossible to make the exact average ion percentages. But the prepared ion percentages were well close to the average ion percentages in the literature. Since a large volume of PW was needed for the experiments, a TDS concentration of about 10.5 ppt was chosen for PW which is within the TDS ranges in the literature (Table 1.1) (Vachon et al., 1991).

The characteristics of the prepared PW were measured for each experiment even though the same method was used to prepare PW for all the experiments, and the average values of the measured parameters were reported.

3.5 Instruments

3.5.1 Filtration unit

LabBrain filtration unit (LiqTech International) was used for membrane filtration of the produced water. This unit can be used for both cross flow and semi-dead end filtration. This unit is equipped with a Back Pulse Hammer (BPH) which generates high frequency “block” pulses from the permeate side back through the membrane and helps to clean the membrane and reject the foulants from the membrane surface.

LabBrain unit is equipped with pressure, temperature, and flow transmitters that measure the operating parameters and log the corresponding data with respect to time (every 3 seconds). In addition, all the settings related to the pump and actual valve positions are stored in the internal memory of the unit and can be transported via an USB port. All the operating parameters can be adjusted through a coloured touch pad. The unit is equipped with a feed pump (Grundfos CRN 3-6) with a capacity of 3 m^3/hour at 5 bars and a PLC (Siemens 6ES7 214-1AE30-OXBO) which controls the valves and the pump of the system (LiqTech, 2013b).

The maximum recommended temperature and pressure of the feed was 95℃ and 6 bars, respectively. All the unit components which were in contact with the liquid were manufactured from stainless steel AISI-316, Viton/EPDM/Nitrile sealing gaskets or Teflon coated components (LiqTech, 2013b).

This unit needs an air supply from an air compressor. An air compressor (MotoMaster) having a tank size of 2.5 US gallons and air delivery capacity of 5.1

SCFM at 40 psi was used and connected to the unit. The BPH system and all the valves of the unit work with air supply and they can be adjusted through the touch pad. The output pressure of the compressor was regularly monitored to have at least 6 bars of pressure.

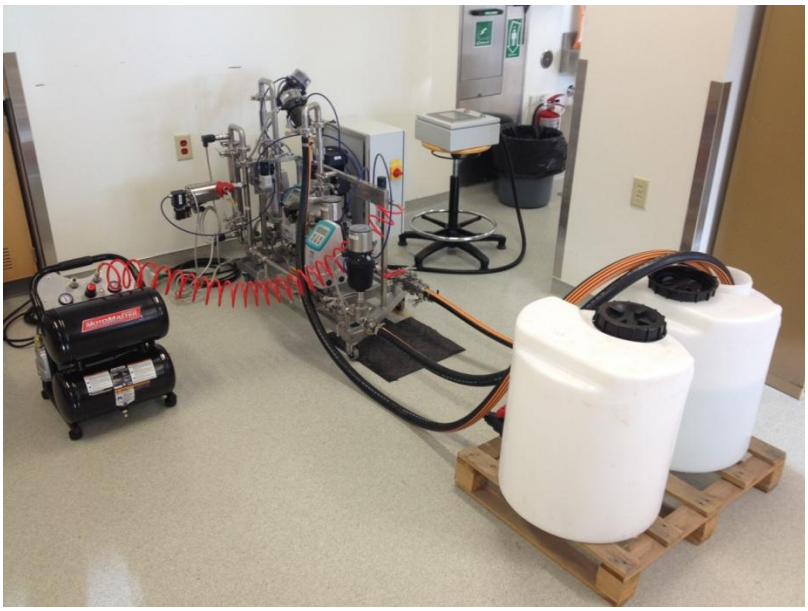

Figure 3.1: LabBrain filtration unit

Figure 3.1 shows the assembled filtration setup. For better representation of the setup, the P&ID of the setup is presented in Figure 3.2. The fluid flow is controlled by different valves including:

- 01V01: Feed valve (Ball valve) from Bürkert
- 01V02: Feed sampling valve (Ball valve) from Uni-valve
- 02V01: Retentate sampling valve (Ball valve) from Uni-valve
- 02V02: Retentate valve (Auto regulating valve) from Bürkert
- 02V03: Loop valve (Auto regulating valve) from Bürkert
- 03V01: Permeate sampling valve (Ball valve) from Uni-valve

- 03V02: On/off valve for BackPulse (Angle seat valve) from Bürkert
- 03V03: On/off valve for BackWash (Angle seat valve) from Bürkert
- 03V04: Solenoid valve for controlling BackWash (2 way) from Bürkert
- 03V05: Check valve for controlling BackWash (Pneumatic) from Bürkert

Furthermore, three manual air pressure adjustment valves exist on the setup to control the air pressure supplied to the valves, BackPulse Hammer (BPH), and permeate tank to provide the necessary air pressure for backwashing. These valves are located on the frame near the feed pump, BackPulse Hammer, and permeate tank, respectively. The setup consists of other parts including:

- 01PT01 is the Feed Pressure Transmitter (max. 6 bars) located after the feed pump giving the user a reading of the pressure leaving the feed pump.
- 02PT01 is the Retentate Pressure Transmitter (max. 6 bars) placed at the outlet side of the membrane element, it gives the retentate pressure.
- 03PT01 is the Permeate Pressure Transmitter (max. 6 bars) placed at the permeate side of the membrane element, it gives the permeate pressure.
- 01FIT01 is the Feed Flow Transmitter (0.2-6 m^3/h) positioned after the feed pump, it gives the cross flow entering the system.
- 02FIT01 is the Retentate Flow Transmitter measuring the amount of retentate leaving the unit.
- 03FIT01 is the Permeate Flow Transmitter (0.01-1.2 m^3/h) located at the permeate side, it measures the flow of the permeate.

- 02TT01 is the Temperature Transmitter giving the temperature of retentate stream.
- 01P01 is a speed controlled Feed Pump (Grundfos multistage pump CRN 3-6).
- 03T01 is the BackWash tank.
- 04BP01 is the BackPulse Hammer.

Two polymeric tanks (each 60 L) were used, which were equipped with manual ball valves. One of the tanks was considered for feed filtration and the other tank was used for membrane cleaning (acid and base cleaning). One immersion heating element model 55044 (SAN Electro Heat) was utilized to heat the acid and base solutions to about 50℃ for membrane chemical cleaning.

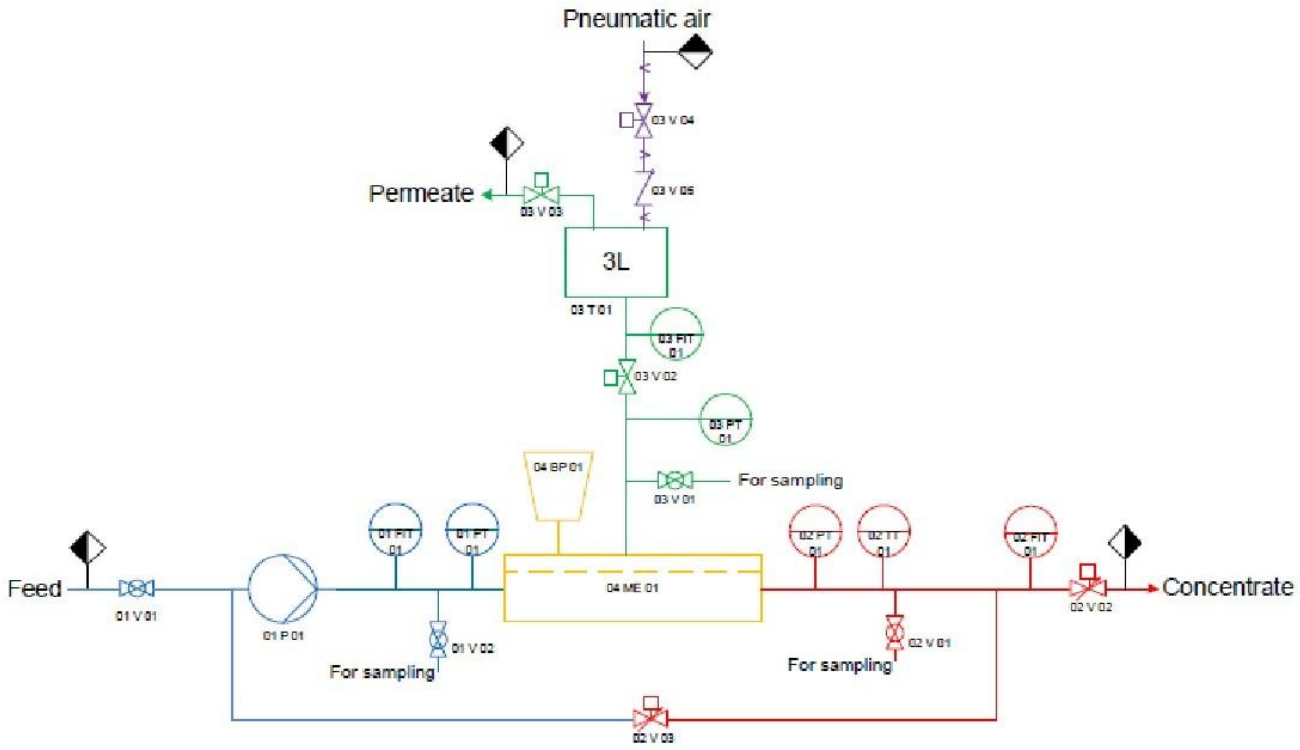

Figure 3.2: P&ID of the LabBrain setup [adapted from (LiqTech, 2013b)]

3.5.2 Mastersizer

A mastersizer 3000 optical unit (Malvern) equipped with hydro LV dispersion unit was used to measure the oil droplet size distribution in the samples. In optical unit, a sample passes between measurement windows of a measurement cell, and red laser light (with 633 nm of wavelength) and blue light (with 470 nm of wavelength to determine the sub-micron particle sizes) are transmitted through the sample and detectors are used to measure the light scattering pattern which is characteristic of the particle sizes of the sample. Larger particles cause smaller angle scattering, and smaller particles cause larger angle scattering. Wet dispersion unit controls the dispersion of the sample in a liquid dispersant (water for the samples) and circulate the sample through the measurement cell. The hydro LV dispersion unit with 600 mL volume is suitable for samples with broad size distributions or have large particles (Malvern, 2011). The mastersizer and dispersion units are presented in Figure 3.3.

Figure 3.3: Masterszier 3000 unit (back) and Hydro LV dispersion unit (front)

The measurement windows were cleaned after each measurement using a dilute concentration of micro 90 solution. If cleaning procedure using the micro 90 solution was not successful, the measurement cells were wiped using Kimwipes. Refractive index, absorption index, and density of sample material were set as 1.45747, 3E-6, and 0.800681 g/cm^3, respectively. Refractive index of the oil which was used to make the synthetic produced water was measured at 25 ℃ using a refractometer model RX-5000α (ATAGO) and absorption index was used from published value in the literature (Król et al., 2006).

The measurement results are presented as the particle sizes versus the volume percentages of particles. The size of the particles in microns, at which 50% of the sample particles are smaller is denoted by Dv50. With a similar concept, Dv10 and Dv90 are used to present the sizes of particles at which 10% and 90% of the particles are smaller, respectively. Dv50 is the median of the volume particle distribution.

3.5.3 Zetasizer

Zetasizer model Nano-ZS (Malvern) was used to measure the zeta potential. All the measurements were performed according to the instructions in the user manual provided with the Zetasizer Nano-ZS (Malvern et al., 2009). The instrument was turned on 30 minutes before the measurement for the laser to stabilize. Folded capillary cell (DTS1060) was used for zeta potential measurements. The cells were cleaned using ethanol or methanol after each measurement. Then, de-ionized water was used several times to wash the cells. All measurements were performed at 25℃. The same refractive index and

absorption index as the ones used for the mastersizer were used for sample material. Water was selected as dispersant and its properties at 25℃ were used. Measurement duration was set to automatic mode, and the number of measurements was set to 3. All other settings were kept unchanged, and the default settings were used.

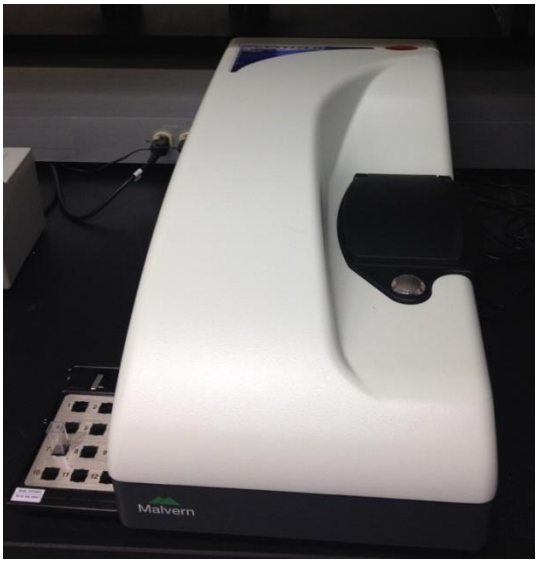

Figure 3.4: Zetasizer

Ions in a liquid may have a positive or negative charge called cations and anions, respectively. Ions of an opposite charge will be attracted to the surface of ions suspended in a liquid. The layer of the ions which are close to the surface of a charged particle, form a strong bound with the charged particle and is called the Stern layer. The layer of ions which are further away from that charged particle form a loose bound with charged particle and is called diffuse layer. Within the diffuse layer there is a boundary called surface of hydrodynamic shear or slipping plane, and when the charged particle moves, all the ions inside this

boundary move with that charged particle. All other ions outside this boundary can move freely independent of the charged particle (Malvern, 2009).

There is a potential between the particle surface and the slipping plane which is a function of the distance between them. The potential at the slipping plane is called the zeta potential (Malvern, 2009).

A combination of measurement techniques is used to measure the zeta potential including electrophoresis and laser doppler velocimetry (laser Doppler electrophoresis). The velocity of the charged particle in an electrical field is measured and based on the measured velocity, the applied electrical field, viscosity and dielectric constant of the sample, the zeta potential is calculated. Charged particles will be attracted to the electrode having the opposite charge. However, viscous forces will prevent the movement of particles. At equilibrium condition, the particles will attain a constant velocity (electrophoretic mobility). The Henry's equation is used to calculate the zeta potential:

$$U_E = \frac{2\,\varepsilon\,z\,f\,(Ka)}{3\eta} \tag{3.1}$$

where ε is the dielectric constant, z is the zeta potential, f(Ka) is Henry's function, η is the viscosity, and U_E is the electrophoretic mobility. f(Ka) was considered as 1.5 and is referred to as the Smoluchowski approximation (Malvern, 2009).

Zeta potential will determine whether the particles tend to flocculate (stick together) or not. If the value of zeta potential is large (negative or positive) then the particles repel each other, and the tendency for flocculation will decrease. However, if particles have a low zeta potential, then particles will stick together and flocculate. Particles having a zeta potential greater than +30 mV or less than

-30 mV are considered stable. Otherwise, the colloid or emulsion of particles will be considered as unstable (Malvern, 2009).

The concept of Zeta potential is useful in waste water treatment and the study of emulsions. The change in pH or the addition of chemical flocculants (e.g. multivalent ions and charged polymers) will alter the flocculation degree of the wastewater. In summary, the zeta potential will determine if an emulsion will be stable or not (Malvern, 2009).

3.5.4 TOC analyzer

TOC-L combustion analyzer model TOC-LCPH (Shimadzu) shown in Figure 3.5, is equipped with autosampler model ASI-L (Shimadzu) for TOC-LC (for 93×9 or 68×40mL VOA vials) and a cylinder of high purity air was used to measure the total organic carbon (TOC) and inorganic carbon (IC) content of the samples. Oxidization of the organic components with platinum pellets catalyst and the generation of carbon dioxide helps to determine the TOC concentration of samples.

Figure 3.5: TOC analyzer (right) and autosampler (left)

All measurements were performed according to the instructions in the TOC-L CPH/CPN user's manual provided with the instrument (Shimadzu, 2010). The combustion tube of the TOC analyzer was filled with TOC standard catalyst. The furnace temperature was set at 680℃ for TOC analysis. Before each measurement, the level of water in the cooler drain vessel, humidifier, dilution water, and rinse bottle was checked and if necessary, the vessels were filled with enough deionized water produced using a Simplicity UV System. The level of acid in the acid container was checked before each measurement, and commercially available special grade concentrated hydrochloric acid was diluted with deionized water to make 1 mol/L hydrochloric acid. CO_2 absorber was installed to remove CO_2 from carrier gas as carrier gas is used to purge the optical system of the detector. The level of IC reagent in the IC reaction vessel was checked regularly and if necessary, the IC reagent was prepared by diluting 50 mL of commercially available phosphoric acid (ACS reagent grade) with deionized water to a final volume of 250 mL to make a 25 wt. % phosphoric acid, and the IC reaction vessel was filled with diluted phosphoric acid.

The TC standard solution was prepared according to the following procedure. 2.125 g of reagent grade potassium hydrogen phthalate was weighed and transferred to a 1 L volumetric flask, and deionised water was added to volumetric flask to 1 L mark, and the solution was stirred well. The carbon concentration of the prepared standard stock solution is 1000 mg C/L. The standard stock solution can be diluted with deionised water to the desired carbon concentrations.

The IC standard solution was prepared according to the following procedure. 3.497 g of ACS reagent grade sodium hydrogen carbonate and 4.412 g of reagent grade sodium carbonate was accurately weighed and transferred into a 1 L volumetric flask, and deionised water was added up to the 1 L mark and the solution was well stirred. The carbon concentration of the prepared standard stock solution was 1000 mg C/L.

The prepared 1000 mg C/L TC and IC standard solutions were stored for 2 months for calibration purpose according to the instruction in TOC-L CPH/CPN user's manual (Shimadzu, 2010).

As field produced water contains suspended solids and TOC is often contained as suspended material, the way of taking a sample is important in TOC analysis, and large variations in TOC measured values may be observed for the same sample if it was handled differently. The tubing that takes the sample from 40 mL vials (PTFE tubing) has an inner diameter of about 0.5 mm, and if suspended particles are larger than this tube, they cannot pass through the tube and the TOC content of those particles won't be measured, and this would be part of the experimental errors (Shimadzu, 2010). The produced water was well homogenized before taking a new sample to assure that the particles were uniformly distributed before a representative sample was taken.

For each TOC measurement, the instrument was turned on and the gas supply pressure was set to about 40 psi. The carrier gas flow rate was set to 150 mL/min. For TOC measurement, the furnace should be turned on and it will take about 30 minutes to reach the set temperature (Shimadzu, 2010).

3.5.5 Oil content analyzer

Oil content analyzer model OCMA-350 (Horiba) shown in Figure 3.6 was used to determine the oil and grease content of the samples. The sample oil was extracted using an S-316 solvent. Before each measurement, the instrument calibrations using 200 mg/L of B-heavy oil in S-316 solvent (span calibration) and pure S-316 solvent (zero calibration) were performed. Initially, hydrochloric acid was used to reduce the sample pH to below 2. Then, 10 mL of sample and 10 mL of S-316 were taken into a vial which was shaken vigorously to extract the oil with the solvent. The vial was kept in an upright position for about 30 seconds to separate the solvent and water phases. The solvent phase remained at the bottom layer and was transferred into the measuring cell. The cell was placed into the analyzer and the oil and grease content was measured in mg/L (Horiba, 1995).

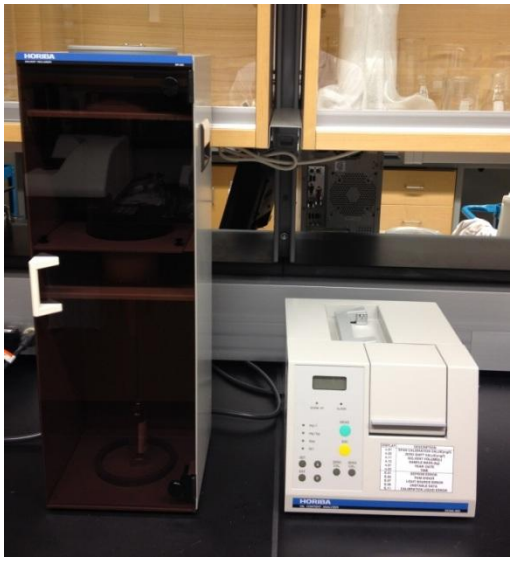

Figure 3.6: Oil content analyzer (right) and solvent reclamation column (left)

The solvent is very expensive. Therefore, solvent reclaimer column model SR-300 (Horiba) was used to reclaim the used solvent. This column uses activated carbon and activated aluminium to reclaim the solvent.

3.5.6 Spectrophotometer

COD measurements of all the samples were performed using a spectrophotometer model DR 5000 UV-Vis (Hach) and the DRB200 reactor shown in Figure 3.7 (Hach LTV082.53.42001). Two types of COD vials were utilized:

a) COD Digestion Vials, High Range (Hach 2125915) for range: 20 -1500 mg/L COD

b) COD Digestion Vials, High Range Plus (Hach 2415925) for range: 200 to 15,000 mg/L COD

These vials contain sulfuric acid, potassium dichromate as a strong oxidizing agent, silver and mercury sulfate. Reaction of organic components with dichromate ion gives a green color trivalent chromium ions. COD was measured based on the intensity of the green color (Hach, 2005).

Figure 3.7: Spectrophotometer (right) and DRB200 reactor (left)

The amount of a specified oxidant that reacts with a sample under controlled condition is called Chemical Oxygen Demand (COD). Oxygen is the equivalent amount of the quantity of oxidant consumed. Oxidation can occur for both organic and inorganic components in a sample; however the majority of oxidation pertains to organic components. COD can be used as an indication of the amounts of pollutants in wastewater and natural waters.

Measurements were performed according to the procedure outlined in "method 8000" (Hach, 2005). A certain volume of homogenized sample was taken and the DRB200 reactor was preheated to 150℃. For analyzing the feed samples for COD concentration, the high range plus (range: 200 to 15,000 mg/L COD) vials were utilized. The caps of the two COD HR+ vials were removed and 0.20 mL of the sample was added to one of the vials while it was positioned at 45-degree angle. 0.20 mL of de-ionized water was added to another COD HR+ vial while it was positioned at 45-degree angle (blank vial). The vials were caped and were rinsed with water and wiped with Kimwipes. The vials were inverted gently several times, and then the vials were inserted into the preheated DRB200 reactor. The vials were heated for two hours. After two hours, the reactor was automatically turned off, and the vials were not removed until the reactor temperature reached to 120 ℃ (it took approximately 20 minutes). Then the vials were removed and inverted several times while they were still warm. The vials were placed into a rack to cool to the room temperature. The spectrophotometer was turned on, and the appropriate measurement program was selected (program number 435 for HR and HR+ vials). The vials were again cleaned using

Kimwipes. The blank vial was inserted into the spectrophotometer, and the instrument was zeroed. Then the sample vial was inserted into the spectrophotometer and the result was read. When HR+ vial was used, the displayed result was multiplied by 10.

The COD concentration of the permeate samples were measured using the high range vials (20 -1500 mg/L COD). The only difference between HR and HR+ vials in the measurement procedure of COD concentration was the amount of sample and de-ionized water which was added to the vials. For HR vials, 2.00 mL of the sample was added to the one of HR vials and 2.00 mL of de-ionized water was added to another HR vial as blank vial. The other steps were the same as the steps described earlier for HR+ vials.

3.5.7 Turbidity meter

Turbidity meter model HI 83414 (Hanna) shown in Figure 3.8 was used to measure the turbidity of the samples. Turbidity causes light to be absorbed and scattered instead of being transmitted. The primary reason for light scattering is the presence of suspended solids in the sample. The intensity and pattern of the scattered light is due to various factors including color, refractive index, size and shape of particles, and wavelength of light (Hanna, 2007).

Figure 3.8: Turbidity meter

The turbidity was measured in Nephelometric Turbidity Units (NTU). The turbidity meter was calibrated regularly using different calibration standards. The samples were transferred into special cuvets and placed in the turbidity meter. Special care should be taken to avoid scratching the cuvets or introducing any air bubble while the sample is being transferred into the cuvet (Hanna , 2007).

3.5.8 pH meter

A pH meter model F-55 (Horiba) shown in Figure 3.9 was used to measure the pH of the samples. The glass electrode was filled with a 3.33 mol/L of potassium chloride solution. The pH meter was calibrated regularly with three pH buffer solutions of 4, 7, and 10. Before calibration or measurement, the filler point of the glass electrode was opened, and after measurement, the electrode was cleaned with acetone and water and wiped with clean tissue paper (Horiba, 2008).

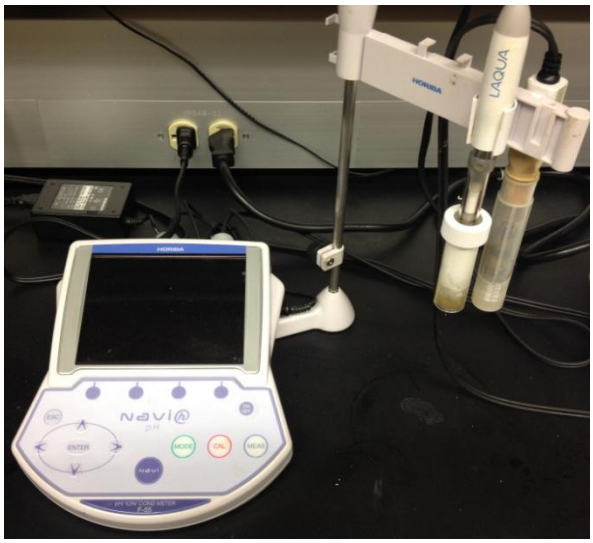

Figure 3.9: pH meter

3.5.9 TDS, conductivity and salinity meter

A TDS meter model HI 4522 (Hanna) shown in Figure 3.10 was used to measure the TDS, conductivity, and salinity of the samples. A platinum conductivity probe model HI 76312 (Hanna) was used for TDS measurement. Regular calibration with a 12.41 g/L TDS standard solution (HI 7036) was performed. After each measurement, the probe was cleaned with acetone and deionized water (Hanna, 2006).

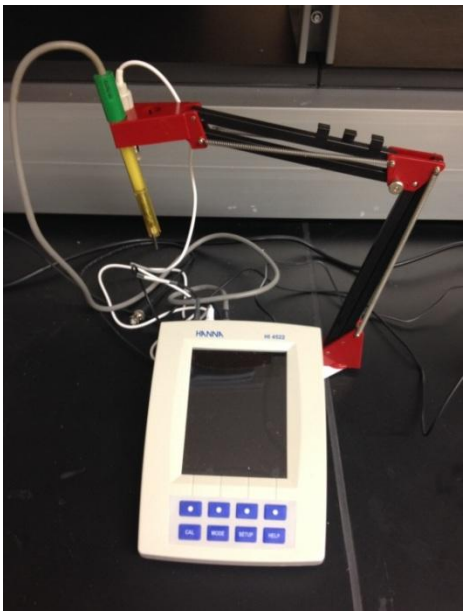

Figure 3.10: TDS, conductivity, and salinity meter

3.6 Experimental procedure

All the experiments were performed in batch mode where the permeate and retentate streams were recycled to the feed tank. The filtration setup had the capability of operating in “cross flow filtration” or “semi-dead end filtration” but all the experiments were conducted in cross flow mode since the degree of fouling in cross-flow mode is less than dead-end mode. The operational conditions including TMP, CFV, Temperature, Valve Opening Percentages, Permeate Flow

Rate, Retentate Flow Rate and Feed Flow Rate were automatically logged every 3 seconds by the filtration setup, and recorded in an internal memory and the stored data could be transferred via flash memories. The TMP and CFV were continuously monitored and the valves were closed or opened to maintain the operating condition constant. The duration of the experiments was 2 hours for which about 24 L of synthetic PW were prepared and the prepared feed was used immediately. The characteristics of the prepared feed were tested for each experiment.

3.6.1 Microfiltration

As described earlier, the purpose of the first part of the experiments was to determine the best MF membrane for the synthetic PW used as feed. To accomplish this aim, the two MF membranes (0.3 μm and 0.1 μm) were tested at the same operating conditions. Table 3.6 presents a review of the operating conditions for MF and UF membranes from the literature. The MF membrane operating ranges for CFV and TMP were 0.2-4.5 m/s and 0.45-4.14 bar, respectively. It seems that the operating conditions were highly dependent on the experimental setup which was available or the type of membrane tested. It was probable that the researchers might have some limitations on the maximum and minimum for CVF and TMP due to experimental setups limitations.

In this research, a CFV of 1 m/s and TMP of 0.8 bar were chosen as the operating conditions for MF membranes which were in the CFV and TMP ranges tested in the literature. Testing the MF 0.1 μm SiC membrane at pressures higher than 0.8 bar was harder since this membrane had a porosity of about 45% and

building a higher pressure demanded much higher pump capacity. Furthermore, a TMP of 0.8 bar was enough to have an acceptable permeate flux for this membrane. To compare the MF membranes together, the MF 0.3 μm membrane was also tested at 0.8 bar of TMP.

To operate the MF 0.3 μm membrane at 1 m/s and 0.8 bar, the pump percentage was set to 62%, and the 02V02 valve was opened to 53%. It was found that the TMP and CFV had some changes with time. Therefore, to maintain the TMP and CFV constant, the 02V02 valve was closed slowly to 51% through the touch pad of the filtration setup and the pump was ramped up to 66%. It should be noted that the adjustments in valve and pump were gradual, and they were changed simultaneously.

For the MF 0.1 μm membrane filtration, the 02V02 valve was initially set to 35% and the pump was set to 63%. Then, the 02V02 valve percentage was gradually increased to 43% to maintain the operating condition constant.

The required adjustment for 02V02 valve and pump were found before each test. Each clean membrane was used with RO water as feed, and the percentages of the 02V02 valve and pump were changed to find the situation where the desired operating condition happens. The percentages of 02V02 valve and pump for PW filtration were slightly different from RO water filtration but this procedure helped to find very good approximate adjustments. When the clean membrane was used with RO water, the probability of membrane fouling was minimum, and it was possible to capture the permeate flux curve from initial fouling step.

Table 3.6: Review of MF and UF membranes operating conditions

Reference	CFV levels (m/s)	Optimum CFV (m/s)	TMP levels (bar)	Optimum TMP (bar)	Membrane pore size
Lobo et al. (2006)	2.5, 3.4, and 4.2	3.4	0.5-4	-	UF: 50 and 300 kDa
Falahati and Tremblay (2011)	1.2	-	0.4-2.7	-	UF: 300 kD
Kyllönen et al. (2006)	0.2-0.6	-	0.9	-	MF: 0.12, 0.19, and 0.25 μm
Mueller et al. (1997)	0.24 and 0.91	-	0.694	-	MF: 0.2 and 0.8 μm
Zhong et al. (2003)	0.58, 1.75, and 2.56	2.56	0.45, 1.10, and 1.55	1.10	MF: 0.2 μm
Shams Ashaghi et al. (2007)	2.56	-	1.10	-	MF: 0.2 μm
Abbasi et al. (2011)	0-2	1.5	0.5-4	3	MF: 0.476 μm
Ebrahimi et al. (2009)	0.6-1.3	-	1	-	MF: 0.1 and 0.2 μm, UF: 0.05 μm and 20 kDa, and NF: 1000 Da
Ebrahimi et al. (2010)	0.6-1.3	-	0.5-2	-	MF: 0.1 and 0.2 μm; UF: 0.05 μm and 20 kDa, and NF: 1 and 0.75 kDa
Abbasi et al. (2010)	0-2	1.5	0.5-4	3	MF: 0.289 μm
Pedenaud et al. (2011)	1-4	-	3.8	-	MF: 0.1 μm; UF: 0.01, 0.04 μm
Rezaei Hosein Abadi et al. (2011)	0.75-2.25	2.25	0.75-1.75	1.25	MF: 0.2 μm
Madaeni et al. (2012)	2	-	15	-	MF: 0.2 μm
Lue et al. (2009)	0.587	-	4.14	-	MF: 0.14 μm
Yang et al. (2011)	4.5	-	1	-	MF: 0.2 μm

Based on the results, the MF 0.1 μm SiC membrane was chosen as the best MF membrane tested. The effect of TMP and CFV on permeate quality and permeate flux of this membrane was investigated. The MF 0.1 μm membrane was tested at CFV of 1 m/s, and three TMPs including 0.4, 0.6 and 0.8 bar. After the TMP of 0.8 bar was selected, filtration was performed at three CFVs including 0.5, 1 and 1.5 m/s. The required adjustments on the filtration setup to operate the filtration at the mentioned operating conditions were presented in Table 3.7. The initial percentages for valve and pump were changed as necessary to the final percentages to maintain the TMP and CFV constant.

Table 3.7: Adjusted percentages for "02V02 valve" and "pump" at different operating conditions for MF 0.1 μm SiC membrane

Operating condition	02V02 valve		Pump	
	Initial	Final	Initial	Final
CFV= 1 m/s, TMP=0.4 bar	58	58	54	54
CFV= 1 m/s, TMP=0.6 bar	46	52	60	60
CFV= 1 m/s, TMP=0.8 bar	35	43	63	63
CFV=0.5 m/s, TMP=0.8 bar	22	28	66	58
CFV=1.5 m/s, TMP=0.8 bar	58	60	75	76

3.6.2 MF & UF in series

After filtration of PW using the MF membranes, it was decided to treat the PW using a combination of the MF and UF membranes (MF and UF membranes in series). The selected MF membrane (0.1 μm SiC membrane) was used as the first filtration step. Then, the permeate of this filtration was used as feed for the two UF membranes (0.04 μm SiC and 150 KDa TiO_2/ZrO_2 membranes).

The MF 0.1 μm SiC membrane was operated at CFV of 1 m/s and TMP of 0.8 bar. The permeate of this filtration was collected in another tank and not recycled

to the feed tank. The CFV of 1 m/s and TMP of 2 bars were chosen as the operating conditions for UF membranes.

Table 3.6 shows that, according to published studies, UF membranes have been operated at CFV and TMP ranges of 0.6-4.2 m/s and 0.4-4 bars. Therefore, the selected operating conditions for UF membranes fell within these ranges.

The UF 0.04 μm SiC membrane failed to operate at CFV of 1 m/s and TMP of 2 bars since this membrane was highly porous, with an approximate porosity of 45%. It was not possible to pressurize the feed inside the filtration setup to 2 bars; therefore, the UF 0.04 μm SiC membrane was operated at CFV of 1 m/s and TMP of 0.8 bar similar to the operating conditions of the MF membranes.

On the other hand, the UF 150 KDa TiO_2/ZrO_2 membrane failed to operate at CFV of 1 m/s and TMP of 0.8 bar. The TMP of 0.8 bar, as the driving force, was very low for this membrane and therefore, no permeate flow was measured. Consequently, the UF 150 KDa TiO_2/ZrO_2 membrane was operated at CFV of 1 m/s and TMP of 2 bars.

3.6.3 Ultrafiltration

The prepared PW was directly used as a feed for the two UF membranes. The UF 0.04 μm SiC membrane was operated at CFV of 1 m/s and a TMP of 0.8 bar, and the UF 150 KDa TiO_2/ZrO_2 membrane operated at CFV of 1 m/s and a TMP of 2 bars.

To operate the UF 0.04 μm membrane at the desired operating condition, the 02V02 valve was set at 46%, and the pump was adjusted to 66%. Then, the

valve percentage was increased gradually to 48% to keep the TMP and CFV unchanged.

For the UF 150 KDa membrane, the 02V02 valve and pump was initially set to 44% and 89%, respectively. Then the valve was closed to 43% and pump was ramped up to 91%.

UF 0.04 μm SiC was selected as the best UF membrane tested (details will be given in the results section). Therefore, the effect of CFV and TMP on the permeate quality and flux of this membrane was investigated. Since the UF 0.04 μm membrane had approximately the same porosity (about 45%) as the MF 0.1 μm membrane tested, the maximum TMP for the UF 0.04 μm SiC membrane was 0.8 bar. It was found that building a higher pressure was hard due to high porosity of this membrane and this membrane had an acceptable permeate flux at TMP of 0.8 bar. Three different TMPs including 0.4, 0.6 and 0.8 bar were used at CFV of 1 m/s, and based on the results, TMP of 0.8 bar was chosen. Then, three CFVs including 0.5, 1 and 1.5 were tested at TMP of 0.8 bar. The required adjustments on filtration setup in the process of the filtration were mentioned in Table 3.8.

Table 3.8: Adjusted percentages for "02V02 valve" and "pump" at different operating conditions for UF 0.04 μm SiC membrane

Operating condition	02V02 valve		Pump	
	Initial	Final	Initial	Final
CFV= 1 m/s, TMP=0.4 bar	59	58	54	56
CFV= 1 m/s, TMP=0.6 bar	50	51	59	61
CFV= 1 m/s, TMP=0.8 bar	46	48	66	66
CFV=0.5 m/s, TMP=0.8 bar	24	31	61	59
CFV=1.5 m/s, TMP=0.8 bar	61	61	76	77

3.6.4 Membrane cleaning

Three different membrane cleaning methods including cleaning-in-place, backwashing and backpulsing have been used to investigate the extent of membrane cleaning by these techniques.

In cleaning-in-place, three concentrations of sodium hydroxide solutions as a base with a constant concentration of nitric acid were used. Then, after one of the base concentrations had been selected based on the membrane cleaning efficiency, three acid concentrations were investigated. Based on the results, the best acid concentration was chosen, and the cleaning efficiency at the selected acid and base concentrations was reported.

For the preparation of the 2%, 3% and 4% sodium hydroxide solutions, 240, 360 and 480 g of sodium hydroxide pellets were dissolved in RO water and then the volume of the solution was increased to 12 L. To make the 2%, 3% and 4% nitric acid solutions by the 69-70% nitric acid, 340, 515 and 690 mL of nitric acid was used and the volume of the solution was increased to 12 L.

The CIP technique in this study is described here. Note that this procedure can be employed to assess the CIP for different types of membranes, but the mentioned operating conditions including the valve and pump percentages are only related to UF 0.04 μm SiC membrane for the PW water tested.

1) RO water flux of the clean membrane was measured before filtration of PW at CFV of 1 m/s and TMP of 0.8 bar (J_{wi}). Note that the 02V02 valve and pump were set to about 48% and 66%, respectively.

2) Filtration setup was drained completely (the draining procedure will be explained later).
3) Membrane was fouled by PW filtration at CFV of 1 m/s and TMP of 0.8 bar for 2 hours.
4) The setup was drained.
5) RO water was filled in the chemical cleaning tank (about 50 L) and the retentate hose was placed in the PW tank. The two valves on permeate line were kept closed, and the pump speed was set to about 50-54% to adjust the cross flow rate to about 1000 L/h. The setup and membrane surface was rinsed with RO water and rinsing continued until drainage about 30 L of RO water volume in the chemical cleaning tank. Then, this operation was stopped.
6) The retentate hose was placed in the chemical cleaning tank, the two permeate valves on the permeate line were opened, and the 02V02 valve percentage and pump percentage were set to about 51% and 63%, respectively, to measure the RO water flux of the fouled membrane at CFV of 1 m/s and TMP of 0.8 bar (J_{ww}).
7) The setup was drained completely.
8) An alkaline solution of sodium hydroxide (NaOH) at the desired concentration was prepared, and the solution temperature was raised to approximately 60 ℃ by the immersion heating element. The two permeate valves (03V02 and 03V03) of the setup were closed and the cross flow rate was set to 1500 L/h (pump percentage was set to about 75%). The

alkaline cleaning continued for 30 min. Note that for the preparation of the alkaline solution and raising the temperature of the prepared solution, about 10 liters of hot tap water was filled in the chemical cleaning tank and the immersion heating element was used to raise the temperature of the water to about 60 ℃. Then the desired amount of NaOH was dissolved in RO water, which was added to the previously heated water in the chemical cleaning tank. The described alkaline preparation and heating method helps to preserve the immersion heating element from being corroded by alkaline solution. As the setup temperature was cooler than the alkaline solution, the equilibrium temperature was about 54 ℃, and the solution was cooled to about 48 ℃ during 30 min. cleaning period.

9) The setup was drained completely and the chemical cleaning tank was washed.
10) Approximately 20 liters of hot tap water was added to the chemical cleaning tank, and the retentate stream was put in the feed tank.
11) To wash the setup and membrane from alkaline solution, while the permeate stream valves (03V02 and 03V03) were closed, the pumping percentage was set to about 50-54% (cross flow rate was about 1000 L/h), and the setup was run until the total water in chemical cleaning tank was drained to the feed tank. It was important to make sure that the pump had water in behind when it was operating. Therefore, it was highly cared to avoid draining the RO water totally in chemical cleaning tank.

12) The desired concentration of nitric acid (HNO_3) solution was prepared and the temperature was raised to approximately 60 ℃. The retentate stream was placed in the chemical cleaning tank and the cross flow rate was set to 1500 L/h. The acidic cleaning continued for 30 min. The acidic solution preparation and heating method were similar to the method of alkaline solution preparation. About 11 L of hot tap water was heated in the chemical cleaning tank and the desired volume of HNO_3 was added to the heated water in the tank. The acidic solution temperature was about 49-53℃ during acidic cleaning period for the same reason as the alkaline cleaning step described earlier.

13) The setup was drained completely and the chemical cleaning tank was washed.

14) About 50 L of the RO water was filled in the chemical cleaning tank and the retentate hose was put in the feed tank. The permeate valves were kept closed and the pump percentage was set to about 50-54% (cross flow rate was about 1000 L/h) and the setup was run until the RO water volume was reached to about 20 L in the chemical cleaning tank. This helps to clean the setup from the acidic solution. Then, this step was stopped.

15) The retentate stream was placed in the chemical cleaning tank, the two permeate valves were opened and the 02V02 valve, and pump percentages were set to about 48% and 66%, respectively, to measure

the RO water flux of the cleaned membrane at CFV of 1 m/s and TMP of 0.8 bar (J_{wc}).

The setup was drained completely via 4 sampling valves (01V02, 02V01, 03V01, and the valve between flow transmitter 03FIT01 and the permeate tank 03T01) in the setup. About 3 liters of the filtered water was remained in the backwash tank (03T01). To drain this water, the clamp of the BackWash tank was opened and the filtered water was drained via the valve between flow transmitter 03FIT01 and the permeate tank 03T01 (this valve is not labeled in P&ID) while the two parts of the backwash tank were kept partially separated. Some amount of water was still in the hoses of the setup. The following connections were opened to drain the remainder water:

- Connection between the flexible hose and the feed tank
- Connection between the flexible hose and the retentate outlet of the unit
- Connection between the flexible hose and the permeate outlet of the unit

For backwashing method, the duration was set to 5 seconds and the interval time to 10 min. When backwashing was performed, it was found that the permeate hose had a very stringent vibration during the backwashing period. Therefore, the permeate hose was carefully kept inside the permeate tank to avoid exiting the permeate hose from the tank. The interval time of the backpulsing was also set to 10 min to have the same interval time for both the

backpulsing and backwashing, and it was possible to compare the results of backwashing and backpulsing.

CHAPTER 4: Results and discussions

4.1 Membrane screening

Table 4.1 shows the average value of the measured feed parameters. The standard deviations (SD) of the parameters were also calculated to find the fluctuations in the measured values for different feeds. It was found that the measured values for COD and oil content had the highest SD values (199 and 25.8, respectively).

Table 4.1: Synthetic PW characteristics

Parameter	Average	SD
Oil content, ppm	117	25.8
Zeta potential, mV	-12.6	4.3
Oil droplet size (Dv 90), μm	46.6	7.1
TOC, mg/L	72.51	5.7
IC, mg/L	20.25	2.5
COD, mg/L	1628	199
TDS, ppt	10.39	0.2
Conductivity, mS/m	20.72	0.3
Turbidity, NTU	60	7.9
pH	7.38	0.2
Salinity, %	40.6	0.7

The average zeta potential of feed was -12.6 mV which is between -30 and 30 mV, which implies that the prepared feed was not stable and the oil droplets tend to attach together. The Dv 90 parameter of oil droplets in the feed was 47.7 μm which means that about 90% of the oil droplets had a smaller size than 47.7

μm. As the prepared feeds had very similar oil droplet size distributions, the oil droplet size analysis of only one of the feeds is presented in Figure A.1 (appendix).

The most suitable membranes should have the highest permeate flux and the highest rejection for different contaminants. The following equation has been used to calculate the "percent removal" for different parameters after filtration using different membranes:

$$Percent\ Removal\ (\%) = (1 - \frac{Permeate\ Concentration}{Feed\ Concentration}) \times 100 \quad (4.1)$$

4.1.1 Microfiltration

The permeate fluxes of the MF 0.1 μm and 0.3 μm membranes versus time were measured for 2 hours and presented in Figure 4.1. The operating conditions for both of the MF membranes were the same. It was found that the MF 0.1 μm SiC membrane had a higher permeate flux than that of MF 0.3 μm TiO_2/ZrO_2 membrane. However, the MF 0.3 μm membrane had a larger pore size, and it was expected to have higher permeate flux for this reason. This may be due to higher porosity of MF 0.1 μm SiC membrane than that of MF 0.3 μm TiO_2/ZrO_2 membrane. The MF 0.3 μm membrane consisted of a support and an active layer. The support layer was made of TiO_2 and the active layer was made of TiO_2 + ZrO_2. The MF 0.1 μm membrane was made of silicon carbide (SiC). Since these two MF membranes were made of different materials which may have different hydrophilicity characteristics, this may be also another reason for having

different permeate fluxes. The SiC membrane may be more hydrophilic than the TiO_2/ZrO_2 membrane.

The initial permeate flux of the MF 0.1 μm membrane was about 3.6 of that of MF 0.3 μm membrane. The permeate fluxes of the MF 0.1 μm and 0.3 μm membranes were reduced by 31% and 27%, respectively, which were about the same values. The permeate flux reduction of the MF 0.1 μm membrane happened mostly in the first 10 min of the filtration, and then the flux was reduced gradually. After about 30 min. of filtration the permeate flux of MF 0.1 μm membrane reached steady state. It seems that that the membrane fouling and the cleaning rates (due to cross flow of feed across the membrane) were reached to the same value and therefore, the membrane permeate flux did not decrease after 30 min. of operation. On the other hand, the permeate flux of the MF 0.3 μm membrane gradually decreased in 30 min. of filtration and then reached to the steady condition.

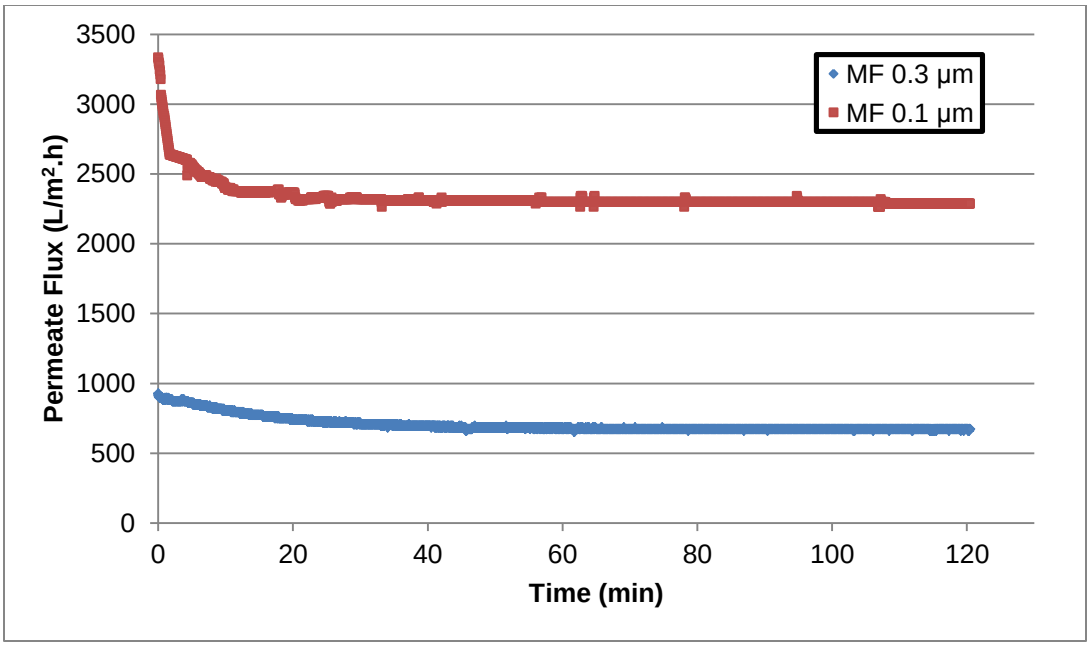

Figure 4.1: MF membranes permeate fluxes versus time (MF 0.3 μm and MF 0.1 μm membranes) [original in color]

The permeate qualities and rejection percentages of the MF 0.3 μm and MF 0.1 μm membranes were shown in Table 4.2 and Table 4.3, respectively. Both of the tested MF membranes had about the same permeate qualities. The MF 0.3 μm membrane had slightly better performance in oil removal (97.2%) than MF 0.1 μm membrane (95.6%). The TOC, COD and turbidity removal percentages of the MF 0.3 μm membrane were about 74.2%, 98.3% and 99.8%, respectively. The TOC, COD and turbidity removal percentages of the MF 0.1 μm membrane were about 72.4%, 98.1% and 99.0%, respectively. The rejection percentages for TDS, conductivity and salinity were very low for both of MF membranes tested.

The MF 0.1 μm SiC membrane was selected as the best MF membrane from the two MF membranes tested for the prepared PW for this experiment. This membrane had much higher permeate flux than the MF 0.3 μm TiO_2/ZrO_2

membrane, and the permeate quality of both of the membranes were relatively close to each other.

Table 4.2: MF 0.3 µm permeate characteristics and rejection percentages PW filtration at CFV of 1 m/s and TMP of 0.8 bar

Parameter	Permeate	Rejection (%)
Oil content (ppm)	3.3	97.2
TOC (mg/L)	1.231	98.3
IC (mg/L)	16.86	16.7
COD (mg/L)	420	74.2
TDS (ppt)	10.35	0.4
Conductivity (mS/m)	20.63	0.4
Turbidity (NTU)	0.1	99.8
Salinity (%)	40.55	0.2

Table 4.3: MF 0.1 µm permeate characteristics and rejection percentages PW filtration at CFV of 1 m/s and TMP of 0.8 bar

Parameter	Permeate	Rejection (%)
Oil content (ppm)	5.2	95.6
TOC (mg/L)	1.384	98.1
IC (mg/L)	19.04	6.0
COD (mg/L)	450	72.4
TDS (ppt)	10.05	3.3
Conductivity (mS/m)	20.45	1.3
Turbidity (NTU)	0.6	99.0
Salinity (%)	39.9	1.8

4.1.2 MF and UF in series

The permeate qualities and rejection percentages of the UF 0.04 µm SiC and 150 KDa TiO_2/ZrO_2 membranes were presented in Table 4.4 and Table 4.5, respectively. The TOC, COD and turbidity for permeate of both the UF membranes were relatively of the same values. The slight differences between the calculated rejection percentages of these parameters were due to slight

differences in the feed characteristics for these two UF membranes. As described earlier, the feed for the UF membranes were the permeate collected from MF 0.1 μm SiC membrane which was prepared in two different experiments. The permeates of the two UF membranes were analyzed for oil content, but no oil concentration was detected.

The rejection percentages for TOC, COD and turbidity of UF 0.04 μm SiC membrane were 30.5%, 22.0% and 66.7%, respectively. The UF 150 KDa TiO_2/ZrO_2 membrane had slightly higher rejection percentages for TOC and turbidity (47.4% and 93.3%, respectively) but it had lower rejection for COD (14.4%). Both the UF membranes had very low rejections for salts.

In operation of MF and UF membranes in series, it was found that the rejection of the UF membranes were very low. Therefore, it was decided to use the prepared PW directly as feed for UF membranes.

Table 4.4: UF 0.04 μm permeate characteristics and rejection percentages (MF 0.1 μm and UF 0.04 μm membranes in series)

Parameter	Feed: Permeate of MF 0.1 μm	Permeate (UF 0.04 μm)	Rejection (%)
TOC (mg/L)	1.384	0.9621	30.5
IC (mg/L)	19.04	18.87	0.9
COD (mg/L)	450	351	22.0
TDS (ppt)	10.05	10.01	0.4
Conductivity (mS/m)	20.45	20.03	2.1
Turbidity (NTU)	0.6	0.2	66.7
Salinity (%)	39.9	39.0	2.3

Table 4.5: UF 150 KDa permeate characteristics and rejection percentages (MF 0.1 μm and UF 150 KDa membranes in series)

Parameter	Feed: Permeate of MF 0.1 μm	Permeate (UF 150 KDa)	Rejection (%)
TOC (mg/L)	1.849	0.9719	47.4
IC (mg/L)	19.15	18.84	1.6
COD (mg/L)	409	350	14.4
TDS (ppt)	10.8	10.33	4.4
Conductivity (mS/m)	21.42	20.74	3.2
Turbidity (NTU)	0.75	0.05	93.3
Salinity (%)	42.1	40.5	3.8

4.1.3 Ultrafiltration

The permeate fluxes versus time for the two UF membranes were presented in Figure 4.2. The initial flux of the UF 0.04 μm SiC membrane was about 5 times the initial flux of the UF 150 KDa TiO_2/ZrO_2 membrane. From the Figure 4.2, it may seem that the percentage flux reduction for the UF 0.04 μm SiC membrane is higher than that of UF 150 KDa TiO_2/ZrO_2 membrane. But in calculation, there was about 30% and 38% flux reductions for the UF 0.04 μm SiC membrane and UF 150 KDa TiO_2/ZrO_2 membrane, respectively. This misreading of graph is due to higher initial flux of the UF 0.04 μm SiC membrane. The permeate flux of both of the membranes had a rapid reduction in about the first 25 min of filtration and then they reached to steady flux values. The final flux of the UF 0.04 μm SiC membrane was about 5.8 times the final flux of UF 150 KDa TiO_2/ZrO_2 membrane.

The permeate qualities of the two UF membranes were presented in Table 4.6 and Table 4.7. The percentages of rejection for both of the UF membranes were very close to each other. The rejection percentages for TOC,

COD and turbidity of UF 0.04 μm SiC membrane were about 96.9%, 76.2% and 100%, respectively. The rejection percentages for TOC, COD and turbidity of UF 150 KDa TiO_2/ZrO_2 membrane were about 97.7%, 78.0% and 99.8%, respectively. The salt rejection for both of the UF membranes was very low.

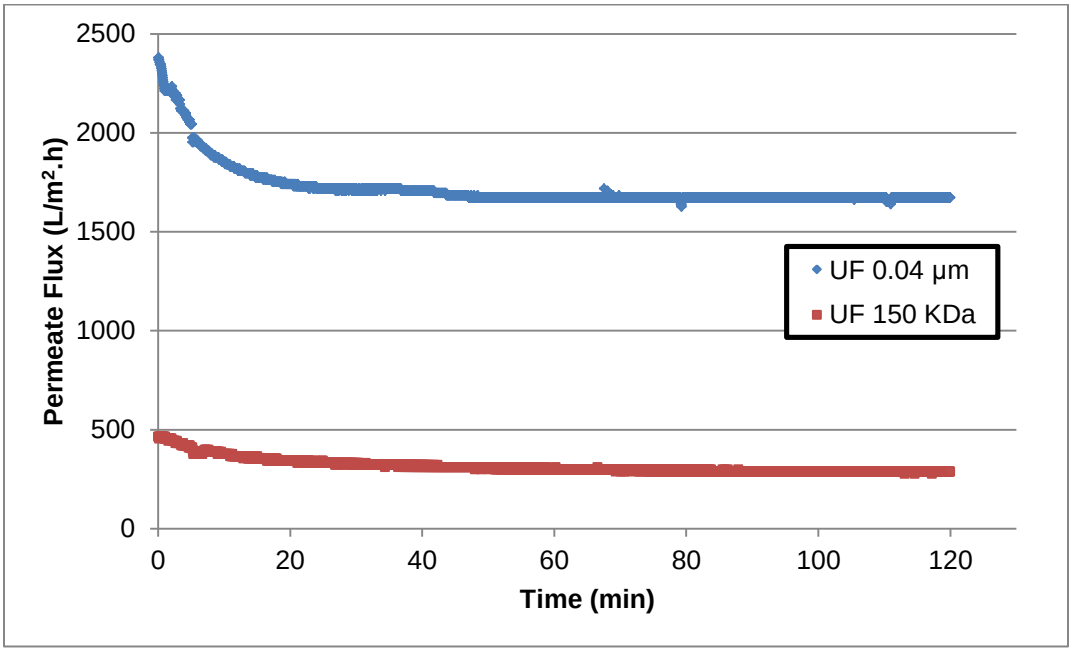

Figure 4.2: MF membranes permeate fluxes versus time (UF 0.04 µm and UF 150 KDa membranes) [original in color]

Table 4.6: UF 0.04 µm permeate characteristics and rejection percentages, PW filtration at CFV of 1 m/s and TMP of 0.8 bar

Parameter	Permeate	Rejection (%)
TOC (mg/L)	2.223	96.9
IC (mg/L)	18.15	10.4
COD (mg/L)	387	76.2
TDS (ppt)	10.35	0.4
Conductivity (mS/m)	20.6	0.6
Turbidity (NTU)	0	100.0
Salinity (%)	40.45	0.4

Table 4.7: UF 150 KDa permeate characteristics and rejection percentages, PW filtration at CFV of 1 m/s and TMP of 2 bars

Parameter	Permeate	Rejection (%)
TOC (mg/L)	1.702	97.7
IC (mg/L)	16.61	18.0
COD (mg/L)	359	78.0
TDS (ppt)	10.35	0.4
Conductivity (mS/m)	20.69	0.1
Turbidity (NTU)	0.1	99.8
Salinity (%)	40.5	0.3

Table 4.8 presents the COD and TOC of the UF 0.04 μm SiC membrane permeate with two different feeds tested. It was found that the COD and TOC were slightly higher for the time when synthetic PW was filtered than filtration of permeate of MF 0.1 μm SiC membrane. This may be due to penetration of more contaminants through the membrane when synthetic PW was used as feed than the time when permeate of the selected MF membrane was tested as feed for UF 0.04 μm SiC membrane.

Table 4.8: Permeate characteristics of UF 0.04 μm membrane with two different feeds

Parameter	Permeate of UF 0.04 μm SiC membrane with two different feeds	
	Feed: Permeate of MF 0.1 μm	Feed: Synthetic PW
COD (mg/L)	351	387
TOC (mg/L)	0.9621	2.223

The COD and TOC of permeate of UF 150 KDa TiO_2/ZrO_2 membrane with the two tested feeds are presented in Table 4.9. It was found that the COD and TOC of the permeate of the two tests were very close to each other, and the permeate

quality of UF 150 KDa TiO_2/ZrO_2 membrane did not change very much with changes in feed characteristics.

Table 4.9: Permeate characteristics of UF 150 KDa membrane with two different feeds

Parameter	Permeate of UF 150 KDa TiO_2/ZrO_2 membrane with two different feeds	
	Feed: Permeate of MF 0.1 μm	Feed: Synthetic PW
COD (mg/L)	350	359
TOC (mg/L)	0.9719	1.702

It was found that the permeate flux of the UF 0.04 μm SiC membrane was higher than that of UF 150 KDa TiO_2/ZrO_2 membrane. It should be noted that the UF 150 KDa membrane was operated at 2 bars, whereas the UF 0.04 μm membrane was tested at a lower TMP (0.8 bar). The UF 0.04 μm SiC membrane had a larger pore size and a high porosity of about 45%, and this may be the cause of the higher permeate flux for this membrane which compensated the operation at a lower TMP. Some other factors like a higher surface hydrophilicity of the UF 0.04 μm membrane (made from SiC) than the UF 150 KDa membrane (support: TiO_2 and active layer: ZrO_2) may cause a higher permeate flux for UF 0.04 μm SiC membrane.

Both of the tested UF membranes had similar permeate qualities. Therefore, the UF 0.04 μm SiC membrane was chosen as the best UF membrane tested with the synthetic PW since it had higher permeate flux.

4.2 Investigation of effect of operating conditions for selected membranes

4.2.1 Microfiltration

It was found that the MF 0.1 μm SiC membrane had a better performance in filtration of synthetic PW compared to MF 0.3 μm TiO2/ZrO2 membrane. The permeate quality of both of the membranes were very close to each other, but the MF 0.1 μm SiC membrane had higher permeate flux than MF 0.3 μm TiO_2/ZrO_2 membrane. Therefore, this membrane was chosen as the best MF membrane tested. To find out how the permeate quality and permeate flux changes when there is a change in the operating condition of filtration, the selected MF membrane was tested at various TMPs and CFVs.

4.2.1.1 Effect of TMP

The MF 0.1 μm SiC membrane was tested at CFV of 1 m/s and TMP of 0.4, 0.6 and 0.8 bar. Figure 4.3 presents the permeate flux of this membrane at different TMPs mentioned. It was found that the MF 0.1 μm SiC membrane had the highest permeate flux at TMP of 0.8 bar. The initial permeate flux of this membrane at TMP of 0.8 bar was about 1.2 and 2.1 times the permeate flux at TMP of 0.6 and 0.4 bar, respectively.

The permeate flux curves of filtration at all the three TMPs have similar shape and trend. At all three TMPs tested, the permeate flux had a very rapid decrease in about 4 min. Then, the degree of permeate flux decrease were lowered, and fluxes gradually decreased to about 20 min of operation, reaching to steady values. The final permeate flux at TMP of 0.8 bar was about 1.8 and 2.6 of fluxes at TMP of 0.6 and 0.4 bar, respectively. The permeate flux decrease percentages

were about 31%, 54% and 44% at TMPs of 0.8, 0.6 and 0.4 bar, respectively, which seems that the filtration at the TMP of 0.8 bar had the lowest permeate flux decline.

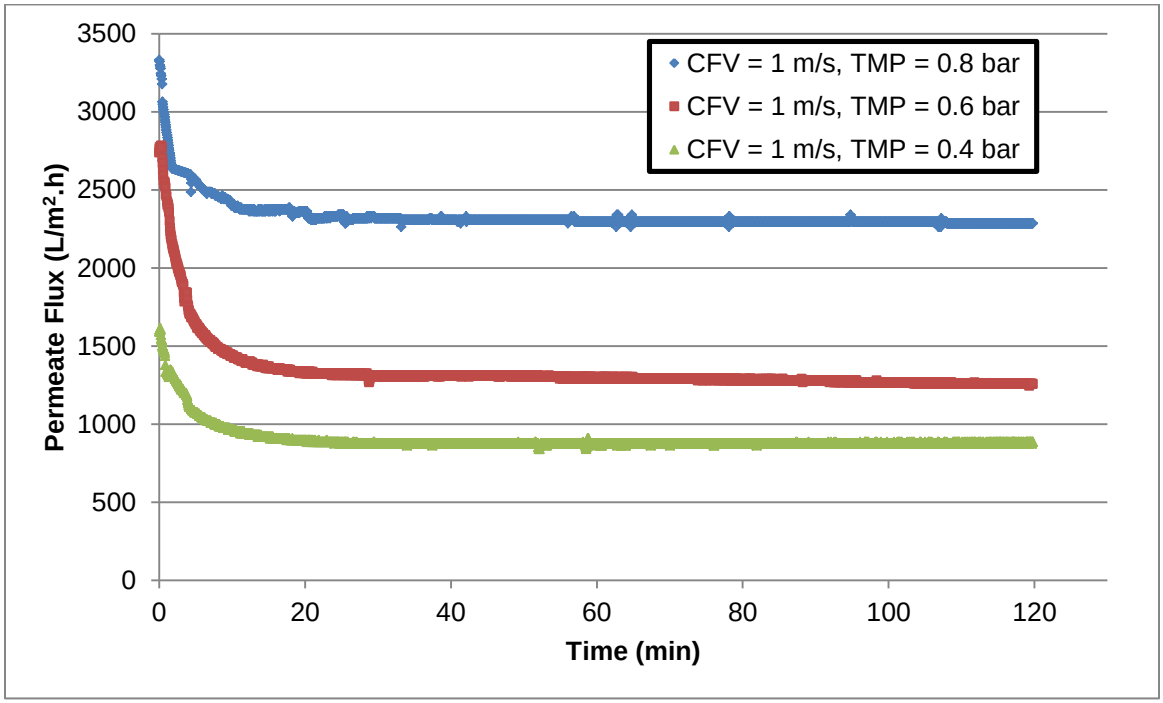

Figure 4.3: MF 0.1 µm membrane permeate fluxes versus time at different TMPs [original in color]

The permeate characteristics of the MF 0.1 µm SiC membrane at CFV of 1 m/s and TMPs of 0.4, 0.6 and 0.8 bar were presented in Table 4.10. TOC, oil content and turbidity rejections of this membrane slightly changed at different TMPs. COD had the highest changes among the other parameters at different TMPs. The COD values were 342, 319 and 450 mg/L at TMPs of 0.4, 0.6 and 0.8 bar, respectively. The oil content rejection percentages were relatively constant at different TMPs. The oil rejections were 95.9%, 97.7% and 95.6% at TMPs of 0.4, 0.6 and 0.8 bar, respectively. The salt rejection percentages of the membrane were very low for all TMPs tested.

Table 4.10: MF 0.1 μm permeate characteristics and rejection percentages, at CFV of 1 m/s and TMPs of 0.4, 0.6 and 0.8 bar

Parameter	TMP = 0.4 bar		TMP = 0.6 bar		TMP = 0.8 bar	
	Permeate	Rejection (%)	Permeate	Rejection (%)	Permeate	Rejection (%)
Oil content (ppm)	4.8	95.9	2.7	97.7	5.2	95.6
TOC (mg/L)	1.253	98.3	1.786	97.5	1.384	98.1
IC (mg/L)	17.63	12.9	10.37	48.8	19.04	6.0
COD (mg/L)	342	79.0	319	80.4	450	72.4
TDS (ppt)	10.13	2.5	10.26	1.3	10.05	3.3
Conductivity (mS/m)	19.92	3.8	20.26	2.2	20.45	1.3
Turbidity (NTU)	0.1	99.8	0.1	99.8	0.6	99.0
Salinity (%)	39.9	1.8	40.6	0.0	39.9	1.8

Since the permeate quality of the MF 0.1 μm SiC membrane at all the TMPs tested were similar and this membrane had the highest permeate flux at the TMP of 0.8 bar, the TMP of 0.8 bar was chosen as the best TMP for this membrane.

4.2.1.2 Effect of CFV

The effect of CFV on the performance of the MF 0.1 μm SiC membrane was investigated. Therefore, the membrane was operated at the selected TMP (0.8 bar) and three CFVs including 0.5, 1 and 1.5 m/s. The permeate flux of this membrane at different CFVs mentioned were presented in Figure 4.4. It was found that the initial permeate flux of the three tests at different CFVs and TMP of 0.8 bar was about the same value. This may be due to operation at a unit TMP (0.8 bar) as the driving force for permeation of water through the membrane. But the flux decrease at the three CFVs was slightly different. In the early 4 min. of the test, there was a rapid flux decline for CFV 1.5 m/s, but for CFV of 1 m/s, the rapid flux decrease was only for the first 2 min. of the test and then the flux decreased gradually and finally, it reached to a steady value after about 15 min.

of the test. For CFV of 0.5 m/s, the sharp flux decrease lasted for about 5 min. and then a gradual permeate flux decrease was observed, and it reached to a steady value after about 16 min. of the operation. It was noticed that the CFV of 1.5 m/s needed the longest time to have a steady permeate flux value. The final flux at the CFVs of 1 and 1.5 m/s were very close to each other, but the final flux at the CFV of 0.5 m/s was very lower (about 70% of the final flux at CFV of 1 m/s). This may be due to higher fouling rate at the lowest CFV (0.5 m/s). The permeate flux decrease percentages were 30%, 31% and 52% at CFVs of 1.5, 1 and 0.5 m/s, respectively.

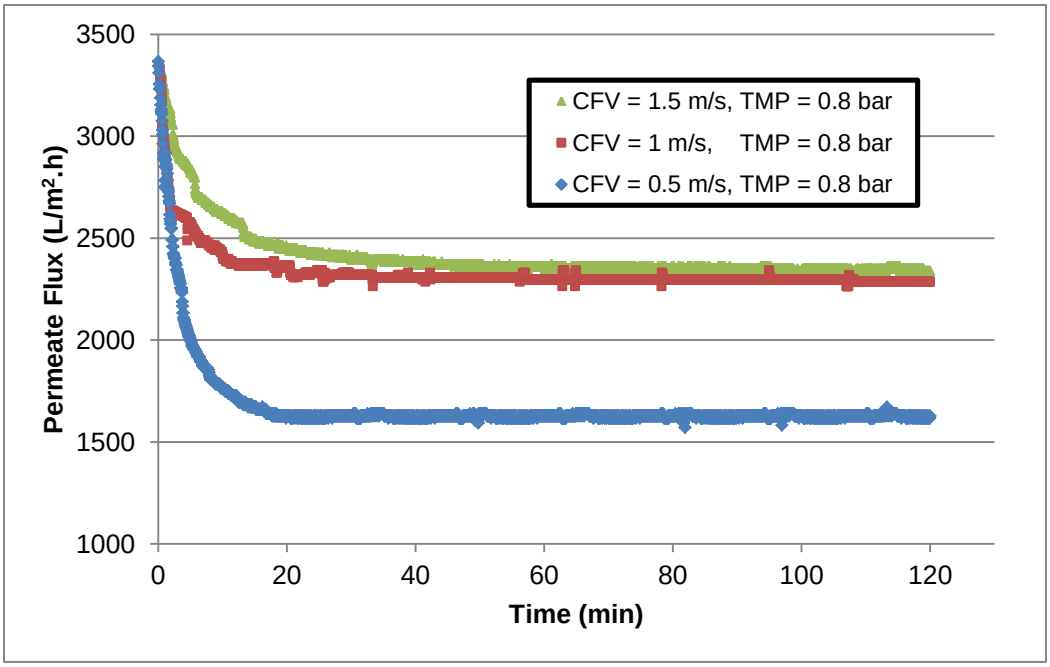

Figure 4.4: MF 0.1 µm membrane permeate fluxes versus time at different CFVs [original in color]

The permeate characteristics of MF 0.1 µm SiC membrane at TMP of 0.8 bar and CFVs of 0.5, 1 and 1.5 m/s are presented in Table 4.11. The oil content, TOC and turbidity rejections at the three tested CFVs were similar. The TOC

concentration at CFV of 1 m/s and TMP of 0.8 bar had the lowest value (1.384 mg/L). However, the COD concentration at this operating condition was the highest value (450 mg/L) compared to other CFVs tested (350 and 364 mg/L at CFVs of 0.5 and 1.5 m/s, respectively). The salt rejections at three CFVs tested were very low.

Based on the results, the CFV of 1 m/s and TMP of 0.8 bar was selected for the MF 0.1 μm SiC membrane since the permeate flux of the membrane at CFV of 1.5 m/s was just slightly higher than the flux at CFV of 1 m/s, and the permeate flux at CFV of 0.5 m/s was much lower than that of 1 m/s CFV. The permeate qualities at the three tested CFVs were similar. The oil content of the permeates were about 5 mg/L at CFVs of 0.5 and 1 m/s and 3 mg/L at CFV of 1.5 m/s. The highest TOC rejection pertains to the CFV of 1 m/s and TMP of 0.8 bar. However, only the COD rejection at CFV of 1 m/s (72.4%) was slightly lower than CFVs of 0.5 and 1.5 m/s (78.5% and 77.6%, respectively).

Table 4.11: MF 0.1 µm permeate characteristics and rejection percentages, at TMP of 0.8 bar and CFVs of 0.5, 1 and 1.5 m/s

Parameter	CFV = 0.5 m/s		CFV = 1 m/s		CFV = 1.5 m/s	
	Permeate	Rejection (%)	Permeate	Rejection (%)	Permeate	Rejection (%)
Oil content (ppm)	5.1	95.7	5.2	95.6	3	97.4
TOC (mg/L)	2.582	96.4	1.384	98.1	2.199	97.0
IC (mg/L)	18.20	10.1	19.04	6.0	18.34	9.4
COD (mg/L)	350	78.5	450	72.4	364	77.6
TDS (ppt)	10.23	1.6	10.05	3.3	10.29	1.0
Conductivity (mS/m)	20.29	2.1	20.45	1.3	20.38	1.6
Turbidity (NTU)	0.2	99.7	0.6	99.0	0.1	99.8
Salinity (%)	40.6	0.0	39.9	1.8	40.6	0.0

4.2.2 Ultrafiltration

4.2.2.1 Effect of TMP

The permeate fluxes versus time for operation of UF 0.04 μm SiC membrane at different TMPs including 0.8, 0.6 and 0.4 bar and CFV of 1 m/s were presented in Figure 4.5. It was found that the permeate flux at TMP of 0.8 bar and CFV of 1 m/s had the highest value for the entire period of operation compared to other two TMPs (0.6 and 0.4 bar). The initial permeate flux at TMP of 0.8 bar was about 1.3 and 2.0 times the permeate fluxes at TMP of 0.6 and 0.4 bar, respectively. The permeate flux curve for TMPs of 0.8 and 0.6 bar had very similar trend and the permeate fluxes decreased at the early stages of the test (about 7 min.), and then flux decreased gradually. For TMP of 0.8 bar, the permeate flux reached to a steady value after about 22 min. of the test while the permeate flux for TMP of 0.6 bar had a continuous gradual declination for the entire test period. For TMP of 0.4 bar, a rapid flux declination was not found and after a gradual flux decrease for about 24 min., the permeate flux reached to a steady value. The final flux at TMP of 0.8 bar was about 1.3 and 1.6 times the permeate fluxes at TMP of 0.6 and 0.4 bar, respectively. The percentages of permeate flux decrease were 30%, 30% and 13% at TMPs of 0.8, 0.6 and 0.4 bar, respectively.

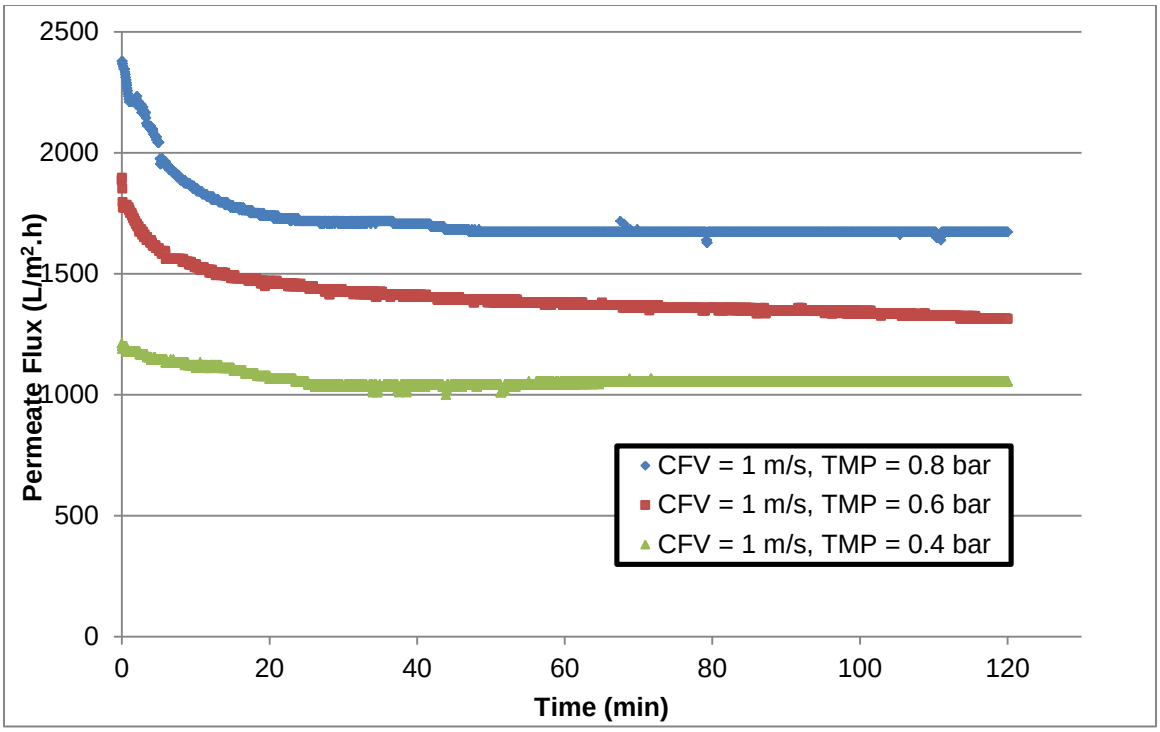

Figure 4.5: UF 0.04 µm membrane permeate fluxes versus time at different TMPs [original in color]

The permeate characteristics of the UF 0.04 µm SiC membrane at different TMPs are presented in Table 4.12. It was found that the TOC, COD and turbidity of the permeate at all TMPs were similar. The COD rejection at TMP of 0.8 bar (76.2%) was slightly lower than the COD rejections at TMPs of 0.6 and 0.4 bar (77.0% and 77.2%, respectively). This may be due to the penetration of more contaminants at higher pressures. The salt rejections at all TMPs tested were very low.

Table 4.12: UF 0.04 μm permeate characteristics and rejection percentages, at CFV of 1 m/s and TMPs of 0.4, 0.6 and 0.8 bar

Parameter	TMP = 0.4 bar		TMP = 0.6 bar		TMP = 0.8 bar	
	Permeate	Rejection (%)	Permeate	Rejection (%)	Permeate	Rejection (%)
TOC (mg/L)	2.140	97.0	2.020	97.2	2.223	96.9
IC (mg/L)	13.01	35.7	13.75	32.1	18.15	10.4
COD (mg/L)	372	77.2	374	77.0	387	76.2
TDS (ppt)	10.37	0.2	10.31	0.8	10.35	0.4
Conductivity (mS/m)	20.72	0.0	20.61	0.5	20.6	0.6
Turbidity (NTU)	0.1	99.8	0.1	99.8	0	100.0
Salinity (%)	40.55	0.2	40.52	0.2	40.45	0.4

The permeate qualities of UF 0.04 μm SiC membrane were similar for all TMPs tested but the permeate flux was highly dependent on the TMP value. The TMP of 0.8 bar had higher permeate flux than the TMPs of 0.6 and 0.4 bar. Therefore, the TMP of 0.8 bar at CFV of 1 m/s was chosen as the most suitable TMP for the UF 0.04 μm SiC membrane.

4.2.2.2 Effect of CFV

The permeate flux curves of UF 0.04 μm SiC membrane at CFVs of 0.5, 1 and 1.5 m/s and TMP of 0.8 bar were presented in Figure 4.6. It was found that the permeate fluxes at different CFVs started from a similar point which may be due to operation at a unit TMP (0.8 bar). The permeate flux curves had a very similar trend except for CFV of 0.5 m/s which had a very sharp flux decrease for the first 15 min. of the test, and then the flux gradually decreased for the entire test period. This may be due to very low CFV chosen (0.5 m/s) which caused very high fouling rate that continuously decreased the permeate flux for the entire

test period. But for CFVs of 1.5 and 1 m/s, there was a sharp permeate flux reduction for about the early 5 min. of the test, and then the flux gradually decreased for more 18 min. when it reached to steady values. This may be due to better membrane surface washing at higher CFVs which caused lower membrane fouling and lower flux reduction. However, the difference between the final permeate fluxes at CFVs of 1.5 m/s and 1 m/s was not very large. But the final permeate flux at CFV of 0.5 m/s was much lower than CFVs of 1.5 and 1 m/s. The CFV of 0.5 m/s with 79% flux reduction percentage had the highest flux reduction. The CFVs of 1 and 1.5 m/s with flux reduction percentages of 30% and 22%, respectively, came after CFV of 0.5 m/s.

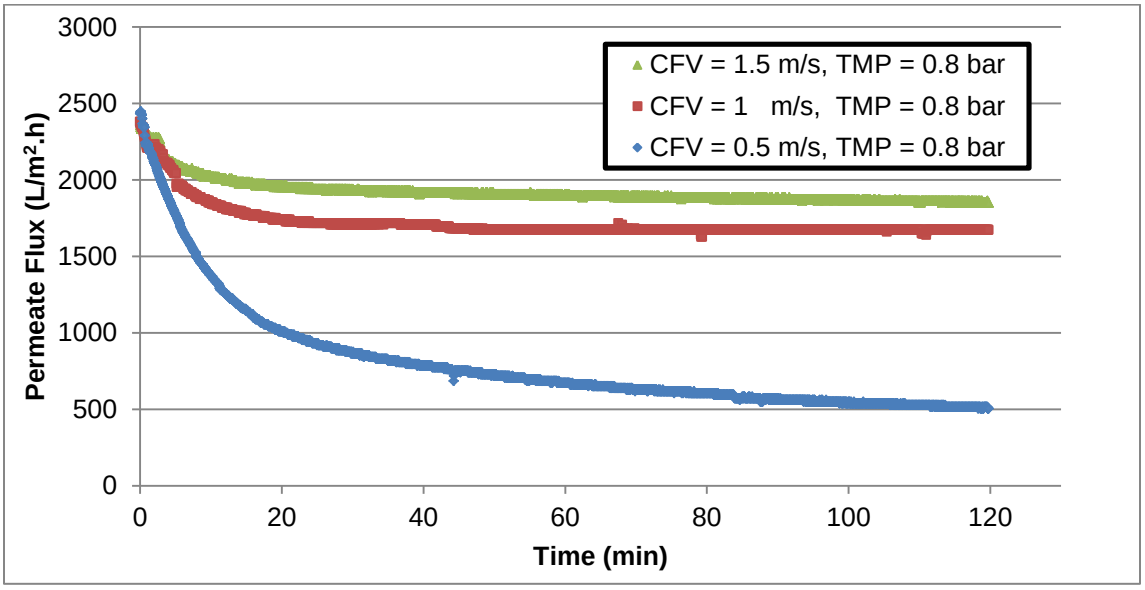

Figure 4.6: UF 0.04 µm membrane permeate fluxes versus time at different CFVs [original in color]

The permeate characteristics of UF 0.04 µm SiC membrane at different CFVs were presented in Table 4.13. The TOC and turbidity rejections were similar at all the CFVs but it was found that the COD rejection decreased as CFV increased.

This may be due to higher flux of contaminants through the membrane at higher CFVs. The salt rejection was very low at all the CFVs.

Table 4.13: UF 0.04 μm permeate characteristics and rejection percentages, at CFVs of 0.5, 1 and 1.5 m/s and TMP of 0.8 bar

Parameter	CFV = 0.5 m/s		CFV = 1 m/s		CFV = 1.5 m/s	
	Permeate	Rejection (%)	Permeate	Rejection (%)	Permeate	Rejection (%)
TOC (mg/L)	2.786	96.2	2.223	96.9	2.513	96.5
IC (mg/L)	16.35	19.2	18.15	10.4	13.05	35.5
COD (mg/L)	364	77.6	387	76.2	410	74.8
TDS (ppt)	10.19	1.9	10.35	0.4	10.15	2.3
Conductivity (mS/m)	20.28	2.1	20.6	0.6	20.29	2.1
Turbidity (NTU)	0.05	99.9	0	100.0	0.1	99.8
Salinity (%)	39.7	2.2	40.45	0.4	39.7	2.2

Based on the results, the CFV of 1 m/s at TMP of 0.8 bar was selected for UF 0.04 μm SiC membrane since the permeate flux at CFV of 1.5 m/s was slightly higher than the CFV of 1 m/s, and the permeate flux at CFV of 0.5 m/s was very low, and it had high fouling rate as well. The permeate qualities for all the CFVs were similar and the COD concentration at CFV of 1 m/s (387 mg/L) was smaller than the COD at a CFV of 1.5 m/s (410 mg/L).

4.3 Membrane fouling and cleaning

In this study, three different membrane cleaning methods including chemical cleaning, backwashing and backpulsing were used to clean the fouled membranes. In the chemical cleaning method, also called cleaning-in-place (CIP), sodium hydroxide as base at three concentrations and nitric acid at three

concentrations was used to find out the effect of the acid and base concentrations on the membrane cleaning extent. The backwashing and backpulsing have also been used to determine the feasibility of using these technologies for the recovery of the membrane permeate.

4.3.1 Effect of chemical cleaning on permeate flux recovery

As described earlier, three base concentrations including 2%, 3% and 4% at a constant acid concentration of 2% were used for the chemical cleaning of membrane. The RO water flux of the clean membrane which is called initial RO water flux (J_{wi}) was measured before the membrane fouling. Then, the membrane was fouled for 2 hours at a constant condition described in experimental section. The RO water flux of the fouled membrane (J_{ww}) was measured and the membrane was cleaned using a base and an acid concentration, and finally the RO water flux of the cleaned membrane was measured (J_{wc}). Based on the measured RO water fluxes, the following equation was used to calculate the flux recovery (FR) in percentage at different concentrations of base and acid:

$$FR(\%) = \frac{J_{wc} - J_{ww}}{J_{wi} - J_{ww}} \times 100 \quad (4.2)$$

The measured RO water fluxes needed for calculation of flux recovery at different base concentrations and an acid concentration of 2% was presented in Table 4.14 and the calculated flux recoveries were presented in Figure 4.7.

Table 4.14: Calculation of the effect of NaOH concentration on flux recovery (%)

	Acid=2%, Base=4%	Acid=2%, Base=3%	Acid=2%, Base=2%
J_{wi}	2368	2368	2368
J_{ww}	909	932	1077
J_{wc}	2256	2166	2121
FR(%)	92	86	81

The calculated flux recoveries at different base concentrations of 2%, 3% and 4% were 81%, 86% and 92%, respectively. It seems that the flux recovery of the membrane increases as the base concentration increases from 2% to 4% at a constant acid concentration of 2%. Therefore, the base concentration of 4% was selected as it had the highest flux recovery percentage from the base concentrations studied.

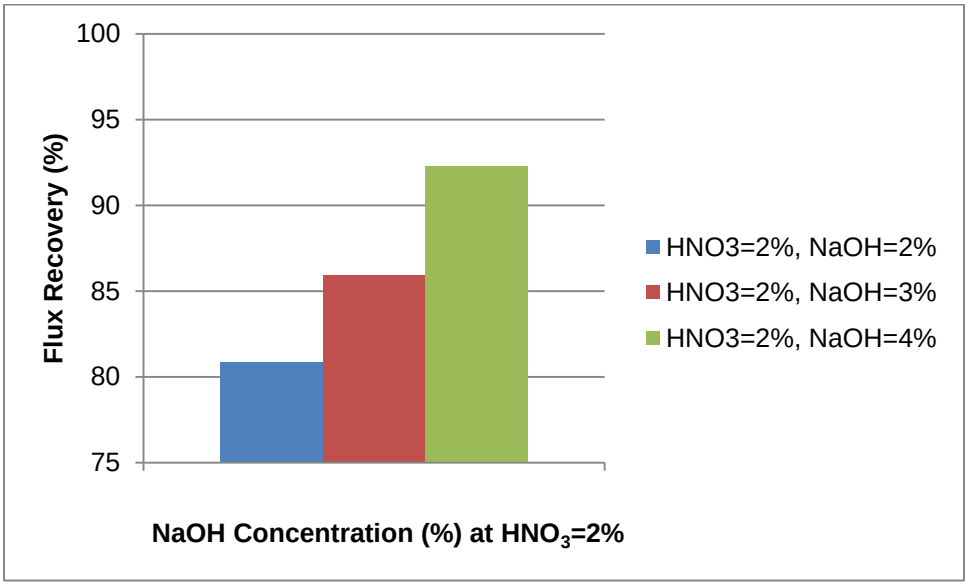

Figure 4.7: Effect of NaOH concentration on flux recovery (%) [original in color]

The selected base concentration of 4% and three acid concentrations of 2%, 3% and 4% were used to clean the fouled membrane. Table 4.15 presents the RO water fluxes measured to calculate the flux recoveries and the calculated flux recovery percentages were presented in Figure 4.8. The flux recoveries were 92%, 95% and 97% for acid concentrations of 2%, 3% and 4%, respectively. It was found that the flux recovery increased with the increase in acid concentration. The highest flux recovery percentage (97%) was related to the acid and base concentrations of 4% and 4%. The difference between the flux recovery percentages at different acid concentrations were small, and it was possible to select the lowest or the medium acid concentration as the optimum acid concentration, but the highest acid concentration was chosen since mixing the used 4% acid solution with the used 4% base solution after the chemical cleaning gave a more neutral solution.

Table 4.15: Calculation of the effect of HNO_3 concentration on flux recovery (%)

	Acid=4%, Base=4%	Acid=3%, Base=4%	Acid=2%, Base=4%
J_{wi}	2368	2368	2368
J_{ww}	1021	1190	909
J_{wc}	2334	2312	2256
FR(%)	97	95	92

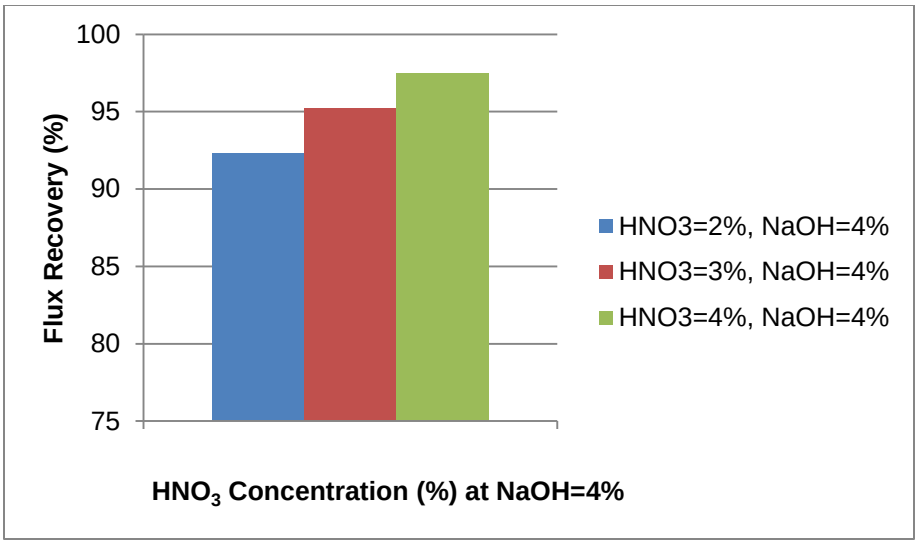

Figure 4.8: Effect of HNO_3 concentration on flux recovery (%) [original in color]

In addition to the measured RO water fluxes mentioned earlier, the cleaned membrane with different acid and base concentrations was tested with PW and the permeate flux of the membrane was measured for 2 hours. Figure 4.9 presents the permeate flux of the UF 0.04 µm SiC membrane cleaned with different acid and base concentrations. It was found that the permeate flux of PW filtration at the highest acid and base concentrations had the highest permeate flux of PW which was also in accordance with the flux recovery percentages calculated.

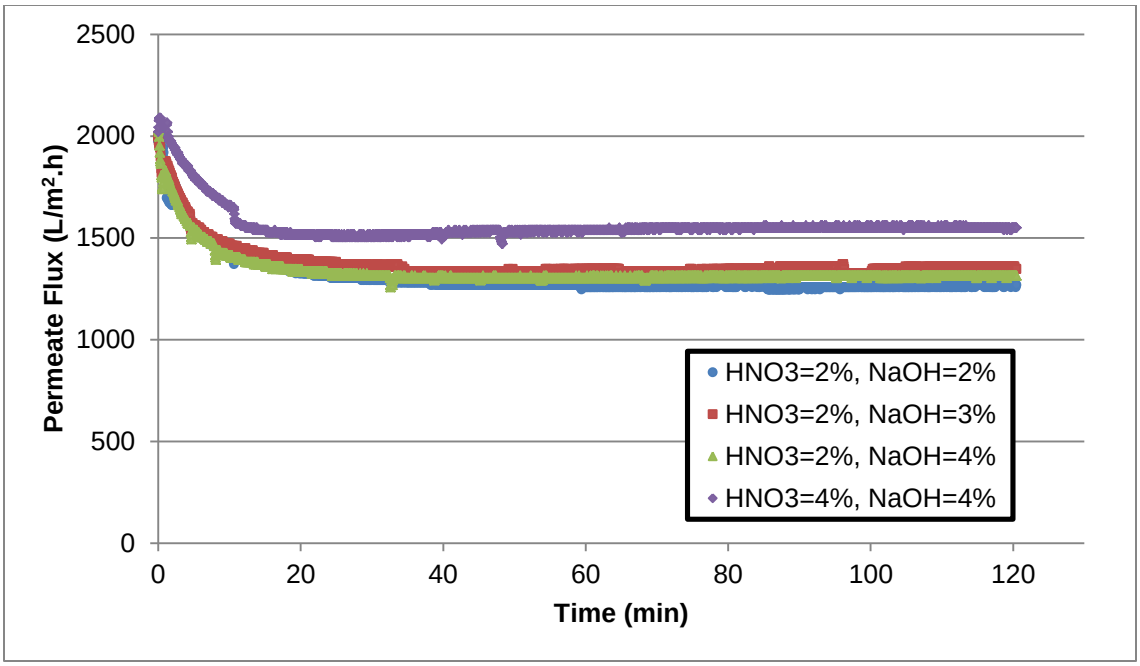

Figure 4.9: Effect of HNO_3 and NaOH concentrations on permeate flux of UF 0.04 µm membrane [original in color]

4.3.2 Effect of backwashing on permeate flux recovery

Backwashing method was applied to recover the permeate flux of the UF 0.04 µm SiC membrane during the filtration. As described earlier, the filtration has to be stopped, in this method, for a few seconds, and the collected permeate in the backwash tank (03T01) was used to flow in the reverse direction through the membrane for the desired backwash period (5 seconds in this study). Then the filtration is started again, and the rejected and fouled materials on the surface of the membrane were washed by the cross flow of feed across the surface of the membrane. The frequency of backwashing was set to 10 min. and the filtration was performed for 2 hours. Figure 4.10 presents the permeate flux of the UF 0.04 µm SiC membrane with the PW used as feed both with backwashing and without backwashing at TMP of 0.8 bar and CFV of 1 m/s. It was found that backwashing could successfully recover the flux of the membrane. It was found

that when filtration was used without any backwashing the permeate flux sharply decreased in about 10 min. of the test and the filtration continued for the rest of filtration period with a lower permeate flux value. It seems that backwashing was a suitable method to recover the permeate flux during the filtration. There was no need to shut down the filtration, and it required only to pause the filtration for a few seconds. It was found that the filtration was paused for about 30 seconds (when backwashing period was set to 5 seconds) during the backwashing which is a short time compared to the time needed for chemical cleaning method. Backwashing uses some volume of the permeate in the backwash tank to reverse the flow. This was one of the drawbacks of this method since the permeate generation needed time and energy and it also fouled the membrane.

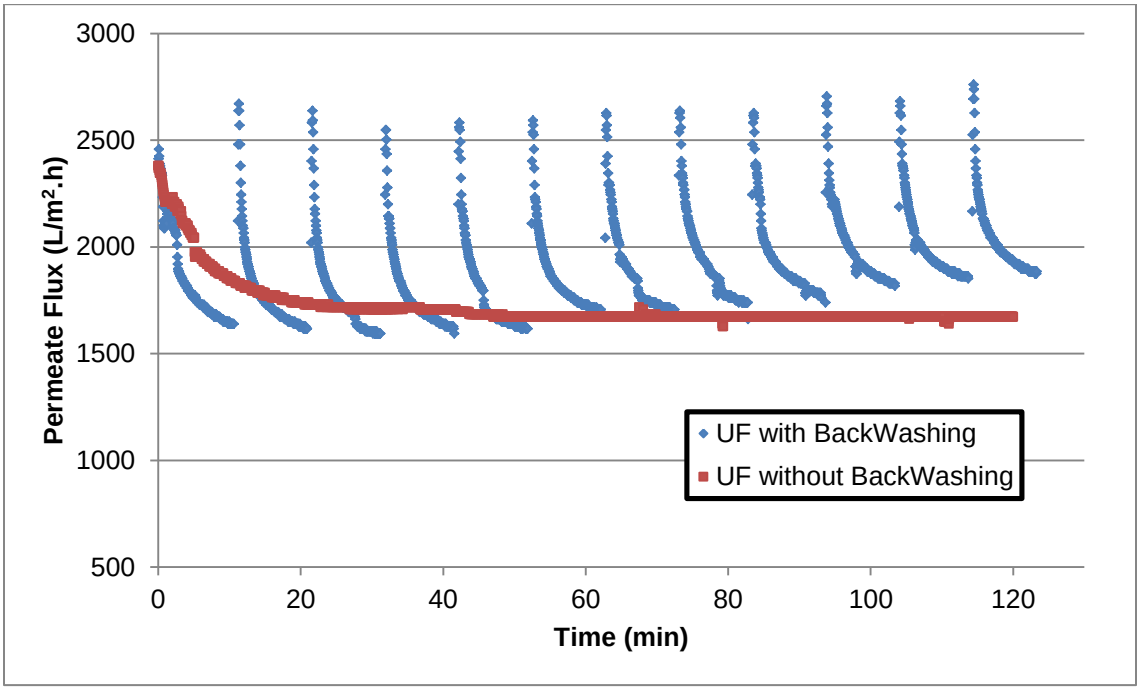

Figure 4.10: Comparison of UF 0.04 µm membrane filtration with and without backwashing [original in color]

4.3.3 Effect of backpulsing on permeate flux recovery

The same membrane (UF 0.04 µm SiC membrane) was used for filtration of PW at the same operating conditions (TMP of 0.8 bar and CFV of 1 m/s). But this time, the backpulsing method was used to recover the permeate flux of the membrane. The backpulsing frequency was set to 10 min. like the frequency used for backwashing in order to compare the results of backwashing and backpulsing. Filtration with backpulsing lasted for 2 hours. Figure 4.11 is a plot showing the permeate fluxes of filtration with and without backpulsing. It is evident that backpulsing could recover the flux of the fouled membrane but the permeate flux of the membrane decreased sharply in about 3 min. after each backpulse.

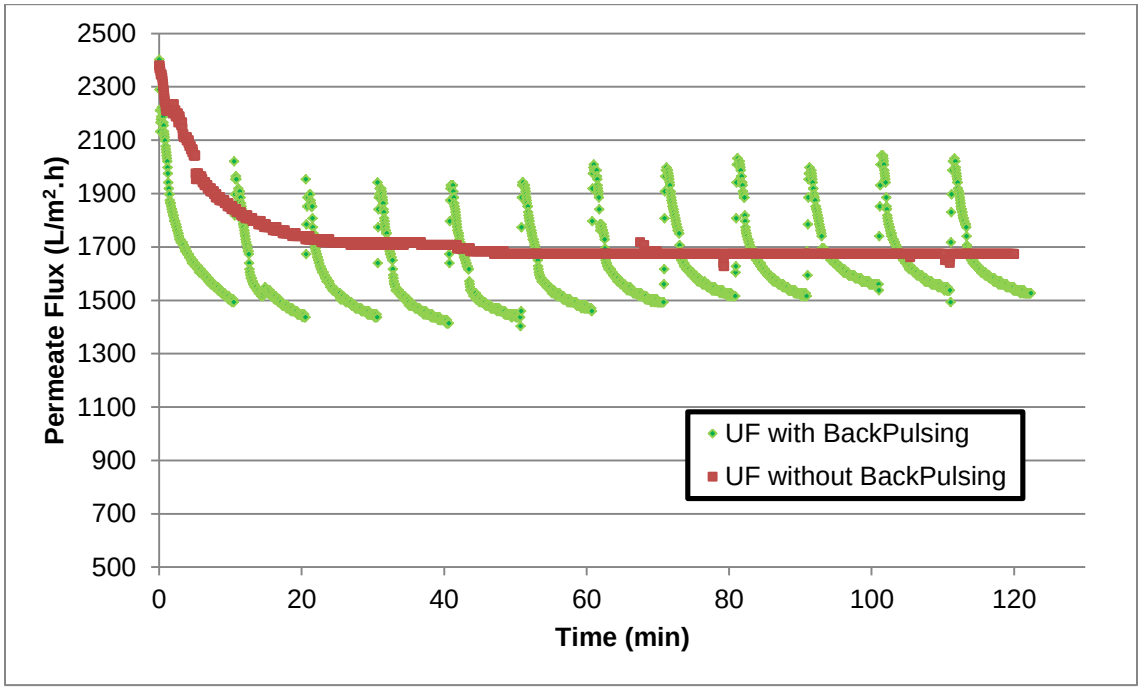

Figure 4.11: Comparison of UF 0.04 µm membrane filtration with and without backpulsing [original in color]

The permeate fluxes versus time of the filtration using backwashing (blue) and backpulsing (green) are presented in Figure 4.12. It was found that the backwashing method had better performance in recovering the permeate flux of the membrane compared to the backpulsing method. The initial permeate fluxes after backwashing were always higher than the initial permeate fluxes after backpulsing. This may be due to a better membrane cleaning using the backwashing. The permeate fluxes after backwashing were also higher than that of after backpulsing for all the 10 min filtration periods.

However, backwashing used more permeate than backpulsing. The backwashing method reversed the permeate flow from the backwash tank, which has collected the permeate during filtration through the membrane for the specified period (5 seconds in this study). However, backpulsing uses a much smaller volume of permeate, collected in the backpulse hammer empty space, to reverse the flow for a very short time (less than 1 second).

By comparing the permeate flux of filtration using backpulsing and filtration without backpulsing (presented in Figure 4.11), it seems that a shorter backpulsing interval may be a better solution since the permeate flux after backpulsing decreased sharply after about 3 min. of filtration. As the backpulsing method used less volume of generated permeate, it may be better to reduce the backpulse interval to about 3 min.

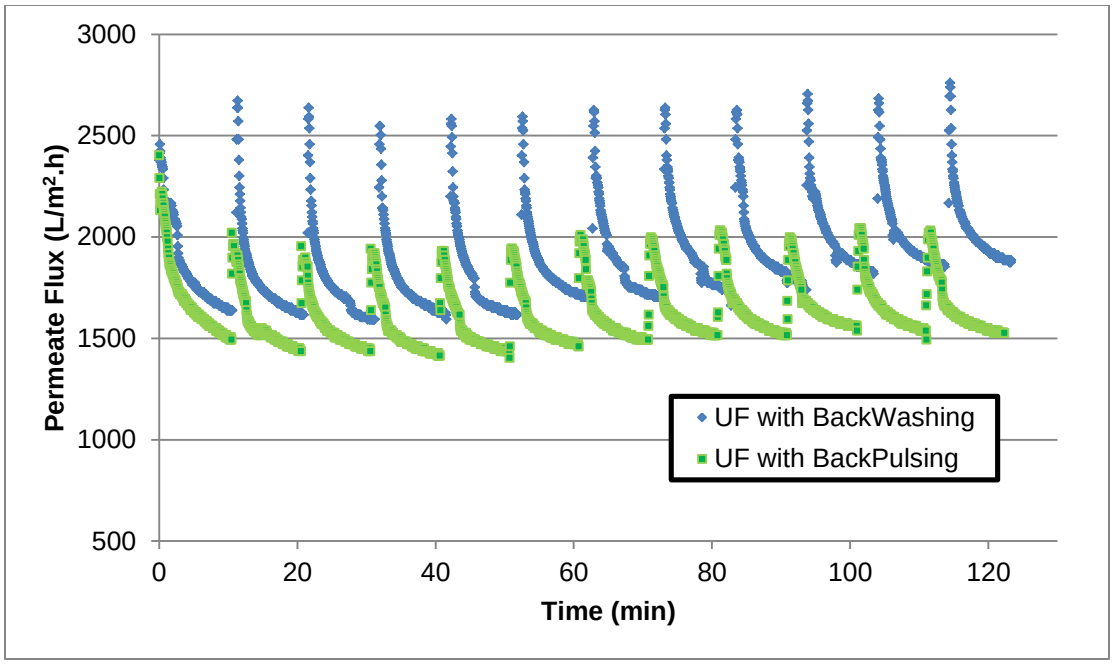

Figure 4.12: Comparison of UF 0.04 µm membrane filtration with backwashing and backpulsing [original in color]

4.3.4 Fouling mechanism of MF and UF treatment of PW

The fouling mechanisms in microfiltration and ultrafiltration of the prepared PW were investigated by Hermia's models. The experimental data were fitted to these models to find out if fouling phenomenon was cake layer formation or pore blocking. Pore blocking may happen inside (standard blocking) or outside the pores (complete blocking and intermediate blocking). When standard blocking occurs, solute molecules penetrate through the membrane pores but if molecules have similar size to the size of membrane pores, the solutes may partially penetrate the membrane pores and cause intermediate blocking. If the solute sizes are bigger than the membrane pores, they cause complete blocking (Vincent Vela et al., 2008).

4.3.4.1 MF membranes

The permeate flux of PW filtration with the two MF membranes were predicted by Hermia's models and presented in Figure 4.13. The R^2 values of the fitted models were also presented in Table 4.16. In the case of MF 0.3 μm TiO_2/ZrO_2 membrane, it was found that the cake layer formation had the highest R^2 value (0.656) and after that, intermediate blocking with a R^2 value of 0.635 had the best fitting. It should be mentioned that comparison of the fitting with the graphs was a little bit difficult since the graph scales were different due to different ranges of the data plotted. Therefore, the best way for comparison of the fittings in this case was the R^2 values. The oil droplet size range was presented in Figure A.1. The minimum oil droplet size was about 0.2 μm which was very close to the pore size of the MF 0.3 μm TiO_2/ZrO_2 membrane But only a small fraction of the oil droplets had a size about 0.2 μm. As most of the oil droplet sizes were bigger than the pores of MF 0.3 μm TiO_2/ZrO_2 membrane, the cake layer formation was more likely to occur, and as some of the oil droplets had a similar size (0.2 μm) to the membrane pores (0.3 μm), the intermediate pore blocking might also happen which is in accordance to the R^2 values of fittings.

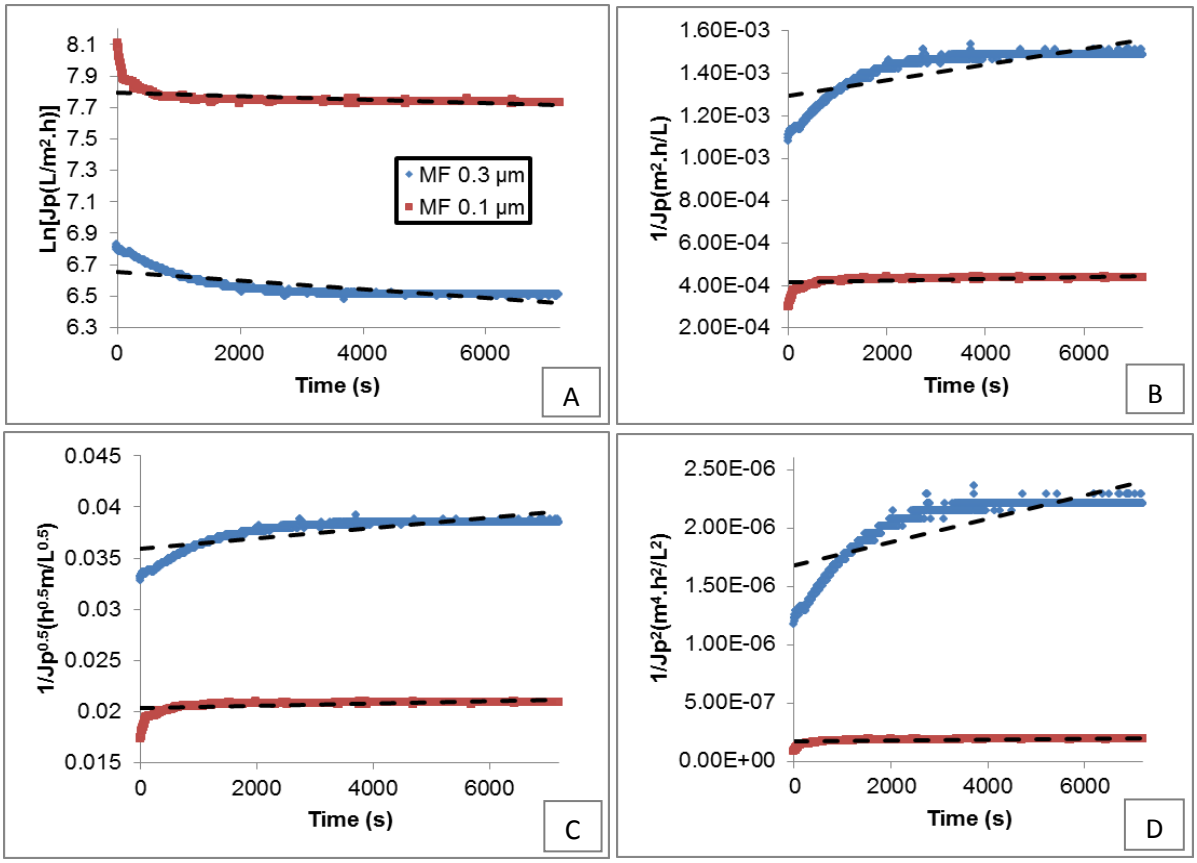

Figure 4.13: Permeate flux prediction of MF membranes at 1 m/s and 0.8 bar A) Complete blocking, B) Intermediate blocking, C) Standard blocking and D) Cake layer formation (broken lines: predicted fluxes) [original in color]

For MF 0.1 µm SiC membrane, the cake layer formation and the intermediate blocking model were found to have to most probability to control the permeate flux of the membrane by comparison of the R^2 values which is similar to the results of MF 0.3 µm TiO_2/ZrO_2 membrane. As mentioned, the minimum oil droplet size was 0.2 µm which is very close to the MF 0.1 µm SiC membrane pore size and therefore, the intermediate blocking is predominant after the cake layer formation.

Table 4.16: Values of R^2 for Hermia's models fitting to the experimental data for MF membranes

	CFV (m/s)	TMP (bar)	Complete blocking	Intermediate blocking	Standard blocking	Cake layer formation
MF 0.3 μm	1	0.8	0.613	0.635	0.624	0.656
MF 0.1 μm	1	0.8	0.321	0.348	0.335	0.374

The obtained Hermia's models parameters for the two MF membranes were presented in Table 4.17. The initial permeate flux was calculated using different Hermia's models for the MF membranes and presented in Table 4.18. It was found that the predicted initial permeate fluxes were very similar for each MF membrane using different models, and in spite of fitting results, the complete blocking and then standard blocking had closer prediction to the measured initial permeate fluxes of MF membranes.

Table 4.17: Hermia's models parameters for MF membranes

	CFV (m/s)	TMP (bar)	$K_c \times 10^5$	K_i	$K_s \times 10^4$	$K_g \times 10^{-2}$
MF 0.3 µm	1	0.8	2.71	0.13	9.47	13.00
MF 0.1 µm	1	0.8	1.09	0.02	2.08	0.47

Table 4.18: Comparison between the predicted initial permeate fluxes for MF membranes and experimental values measured at 1 m/s

	TMP (bar)	Complete blocking	Intermediate blocking	Standard blocking	Cake layer formation	Measured
MF 0.3 µm	0.8	776	774	775	772	927
MF 0.1 µm	0.8	2423	2419	2421	2414	3333

The permeate flux of MF 0.1 µm SiC membrane was modeled at different TMPs and CFVs and presented in Figure 4.14 and Figure 4.15, respectively. The

R2 values for fittings were also presented in Table 4.19. It was previously reported (Gu, 2007; Vincent Vela et al., 2008) that the obtained values of R2 were not sufficient to compare the fittings using the same model at different operating condition, but R2 values were suitable indicative for comparison of the fittings at the same operating condition for different models. Therefore, the graphs were used for comparison of fittings of the same model at different operating conditions which was also possible since the plotted graph data had the same data range for the same models. But the R2 values were used for comparison of the fittings at the same operating condition and for different models.

By comparison of the R^2 values for different models, it was found that the cake layer formation and then the intermediate blocking model were the most predominant fouling mechanisms controlling the permeate flux of the MF 0.1 μm SiC membrane at all the operating conditions tested.

The Hermia's models parameters for MF 0.1 μm SiC membrane are presented in Table 4.20. The model parameters would have higher values at operating conditions that membrane fouling is more severe (Vincent Vela et al., 2008). It was found that the model parameters were higher at low TMPs (0.4 and 0.6 bar) and at the lowest CFV tested (0.5 m/s).

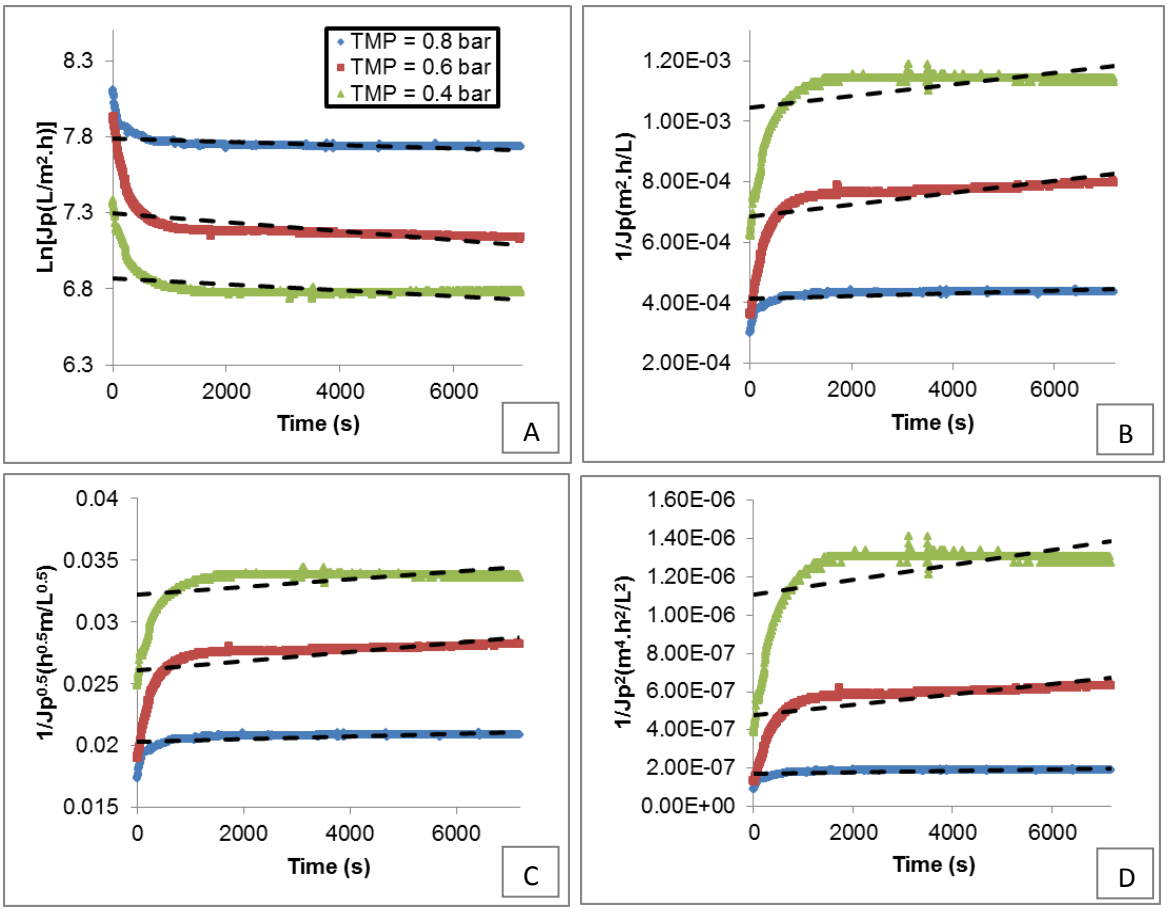

Figure 4.14: Permeate flux prediction of MF 0.1 μm SiC membrane at 1 m/s and different TMPs, A) Complete blocking, B) Intermediate blocking, C) Standard blocking and D) Cake layer formation (broken lines: predicted fluxes) [original in color]

Table 4.19: Values of R^2 for Hermia's models fitting to the experimental data for MF 0.1 μm SiC membrane

CFV (m/s)	TMP (bar)	Complete blocking	Intermediate blocking	Standard blocking	Cake layer formation
1	0.8	0.321	0.348	0.335	0.374
	0.6	0.330	0.398	0.364	0.464
	0.4	0.243	0.265	0.254	0.284
1.5	0.8	0.428	0.456	0.442	0.484
1		0.321	0.348	0.335	0.374
0.5		0.198	0.219	0.209	0.239

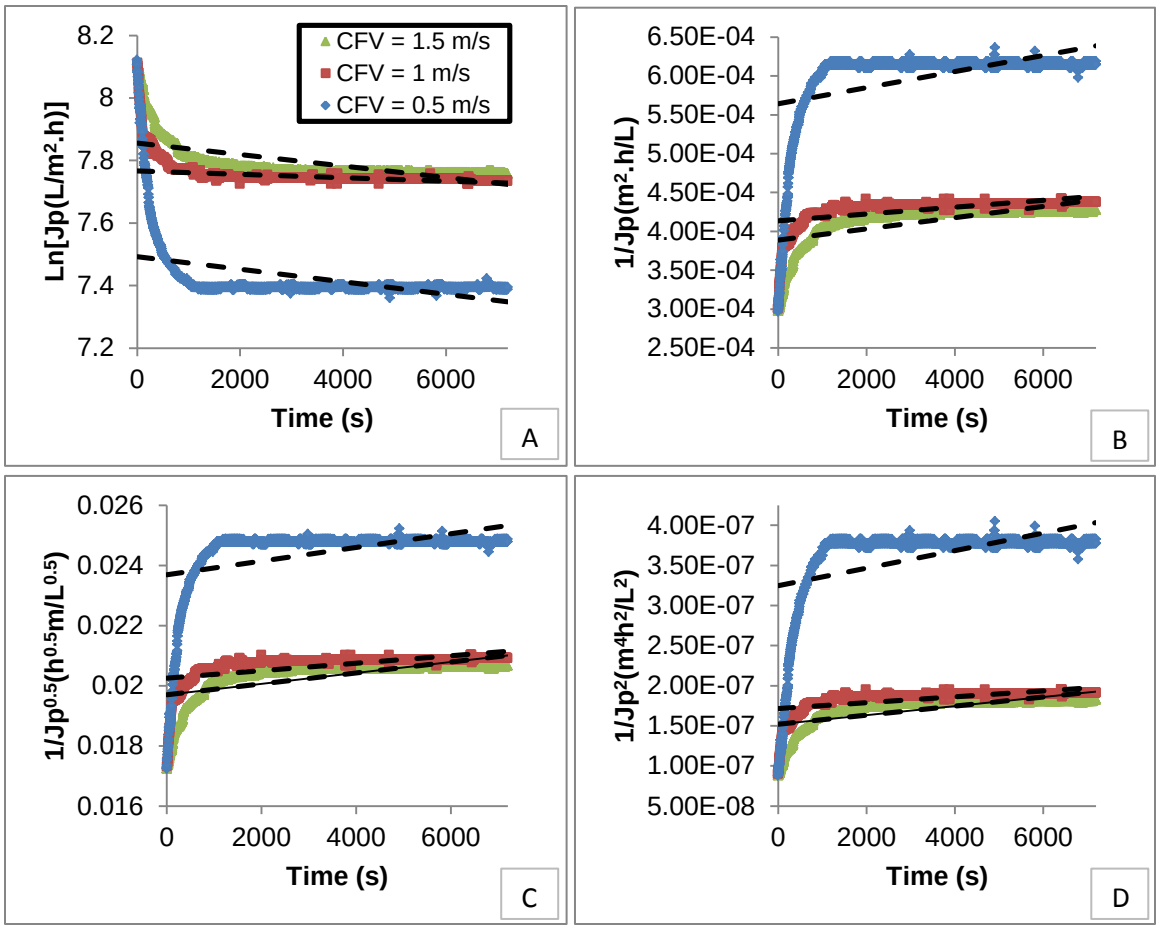

Figure 4.15: Permeate flux prediction of MF 0.1 µm SiC membrane at 0.8 bar and different CFVs, A) Complete blocking, B) Intermediate blocking, C) Standard blocking and D) Cake layer formation (broken lines: predicted fluxes) [original in color]

Table 4.20: Hermia's models parameters for MF 0.1 μm SiC membrane

CFV (m/s)	TMP (bar)	$K_c \times 10^5$	K_i	$K_s \times 10^4$	$K_g \times 10^{-2}$
1	0.8	1.09	0.02	2.08	0.47
	0.6	2.95	0.07	7.20	3.50
	0.4	1.96	0.07	5.83	5.04
1.5	0.8	1.84	0.03	3.45	0.73
1		1.08	0.02	2.08	0.47
0.5		2.01	0.04	4.31	1.41

The initial permeate fluxes were predicted using different models at different operating conditions (Table 4.21). Similar to the results of the MF membranes

presented earlier, the complete and then the standard blocking models had better predictions of initial permeate flux.

Table 4.21: Comparison between the predicted initial permeate fluxes for MF 0.1 μm SiC membrane and experimental values measured

CFV (m/s)	TMP (bar)	Complete blocking	Intermediate blocking	Standard blocking	Cake layer formation	Measured
1	0.8	2423	2419	2421	2414	3333
	0.6	1480	1461	1470	1448	2738
	0.4	965	957	961	949	1594
1.5	0.8	2581	2573	2577	1755	3360
1		2423	2419	2421	2414	3333
0.5		1794	1772	1782	2565	3367

4.3.4.2 UF membranes

The two permeate fluxes of the two UF membranes tested were also modeled using the Hermia's models and the results are presented in Figure 4.16. It should be noted that the UF 0.04 μm SiC membrane was tested at 0.8 bar and 1 m/s, but the UF 150 KDa TiO2/ZrO2 membrane was tested at 2 bars and 1 m/s. The R2 values were presented in Table 4.22. Both of the UF membranes had higher R2 values for cake layer formation and the intermediate blocking models which were similar to the results of the MF membranes tested.

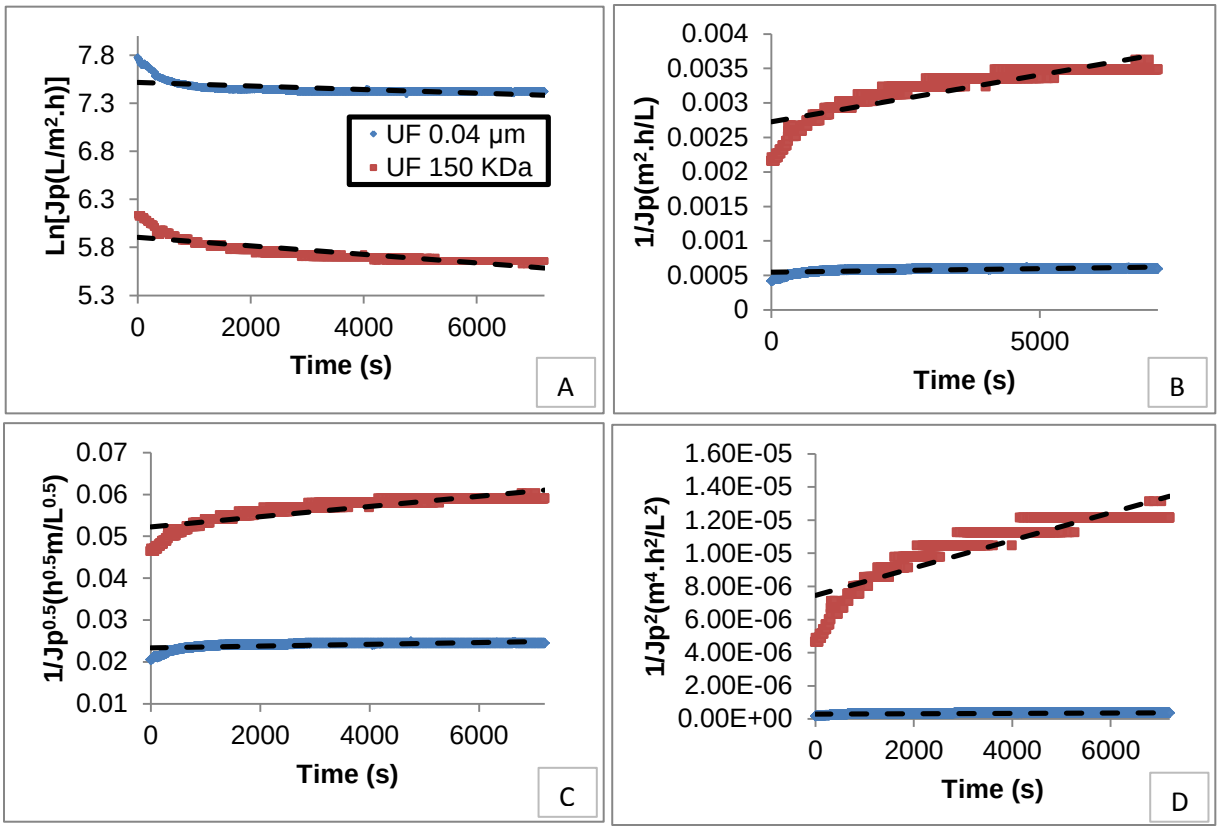

Figure 4.16: Permeate flux prediction of UF membranes
A) Complete blocking, B) Intermediate blocking, C) Standard blocking and D) Cake layer formation (broken lines: predicted fluxes) [original in color]

Table 4.22: Values of R^2 for Hermia's models fitting to the experimental data for UF membranes at 1 m/s

	TMP (bar)	Complete blocking	Intermediate blocking	Standard blocking	Cake layer formation
UF 0.04 µm	0.8	0.415	0.441	0.428	0.467
UF 150 Kda	2	0.736	0.782	0.760	0.821

The Hermia's models parameters were presented in Table 4.23. The predicted initial permeate flux of the membranes are presented in Table 4.24. The predicted initial permeate fluxes of UF 150 KDa membrane were very similar, but the predicted fluxes of complete and standard blocking models were slightly closer to the measured value for UF 0.04 µm membrane.

Table 4.23: Hermia's models parameters for UF membranes

	CFV (m/s)	TMP (bar)	$K_c \times 10^5$	K_i	$K_s \times 10^4$	$K_g \times 10^{-2}$
UF 0.04 µm	1	0.8	1.85	0.04	4.10	1.45
UF 150 Kda	1	2	4.46	0.49	23.29	107.94

Table 4.24: Comparison between the predicted initial permeate fluxes for UF membranes and experimental values measured at 1 m/s

	TMP (bar)	Complete blocking	Intermediate blocking	Standard blocking	Cake layer formation	Measured
UF 0.04 µm	0.8	1836	1830	1833	1824	2379
UF 150 Kda	2	367	366	367	366	464

The modeled permeate fluxes of the UF 0.04 µm SiC membrane at different TMPs and CFVs were presented in Figure 4.17 and Table 4.18, respectively. The obtained R2 values were presented in Table 4.25. By comparison of the R2 values of fittings, it was found that the cake layer formation and the intermediate blocking models were the most predominant fouling mechanisms at all the operating conditions testes but at TMP of 0.4 bar and CFV of 1 m/s, these two fouling mechanisms were slightly less effective, and it seems that all the mechanisms had very similar effects on permeate flux at this operating condition. This may be due to operation at a lower TMP which causes less cake layer formation.

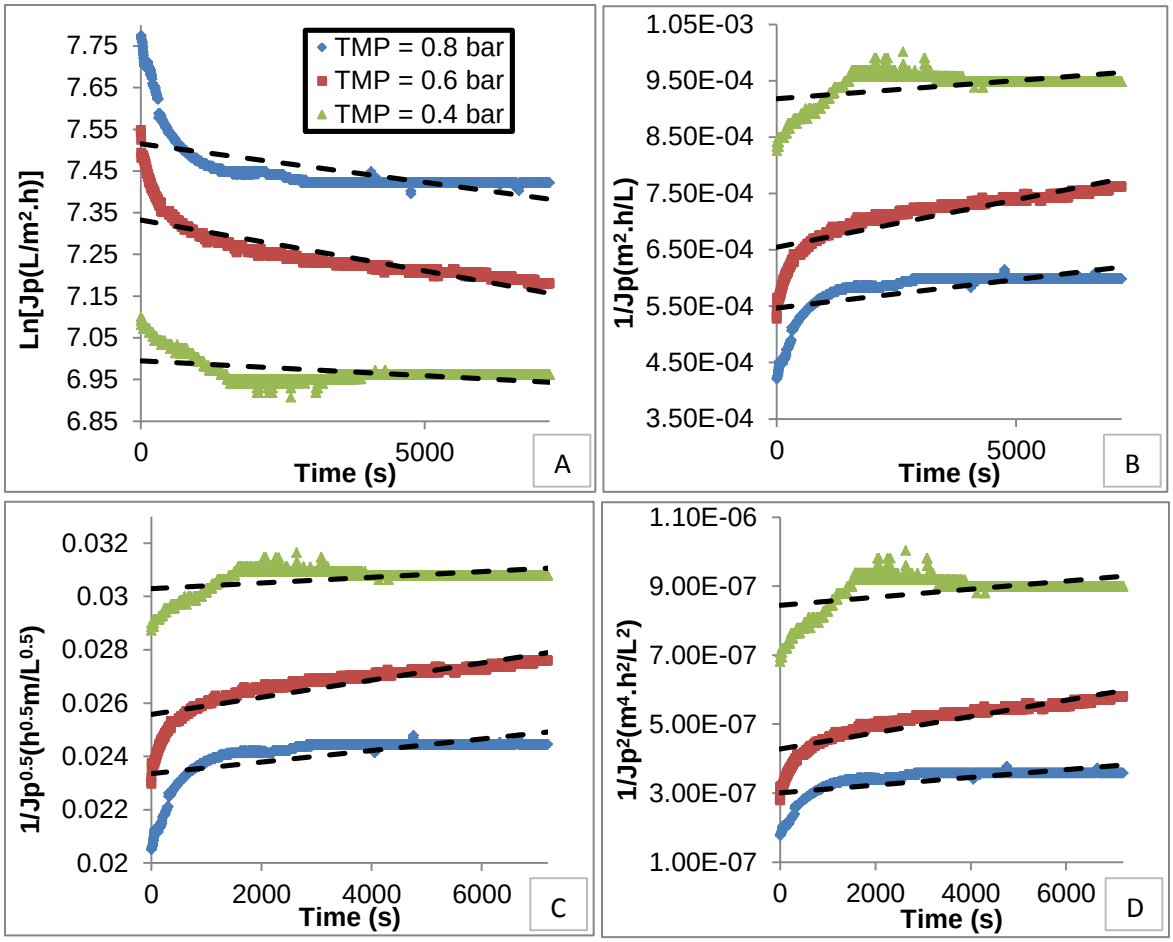

Figure 4.17: Permeate flux prediction of UF 0.04 µm SiC membrane at 1 m/s and different TMPs, A) Complete blocking, B) Intermediate blocking, C) Standard blocking and D) Cake layer formation (broken lines: predicted fluxes) [original in color]

By the comparison of the fitted curves, it was found that as TMP increases, the fitting results were better for cake layer formation which was also in accordance to the R2 values obtained. The models parameters and initial permeate fluxes were presented in Table 4.26 and Table 4.27, respectively.

Table 4.25: Values of R^2 for Hermia's models fitting to the experimental data for UF 0.04 µm SiC membrane

CFV (m/s)	TMP (bar)	Complete blocking	Intermediate Blocking	Standard blocking	Cake layer formation
1	0.8	0.415	0.441	0.428	0.467
	0.6	0.752	0.787	0.770	0.819
	0.4	0.254	0.249	0.251	0.244
1.5	0.8	0.609	0.639	0.624	0.668
1		0.415	0.441	0.428	0.467
0.5		0.830	0.948	0.899	0.994

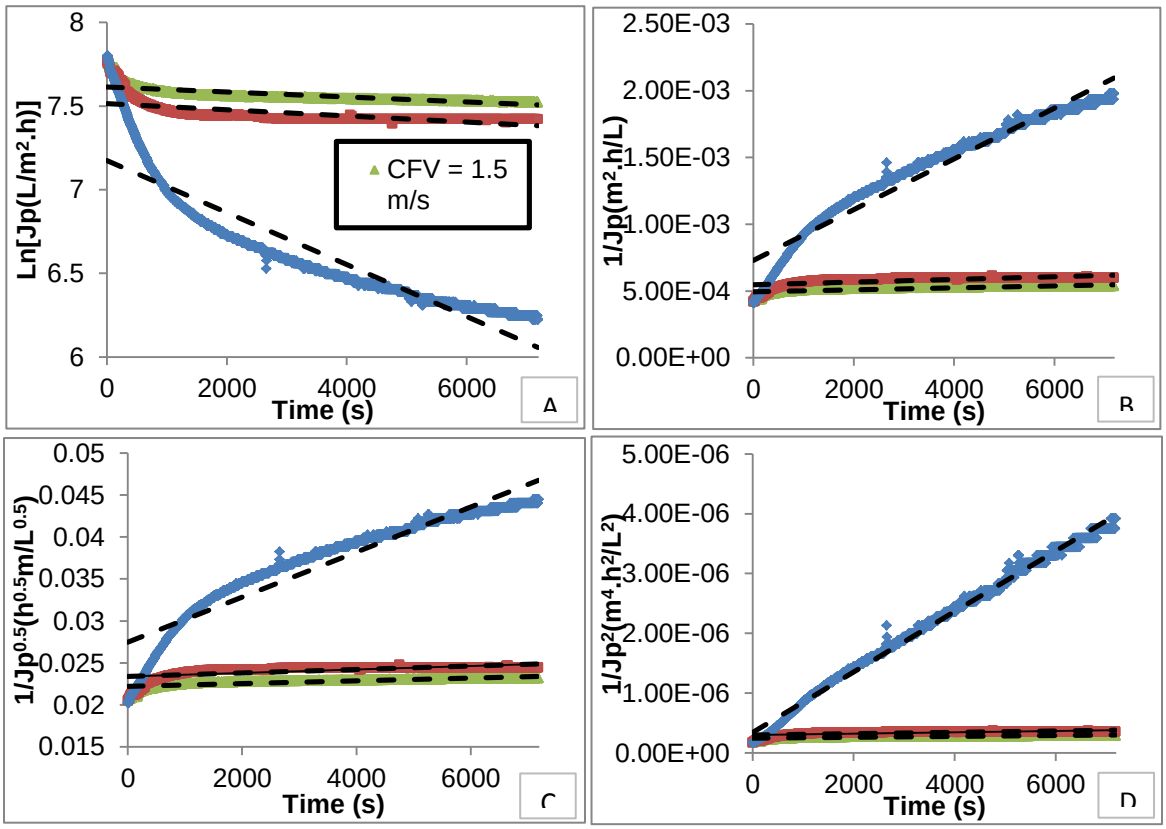

Figure 4.18: Permeate flux prediction of UF 0.04 µm SiC membrane at 0.8 bar and different CFVs, A) Complete blocking, B) Intermediate blocking, C) Standard blocking and D) Cake layer formation (broken lines: predicted fluxes) [original in color]

Table 4.26: Hermia's models parameters for UF 0.04 µm SiC membrane

CFV (m/s)	TMP (bar)	$K_c \times 10^5$	K_i	$K_s \times 10^4$	$K_g \times 10^{-2}$
1	0.8	1.85	0.04	4.10	1.45
	0.6	2.43	0.06	6.08	3.06
	0.4	0.71	0.02	2.04	1.52
1.5	0.8	1.49	0.03	3.18	0.99
1		1.85	0.04	4.10	1.45
0.5		15.54	0.68	50.95	65.57

Table 4.27: Comparison between the predicted initial permeate fluxes for UF 0.04 µm SiC membrane and experimental values measured

CFV (m/s)	TMP (bar)	Complete blocking	Intermediate blocking	Standard blocking	Cake layer formation	Measured
1	0.8	1836	1830	1833	1824	2379
	0.6	1529	1528	1528	1528	1886
	0.4	1091	1089	1090	1088	1212
1.5	0.8	2028	2026	2027	2025	2379
1		1836	1830	1833	1824	2379
0.5		1306	1371	1325	1712	2435

CHAPTER 5: Summary and conclusions

5.1 Summary

Two ceramic MF membranes, 0.3 μm TiO_2/ZrO_2 (TAMI Industries) and 0.1 μm SiC (Liqtech International), and two ceramic UF membranes, 0.04 μm SiC (Liqtech International) and 150 kg/mol TiO_2/ZrO_2 (TAMI Industries) were tested for produced water treatment. The synthetic produced water with average concentrations of oil content, TOC, COD, TDS and turbidity of 117 ppm, 72.51 mg/L, 1628 mg/L, 10.39 ppt and 60 NTU, respectively was used as a feed for the MF and UF membranes. The two MF membranes and UF 0.04 μm SiC membrane were tested at TMP of 0.8 bar and CFV of 1 m/s. The UF 150 kg/mol TiO2/ZrO2 membrane was operated at TMP of 2 bars and CFV of 1 m/s.

The MF 0.3 μm TiO_2/ZrO_2 membrane had slightly higher rejection percentages for oil, TOC and COD (97.2%, 74.2% and 98.3%, respectively) than MF 0.1 μm SiC membrane (95.6%, 72.4% and 98.1%, respectively). But the steady permeate flux of MF 0.1 μm SiC membrane was about 2285 $L/m^2 \cdot h$, while the steady permeate flux of MF 0.3 μm TiO_2/ZrO_2 membrane was about 673 $L/m^2 \cdot h$. Salt rejections of both of the MF membranes were low. Therefore, the MF 0.1 μm SiC membrane was selected from the MF membranes since it had higher permeate flux and similar permeate characteristics to MF 0.3 μm TiO_2/ZrO_2 membrane.

The permeate of the selected MF membrane was used as a feed for two UF membranes (MF and UF in series). It was found that the oil was totally rejected by UF membranes but the rejection percentages of UF membranes for the other

parameters were very low. Therefore, the produced water was used directly as a feed for UF membranes.

The UF 150 kg/mol TiO_2/ZrO_2 membrane rejections for TOC and COD were 97.7% and 78.0%, respectively, which were slightly higher than TOC and COD rejections of UF 0.04 μm SiC membrane (96.9% and 76.2%, respectively). The salt rejections were low for both of UF membranes. The final permeate flux of the UF 0.04 μm SiC membrane was about 1672 $L/m^2 \cdot h$ which was about 5.8 times the final flux of the UF 150 KDa TiO_2/ZrO_2 membrane. Therefore, the UF 0.04 μm SiC membrane was selected since it had higher permeate flux and similar permeate quality as UF 150 KDa TiO_2/ZrO_2 membrane.

The performances of the selected MF and UF membranes were investigated at different TMPs (0.4, 0.6 and 0.8 bar) and CFVs (0.5, 1 and 1.5 m/s). It was found that the permeate quality of the MF 0.1 μm SiC and UF 0.04 μm SiC membranes did not change very much at different TMPs and CFVs. However, at highest TMP (0.8 bar) and the highest CFV (1.5 m/s), the highest permeate fluxes were observed. The permeate fluxes at CFV of 1 m/s and 1.5 m/s were very close. Therefore, the CFV of 1 m/s and TMP of 0.8 bar were selected for MF and UF membranes. Finally, the UF 0.04 μm SiC membrane was chosen as the best membrane since it had 100% oil removal and a permeate COD concentration of 387 mg/L. The oil removal percentage and COD concentration of MF 0.1 μm SiC membrane were 95.6% and 450 mg/L, respectively. The treated water can be disposed into sea or injected into oil reservoirs for enhanced oil recovery.

Cleaning-in-place method was used to clean the fouled UF 0.04 μm SiC membrane at different concentrations of NaOH (2%, 3% and 4%) and HNO_3 (2%, 3% and 4%), and based on the flux recoveries, the highest acid and base concentrations were selected. The backwashing (5 seconds duration) and backpulsing were also tested at 10 min. intervals. It was found that these two methods can successfully recover the permeate flux of the UF membrane without stopping the filtration. These two methods may be used along with the CIP method for cleaning of the fouled membranes.

The Hermia's models were used to investigate the fouling mechanisms in filtrations. It was found that the cake layer formation had the best results in the fittings. The intermediate blocking model was found to be the second predominant fouling mechanism involved in the filtration experiments.

5.2 Conclusions

The MF 0.1 μm SiC membrane was selected as the best MF membrane and the UF 0.04 μm SiC membrane was chosen as the best UF membrane. A CFV of 1 m/s and a TMP of 0.8 bar were found to be the best operating conditions for the selected MF and UF membranes. Finally, the UF 0.04 μm SiC membrane was selected as the best membrane since it had 100% oil rejection.

NaOH and HNO_3 concentrations of 4% and 4% were found to be the best acid and base concentrations for the cleaning-in-place method. The backpulsing and backwashing methods could successfully recover the permeate flux of the membrane during filtration. Cake layer formation and intermediate blocking models were the most predominant fouling mechanisms.

CHAPTER 6: Future work

The following recommendations are made to extend the study of ceramic filtration of produced water:

- The critical flux of the new and tested membranes can be determined.
- Another synthetic produced water preparation method like using a homogenizer instead of the polymeric filtration setup can be used for preparation of the feed.
- The effect of produced water oil content on permeate flux and permeate quality of different membranes can be assessed.
- Ceramic membranes with another channel configuration and size can be tested.
- The filtrations can be performed for longer periods. To accomplish this aim, higher volumes of feed should be prepared, and some new feed can be added in predetermined intervals to keep the feed characteristics unchanged.
- The accuracy of spectrophotometer can be compared with the oil content analyzer (OCMA-350) for oil content analysis of the samples, and the most accurate method can be used for future analysis.
- Field produced water can be used as a feed for membranes.
- Other cleaning methods like ultrasonic radiation can be used.
- Other chemicals can be used for CIP method.
- Different interval times for backwashing and backpulsing methods and different backwashing durations can be investigated.

- Different combinations of cleaning methods with different interval times can also be assessed.
- The polymeric RO membranes can be used after the selected ceramic UF membrane to reject the salts and therefore, make the produced water usable for agricultural or industrial use.

REFERENCES

Abbasi, M., Mirfendereski, M., Nikbakht, M., Golshenas, M., and Mohammadi, T. (2010). Performance study of mullite and mullite–alumina ceramic MF membranes for oily wastewaters treatment. *Desalination, 259*, 169-178.

Abbasi, M., Sebzari, M. R., and Mohammadi, T. (2011). Enhancement of oily wastewater treatment by ceramic microfiltration membranes using powder activated carbon. *Chemical Engineering & Technology, 34*, 1252–1258.

Badrnezhad, R., and Heydari Beni, A. (2013). Ultrafiltration membrane process for produced water treatment: experimental and modeling. *Journal of Water Reuse and Desalination*. doi:10.2166/wrd.2013.092.

Bhattacharjee, C., and Datta, S. (2003). Analysis of polarized layer resistance during ultrafiltration of PEG-6000: an approach based on filtration theory. *Separation and Purification Technology, 33*, 115-126.

Bowen, W., Calvo, J., and Hernández, A. (1995). Steps of membrane blocking in flux decline during protein microfiltration. *Journal of Membrane Science, 101*, 153-165.

Çakmakce, M., Kayaalp, N., and Koyuncu, I. (2008). Desalination of produced water from oil production fields by membrane processes. *Desalination, 222*, 176-186.

Canada Oil and Gas Lands Administration (1990). Offshore waste treatment guidelines. Ottawa, ON, Canada.

Chai, X., Kobayashi, T., and Fujii, N. (1999). Ultrasound-associated cleaning of polymeric membranes for water treatment. *Separation and Purification Technology, 15*, 139-146.

Chakrabarty, B., Ghoshal, A., and Purkait, M. (2008). Ultrafiltration of stable oil-in-water emulsion by polysulfone membrane. *Journal of Membrane Science, 325*, 427-437.

Cheryan, M. (1998). *Ultrafiltration and Microfiltration Handbook.* CRC Press.

Cheryan, M., and Rajagopalan, N. (1998). Membrane processing of oily streams. wastewater treatment and waste reduction. *Journal of Membrane Science, 151*, 13-28.

Clark, C., and Veil, J. (September 2009). *Produced water volumes and management practices in the United States.* prepared by the Environmental Science Division, Argonne National Laboratory for the U. S. Department of Energy, Office of Fossil Energy, National Energy Technology Laboratory.

Cui, J., Zhang, X., Liu, H., Liu, S., and Yeung, K. L. (2008). Preparation and application of zeolite/ceramic microfiltration membranes for treatment of oil contaminated water. *Journal of Membrane Science, 325*, 420–426.

Czermak, P., Ebrahimi, M., Ashaghi, K. S., Engel, L., and Mund, P. (April 14-18, 2008). Feasibility of using ceramic micro-, ultra- and nanofiltration

membranes for efficient treatment of produced water. *10th World Filtration Congress.* Leipzig, Germany.

Daiminger, U., Nitsch, W., Plucinski, P., & Hoffmann, S. (1995). Novel techniques for oil/water separation. *Journal of Membrane Science, 99*, 197–203.

de Barros, S., Andrade, C., Mendes, E., and Peres, L. (2003). Study of fouling mechanism in pineapple juice clarification by ultrafiltration. *Journal of Membrane Science, 215*, 213-224.

Duraisamy, R. T., Heydari Beni, A., and Henni, A. (2013). State of the Art Treatment of Produced Water. In *Water Treatment* (pp. 199-222). Rijeka, Croatia: InTech.

Ebrahimi, M., Shams Ashaghi, K., Engel, L., Willershausen, D., Mund, P., Bolduan, P., and Czermak, P. (2009). Characterization and application of different ceramic membranes for the oil-field produced water treatment. *Desalination, 245*, 533-540.

Ebrahimi, M., Willershausen, D., Shams Ashaghi, K., Engel, L., Placido, L., Mund, P., Bolduan, P., and Czermak, P. (2010). Investigations on the use of different ceramic membranes for efficient oil-field produced water treatment. *Desalination, 250*, 991-996.

El-Kayar, A., and Hussein, M. (1993). Removal of oil from stable oil-water emulsion by induced air flotation technique. *Separations Technology, 3*, 25–31.

Environment Canada (2004). Threats to Water Availability in Canada. In *National Water Research Institute.* Burlington, Ontario.

Facciotti, M., Boffa, V., Magnacca, G., Jørgensen, L. B., Kristensen, P. K., Farsi, A., König, K., Christensen, M. L., and Yue, Y. (2014). Deposition ofthinultrafiltration membranesoncommercial SiC microfiltration tubes. *Ceramics International, 40*, 3277–3285.

Fakhru'l-Razi, A., Pendashteh, A., Abidin, Z. Z., Abdullah, L. C., Biak, D. R., and Madaeni, S. S. (2010). Application of membrane-coupled sequencing batch reactor for oilfielld produced water recycle and beneficial re-use. *Bioresource Technology, 101*, 6942-6949.

Falahati, H., and Tremblay, A. (2011). Flux dependent oil permeation in the ultrafiltration of highly concentrated and unstable oil-in-water emulsions. *Journal of Membrane Science, 371*, 239-247.

Field, R., Hang, S., and Arnot, T. (1994). The influence of surfactant on water flux through microfiltration membranes. *Journal of Membrane Science, 86*, 291–304.

Glimmerman, E. D. (2006). *Assessment of the available technologies for slop and bilge water treatment and monitoring offshore.* Master thesis: Chalmers University of Technology, Sweden.

Gorouhi, E., Sadrzadeh, M., and Mohammadi, T. (2006). Microfiltration of oily wastewater using PP hydrophobic membrane. *Desalination, 200*, 319-321.

Gu, Z. (2007). Across-sample Incomparability of R^2s and Additional Evidence on Value Relevance Changes Over Time. *Journal of Business Finance & Accounting, 34*, 1073–1098.

Hach. (2005). *DR5000 spectorphotometer procedures manual.* Hach Company.

Hanna. (2006). *HI 4521 & HI 4522 pH/mV/ISE/temperature/conductivity/resistivity /TDS/salinity bench meters instruction manual.* Hanna Instruments.

Hanna. (2007). *HI 83414 turbidity and free/total chloride meter instructon manual.* Hanna Instruments.

Hermia, J. (1982). Constant pressure blocking filtration laws: application to power-law non-Newtonian fluids. *Trans. Inst. Chem. Eng., 60a*, 183 - 187.

Horiba. (1995). *Oil content analyzer OCMA-350 instruction manual.* Kyoto, Japan: Horiba Ltd.

Horiba. (2008). *pH meter F-52/F-53/F-54/F-55 instruction manual.* Horiba Ltd.

Hua, F., Tsang, Y., Wang, Y., Chan, S., Chua, H., and Sin, S. (2007). Performance study of ceramic microfiltration membrane for oily wastewater treatment. *Chemical Engineering Journal, 128*, 169–175.

Hwang, K. J., and Lin, T. T. (2002). Effect of morphology of polymeric membrane on the performance of cross-flow microfiltration. *Journal of Membrane Science, 199*, 41-52.

International Advanced Resources (November 2002). *Powder River Basin coal bed methane development and produced water management study.* prepared for the U.S. Department of Energy, National Energy Technology Laboratory.

Khatib, Z., and Verbeek, P. (2003). Water to Value – Produced water management for sustainable field development of mature and green fields. *Journal of Petroleum Technology, 55*, 26-28.

Koltuniewiz, A., and Field, R. (1996). Process factors during removal of oil-in-water emulsions with cross-flow microfiltration. *Desalination, 105*, 79-89.

Kong, J., and Li, K. (1999). Oil removal from oil-in-water emulsions using PVDF membranes. *Seperation and Purification Technology, 16*, 83–93.

Król, T., Stelmaszewski, A., and Freda, W. (2006). Variability in the optical properties of a crude oil – seawater emulsion. *Oceanologia, 48*, 203-211.

Kukizaki, M., and Masahiro, G. (2008). Demulsification of water-in-oil emulsions by permeation through Shirasu-porous-glass (SPG) membranes. *Journal of Membrane Science, 322*, 196–203.

Kyllönen, H., Pirkonen, P., Nyström, M., Nuortila-Jokinen, J., and Grönroos, A. (2006). Experimental aspects of ultrasonically enhanced cross-flow membrane filtration of industrial wastewater. *Ultrasonics Sonochemistry, 13*, 295–302.

Lee, K. P., Arnot, T. C., and and Mattia, D. (2011). A review of reverse osmosis membrane materials for desalination—Development to date and future potential. *Journal of Membrane Science, 370*, 1–22.

Lee, S. m., Jung, J. y., and Chung, Y. c. (2001). Novel method for enhancing permeate flux of submerged membrane system in two-phase anaerobic reactor. *Water Research, 35*, 471-477.

Lescoche, P., and Bergel, J. Y. (2004). FILTANIUMTM: The 100% titanium dioxide ceramic membrane. *Proceedings of the 8th International Conference on Inorganic Membranes*, (pp. 430-433). Cincinnati, USA.

Lim, A., and Bai, R. (2003). Membrane fouling and cleaning in microfiltration of activated sludge wastewater. *Journal of Membrane Science, 216*, 279-290.

Lin, H. F. (2006). *Ceramic membrane technology applied to oily wastewater separation.* PhD dissertation: Hong Kong Polytechnic University, Japan.

LiqTech. (2013a). *Flux maintenance on ceramic silicon carbide membranes from LiqTech International A/S.* Ballerup, Denmark: LiqTech International A/S.

LiqTech. (2013b). *User manual for LabBrain CFU025.* Ballerup, Denmark: LiqTech International.

LiqTech. (2014). *Future filtraton silicon carbide ceramic membranes.* Ballerup, Denmark: LiqTech International.

Lobo, A., Cambiella, Á., Benito, J. M., Pazos, C., and Coca, J. (2006). Ultrafiltration of oil-in-water emulsions with ceramic membranes: Influence of pH and crossflow velocity. *Journal of Membrane Science, 278*, 328-334.

Lue, S. J., Chow, J., Chien, C., and Chen, H. (2009). Cross-flow microfiltration of oily water using a ceramic membrane: Flux decline and oil adsorption. *Separation Science and Technology, 44*, 3435-3454.

Madaeni, S. S., Ahmadi Monfared, H., Vatanpour, V., Arabi Shamsabadi, A., Salehi, E., Daraei, P., Laki, S., and Khatami, S. M. (2012). Coke removal from petrochemical oily wastewater using γ-Al2O3 based cermic microfiltration membrane. *Desalination, 293*, 87-93.

Madaeni, S., Gheshlaghi, A., and Rekabdar, F. (2013). Membrane treatment of oily wastewater from refinery processes. *Asia-Pacific Journal of Chemical Engineering, 8*, 45–53.

Mallada, R., and Menéndez, M. (2008). *Inorganic Membranes: Synthesis, Characterization and Applications.* Amsterdam, The Netherlands: Elsevier.

Malvern. (2009). *Zetasizer nano series user manual.* Worcestershire, United Kingdom: Malvern Instruments Ltd.

Malvern. (2011). *Mastersizer 3000 User Manual.* Worcestershire, United Kingdom: Malvern Instruments Ltd.

Mohammadi, T., Kazemimoghadam, M., and Saadabadi, M. (2003). Modeling of membrane fouling and flux decline in reverse osmosis during separation of oil in water emulsions. *Desalination, 157*, 369–375.

Mueller, J., Cen, Y., and Davis, R. (1997). Crossflow microfiltration of oily water. *Journal of Membrane Science, 129*, 221-235.

Munoz-Aguado, M., Wiely, D., and Fane, A. (1996). Enzymatic detergent cleaning of polysulphone membrane fouled with BSA and whey. *Journal of Membrane Science, 117*, 175-187.

Nandi, B., Uppaluri, R., and Purkait, M. (2009). Treatment of Oily Waste Water Using Low-Cost Ceramic Membrane: Flux Decline Mechanism and Economic Feasibility. *Separation Science and Technology, 44*, 2840-2869.

OGP. (2005). *Fate and effects of naturally occurring substances in produced water on the marine environment.* Report no. 364.

Ohya, H., Kim, J., Chinen, A., Aihara, M., Semenova, S., Negishi, Y., Mori, O., and Yasuda, M. (1998). Effects of pore size on separation mechanisms of microfiltration of oily water using porous glass tubular membrane. *Journal of Membrane Science, 145*, 1-14.

Peachey, B. (2005). *Strategic needs for energy related water use technologies. Water and the EnergyINet.* Calgary: Alberta Energy Research Institute.

Pedenaud, P., Heng, S., Evans, W., and Bigeonneau, D. (October 4-6, 2011). Ceramic membrane and core pilot results for produced water management. *Offshore Technology Conference Brazil.* Rio de Janeiro, Brazil.

Ramirez, J. A., and Davis, R. H. (1998). Application of cross-flow microfiltration with rapid backpulsing to wastewater treatment. *Journal of Hazardous Materials, 63*, 179–197.

Ray, J., and Engelhardt, R. (1992). Produced water, technological/environmental issues and solutions. In *Proceedings of the 1992 International Produced Water Symposium.* San Diego, USA: Plenum Publishing Corporation.

Rezaei Hosein Abadi, S., Sebzari, M. R., Hemati, M., Rekabdar, F., and Mohammadi, T. (2011). Ceramic membrane performance in microfiltration of oily wastewater. *Desalination, 265*, 222-228.

Salahi, A., Abbasi, M., and Mohammadi, T. (2010a). Permeate flux decline during UF of oily wastewater: Experimental and modeling. *Desalination, 251*, 153-160.

Salahi, A., Gheshlaghi, A., Mohammadi, T., and Madaeni, S. S. (2010b). Experimental performance evaluation of polymeric membranes for treatment of an industrial oily wastewater. *Desalination, 262*, 235-242.

Salahi, A., Mohammadi, T., Abbasi, M., and Rekabdar, F. (2010c). Chemical cleaning of ultrafiltration membrane after treatment of oily wastewater. *Iranian Journal of Chemical Engineering, 7*, 17-28.

Salahi, A., Mohammadi, T., Rekabdar, F., and Mahdavi, H. (2010d). Reverse osmosis of refinery oily wastewater effluents. *Iranian Journal of Rnvironmental Health Science & Engineering, 7*, 413-422.

Sarfaraz, M. V., Ahmadpour, E., Salahi, S., Rekabdar, F., and Mirza, B. (2012). Experimental investigation and modeling hybrid nano-porous membrane process for industrial oily wastewater treatment. *Chemical Engineering Research and Design, 90*, 1642-1651.

Scurtu, C. T. (2009). *Treatment of produced water: targeting dissolved compounds to meet a zero harmful discharge.* Trondheim: PhD thesis, NTNU.

Shams Ashaghi, K., Ebrahimi, M., and Czermak, P. (2007). Ceramic Ultra- and Nanofiltration Membranes for Oilfield Produced Water Treatment: A Mini Review. *The Open Environmental Journal, 1*, 1-8.

Shimadzu. (2010). *TOC-L CPH/CPN user's manual .* Kyoto, Japan: Shimadzu Corporation.

Silalahi, S. H., and Leiknes, T. (2009). Cleaning strategies in ceramic microfiltration membranes fouled by oil and particulate matter in produced water. *Desalination, 236*, 160-169.

Sohrabi, M., Madaeni, S., Khosravi, M., and Ghaedi, A. (2011). Chemical cleaning of reverse osmosis and nanofiltration membranes fouled by licorice aqueous solutions. *Desalination, 267*, 93-100.

Sutrisna, P., Lingganingrum, F., and Wenten, I. (2012). Separation of oil-in-water emulsion using slotted pore membrane. *Jurnal Teknik Kimia Indonesia, 11*, 57-65.

Syncrude.(2004). *http://sustainability.syncrude.ca/sustainability2004/download /SyncrudeSD2004.pdf.* Syncrude.

Thoma, G., Bowen, M., and Hollensworth, D. (1999). Dissolved air precipitation/solvent sublation for oil-field produced water treatment. *Separation and Purification Technology, 16*, 101–107.

Thomas, D., Greene, G., Duval, W., Milne, K., and Hutcheson, M. (1983). *Offshore oil and gas production waste characteristics, treatment methods, biological effects and their applications to Canadian regions.* Ottawa, ON, Canada: Prepared for EPS, Environment Canada.

Thompson, D., Taylor, A., and Graham, D. (1985). Emulsification and demulsification related to crude oil production. *Colloids and Surfaces, 15*, 175–189.

United States Environmental Protection Agency (1991). Proposed Rules (Vol. 56). Federal Register.

Vachon, D., Zaidi, A., and and Kok, S. (1991). A data base on the characteristics of produced waters from insitu heavy oil recovery operations in western Canada. *Petroleum Society of CIM and AOSTRA*, 91-38.

Vasanth, D., Pugazhenthi, G., and Uppaluri, R. (2011). Fabrication and properties of low cost ceramic microfiltration membranes for separation of oil and bacteria from its solution. *Journal of Membrane Science, 379*, 154-163.

Vigo, F., Uliana, C., and Ravina, E. (1990). The Vibrating Ultrafiltration Module. Performance in the Low Frequency Region. *Separation Science and Technology, 25*, 63-82.

Vincent Vela, M. C., Blanco, S. Á., García, J. L., and Rodríguez, E. B. (2008). Analysis of membrane pore blocking models applied to the ultrafiltration of PEG. *Separation and Purification Technology, 62*, 489-498.

Wandera, D. (2012). *Design of advanced fouling-resistant and self-cleaning membranes for treatment of oily and impaired waters.* University of Clemson, United States: Ph.D dissertation.

Yan, L., Hong, S., Li, M. L., and Li, Y. S. (2009). Application of the Al2O3–PVDF nanocomposite tubular ultrafiltration (UF) membrane for oily wastewater treatment and its antifouling research. *Separation and Purification Technology, 66*, 347-352.

Yang, Y., Chen, R., and Xing, W. (2011). Integration of ceramic membrane microfiltration with powdered activated carbon for advanced treatment of oil-in-water emulsion. *Separation and Purification Technology, 76*, 373-377.

Zaidi, A., Simms, K., and Kok, S. (1992). The use of micro/ultrafiltration for the removal of oil and suspended solids from oilfield brines. *Water Science and Technology, 25*, 163-176.

Zeevalkink, J., and Brunsmann, J. (1983). Oil removal from water in parallel plate gravity-type separators. *Water Research, 17*, 365–373.

Zhang, H., and Fang, S. (2008). Treatment of waste filature oil/water emulsion by combined demulsification and reverse osmosis. *Separation and Purification Technology, 63*, 264–268.

Zhang, H., Zhong, Z., and Xing, W. (2013). Application of ceramic membranes in the treatment of oilfield-produced water: Effects of polyacrylamide and inorganic salts. *Desalination, 309*, 84-90.

Zhao, Y., Tan, Y., Wong, F., Fane, A., and Xu, N. (2005). Formation of dynamic membranes for oily water separation by crossflow filtration . *Separation and Purification Technology, 44*, 212–220.

Zhong, J., Sun, X., and Wang, C. (2003). Treatment of oily wastewater produced from refinery processes using flocculation and ceramic membrane filtration. *Separation and Purification Technology, 32*, 93-98.

Zydney, A. L., and Ho, C. C. (2002). Scale-up of microfiltration systems: fouling phenomena and Vmax analysis. *Desalination, 146*, 75-81.

APPENDIX

Analysis

Created by: Malvern Instruments Ltd
Last edited: 10/20/2011 4:38:58 AM

Measurement Details

Sample Name	August 21, 2013	**Measurement Date**	8/21/2013 9:34:27 AM
Operator Name	softinstall	**Analysis Date Time**	8/21/2013 9:34:27 AM
Sop Name	Balkan Oil.msop	**Result Source**	Measurement

Analysis

Particle Name	Bakken area oil	**Particle Refractive Index**	1.457
Dispersant Name	Water	**Dispersant Refractive Index**	1.330
Particle Absorption Index	0.000	**Laser Obscuration**	2.37 %
Weighted Residual	0.37 %	**Scattering Model**	Mie
Analysis Model	General Purpose	**Analysis Sensitivity**	Normal
Scattering Model	Mie		

Result

Concentration	0.0043 %	**Span**	1.886
Uniformity	1.267	**Result Transformation Type**	Volume
Specific Surface Area	1055 m^2/kg	**Dv 10**	5.90 µm
D[3,2]	7.11 µm	**Dv 50**	24.2 µm
D[4,3]	43.9 µm	**Dv 90**	51.6 µm

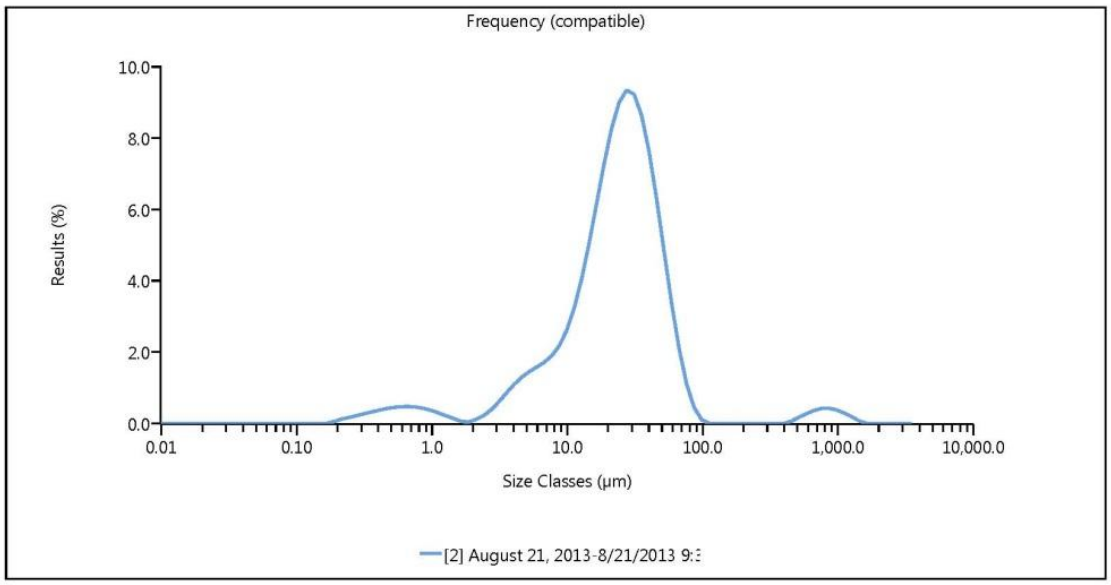

Malvern

Figure A.1: Oil droplet size analysis of synthetic PW

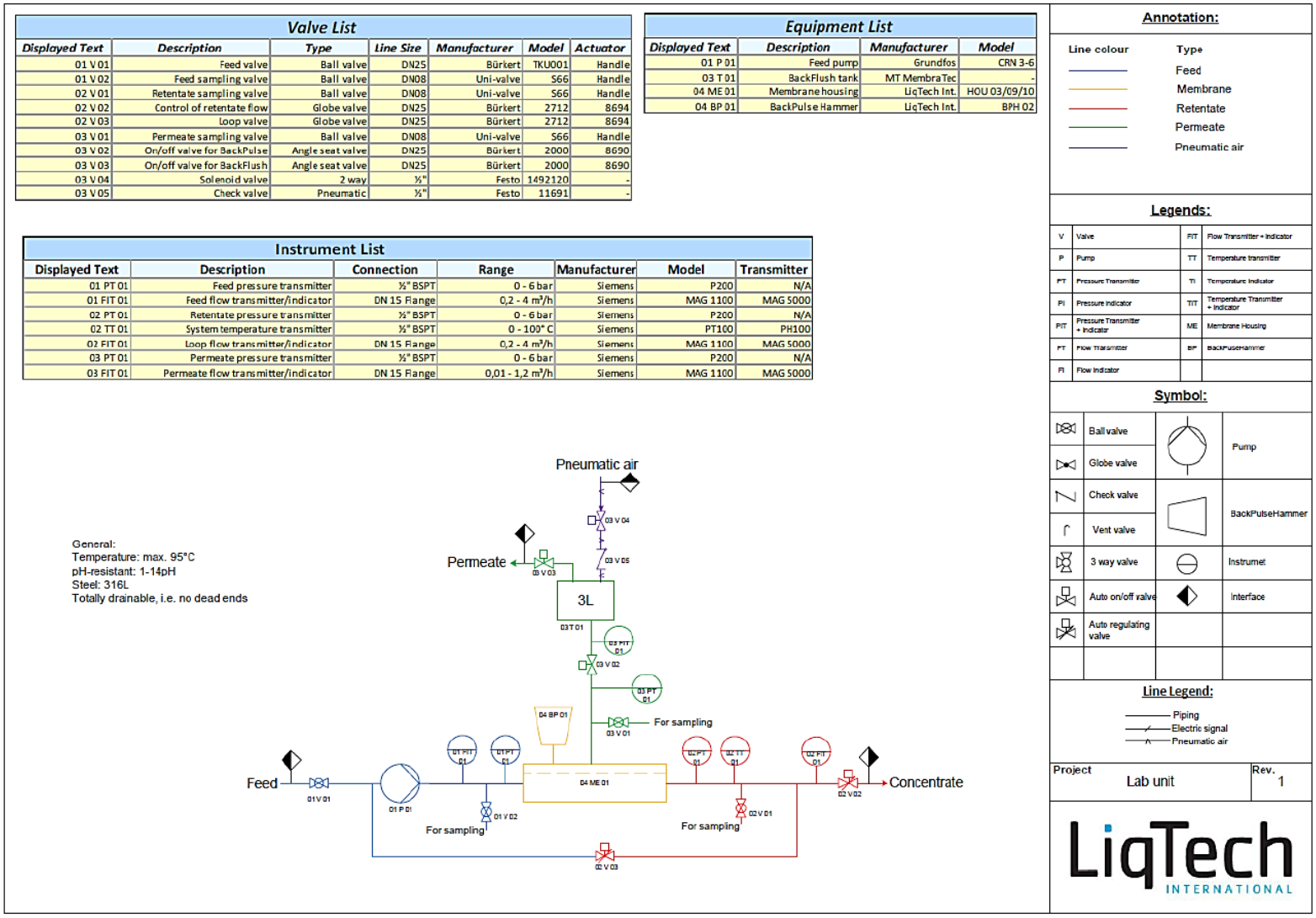

Figure A.2: P&ID diagram of the LabBrain unit (with details about different parts of setup) [adapted from (LiqTech, 2013b)]